DIEL CHARACTERISTICS OF *PROCHLOROCOCCUS* AND *SYNECHOCOCCUS* POPULATIONS IN THE WESTERN SARGASSO SEA

by

BRAD JAMES BLYTHE

(Under the Direction of Brian J. Binder)

ABSTRACT

Prochlorococcus and *Synechococcus* are ubiquitous marine picocyanobacteria that contribute significantly to oceanic primary production. The tightly phased patterns of cell growth and division in these groups provide a basis for evaluating their *in situ* growth and mortality. In particular, the daily progression of *Prochlorococcus* populations through their cell cycle can be used to estimate the growth rate (and by inference, the loss rate) of these populations. In this dissertation, the diel dynamics of cell abundance, cellular growth, and cell cycle progression are presented for *Prochlorococcus* and *Synechococcus* populations in the Western Sargasso Sea. I use these data to critically evaluate two methods of calculating *in situ* growth rates of *Prochlorococcus* populations in this environment. I also utilize concurrently sampled incubation bottles to test the efficacy of commonly used incubation techniques to accurately simulate the dynamics of natural picoplankton populations. Finally, I report on a numerical simulation model of *Prochlorococcus* based on the current state of knowledge of the biology and ecology of these organisms. My results demonstrate that while as a group *Prochlorococcus* growth rates estimated by the two cell cycle-based approaches do not vary systematically, individual estimates can differ significantly between these two approaches.

Growth rates varied widely over depth and between stations; no significant seasonality was detected. Regarding the bottle incubations, the physiology of *in situ Prochlorococcus* populations (as reflected in growth rate) appears to be reasonably reflected in the bottles. In contrast, grazing on *Prochlorococcus* was dramatically reduced in the bottles, relative to the *in situ* rates. Thus, traditional bottle incubations may not accurately replicate the ecological dynamics of *in situ* populations. Finally, the biology-based cell cycle model produced diel patterns in cell size and cell cycle dynamics that were qualitatively similar to those observed in natural populations. The model predicted strong day to day variability in these dynamics, and in the resultant growth rates, suggesting that estimates based on 24 h sampling may not accurately reflect the true growth rate of these populations on ecologically relevant time scales.

INDEX WORDS: Cyanobacteria, Sargasso Sea, Cell Cycle, Flow Cytometry

DIEL CHARACTERISTICS OF *PROCHLOROCOCCUS* AND *SYNECHOCOCCUS* POPULATIONS IN THE WESTERN SARGASSO SEA

by

BRAD JAMES BLYTHE

B.S., Coastal Carolina University, 2001

A Dissertation Submitted to the Graduate Faculty of the University of Georgia in Partial Fulfillment of the Requirements for the Degree

DOCTOR OF PHILOSOPHY

ATHENS, GEORGIA

2008

DIEL CHARACTERISTICS OF *PROCHLOROCOCCUS* AND *SYNECHOCOCCUS* POPULATIONS IN THE WESTERN SARGASSO SEA

by

BRAD JAMES BLYTHE

Major Professor: Brian J. Binder

Committee: James T. Hollibaugh
Mary Ann Moran
Peter Verity
Elizabeth Mann

Electronic Version Approved:

Maureen Grasso
Dean of the Graduate School
The University of Georgia
December 2008

TABLE OF CONTENTS

Page

CHAPTER

1 INTRODUCTION AND LITERATURE REVIEW…….1

References……..……8

2 A CRITICAL ANALYSIS OF THE CELL CYCLE METHOD FOR CALCULATING *IN SITU* GROWTH RATES IN *PROCHLOROCOCCUS* POPULATIONS……13

Introduction……14

Methods……..16

Results and Discussion …….18

Conclusions……26

References……..28

Tables and Figures…….30

3 *PROCHLOROCOCCUS* GROWTH AND MORTALITY IN THE WESTERN SARGASSO SEA: DIEL OBSERVATIONS FROM COUPLED *IN SITU* AND INCUBATION STUDIES……46

Introduction……47

Methods……..47

Results……49

Discussion……..53

References……..59

Tables and Figures…….61

4 AN INDIVIDUAL-BASED MODEL FOR THE ANALYSIS OF *PROCHLOROCOCCUS* DIEL CELL CYCLE BEHAVIOR……..71

Introduction……72

Model Description…….76

Results……79

Discussion……..83

References..……88

Tables and Figures……..91

Appendix……...101

5 DISSERTATION CONCLUSIONS……107

References…….112

CHAPTER 1

INTRODUCTION AND LITERATURE REVIEW

Two groups of picocyanobacteria have a particularly important role in the oligotrophic, open ocean environment: *Synechococcus* and *Prochlorococcus.* The importance of Synechococcus was recognized in 1979 (Johnson & Sieburth 1979, Waterbury et al. 1979), while *Prochlorococcus* were not identified until 1988 (Chisholm et al. 1988). In fact, *Prochlorococcus* had been observed earlier, (Johnson & Sieburth 1979) but it was not until the shipboard application of flow-cytometry that it was characterized as a distinct and abundant picocyanobacterial group (Chisholm et al. 1988).

Prochlorococcus and *Synechococcus* are ubiquitous in tropical and temperate oceans (Partensky et al. 1999) and can contribute significantly to photosynthetic standing stock and primary production in these environments (Campbell et al. 1994, Liu et al. 1998, DuRand et al. 2001). *Prochlorococcus* has been estimated to be responsible for over 50% of total primary production in the Sargasso Sea (Li 1994). *Synechococcus* has also been shown to have a major contribution in both coastal and open-ocean environments (Waterbury 1986).

While similar in size and closely related (~96% similarity in 16s rRNA content) (Rocap et al. 2002), *Prochlorococcus* and *Synechococcus* are nevertheless genetically and physiologically distinct. *Synechococcus* is found in oceanic and coastal regions, and along with chlorophyll a, contains phycobiliproteins (Waterbury 1986). *Prochlorococcus*, by contrast, is found predominantly in oceanic regions, lacks phycobiliproteins, and possesses divinyl

chlorophyll a and b (chl a_2 and b_2) (Chisholm et al. 1988). *Prochlorococcus* is also slightly smaller (~0.7μm in diameter) than *Synechococcus* (~1μm in diameter) (Partensky et al. 1999).

Recently the existence of distinct ecotypes of *Prochlorococcus* (and to a lesser extent *Synechococcus)* has been recognized. These ecotypes are distributed differentially in the water-column, and show latitudinal gradients as well (Johnson et al. 2006, Zinser et al. 2006). *Prochlorococcus* ecotypes have been shown to differ markedly in light physiology, nutrient preference and temperature response (Moore et al. 1998, Rocap et al. 2003, Johnson et al. 2006, Zinser et al. 2006). Moore et al. (2002) also showed a correlation between the nitrogen source preference of *Prochlorococcus* ecotypes (and *Synechococcus*) and the dominant nitrogen source available at their optimal depth range (Moore et al. 2002).

Prochlorococcus and *Synechococcus* exhibit strong diel patterns of cell growth and division. In *Prochlorococcus* populations, division is tightly phased, with all members of the population that are going to divide on a given day entering into the division cycle a few hours after the maximal solar irradiance, and completing their division a few hours before sunrise the next day, with most of the process taking place in the evening hours (Jacquet et al. 2001a, Jacquet et al. 2001b, Binder & DuRand 2002). Flow cytometrically measured cellular parameters also exhibit strong daily cycles. Both light scatter (a proxy for size) and chlorophyll fluorescence increase during the early day until cells begin dividing, at which point these parameters begin to decrease until sunrise the next day (Binder & DuRand 2002). *Synechococcus* strains have also been shown to divide in a diel pattern in the laboratory and in the field (Binder & Chisholm 1995, Jacquet et al. 2001a, Binder & DuRand 2002). **T**hus both groups exhibit highly timed cycles of cell growth and division over 24 hour light:dark cycles.

The tightly timed division cycle of *Prochlorococcus* populations can be useful in evaluating the processes that control the dynamics of these populations. Using flow cytometric analyses, it is possible to measure abundance, fluorescence patterns and DNA content of these picocyanobacteria (Binder et al. 1996). By assessing diel changes in the population DNA distributions, growth rates (and by inference, mortality rates) for *Prochlorococcus* populations in the field can be estimated (Binder et al. 1996, Liu et al. 1997, Shalapyonok et al. 1998, Worden & Binder 2003). It is one of the goals of my thesis to utilize information from in-situ and incubation studies to infer relationships between *Prochlorococcus* and its top-down controls. Unfortunately, *Synechococcus* is less amenable to this approach, due to greater variability in cell cycle behavior, and to difficulties in analyzing *Synechococcus* DNA distributions in the field.

The theory underlying cell-cycle based approaches for calculating growth rates was developed by McDuff & Chisholm (1982) in the context of their clarification of the "frequency of dividing cells" method. This approach relies on estimating both the fraction of cells in the process of division over the course of the day, and the duration of the division phase in any given cell. Estimation of the latter is the main source of error for these calculations. Carpenter and Chang (1988) expanded this idea, and utilized the concept of a generalized "terminal event" (which can be any cell cycle stage the ends in cell division). They used the combined cell cycle phases S+G2 as the terminal event and showed that the duration of this event can be estimated as twice the time between the peaks of cells in S-phase and G2-phase, based upon a time-series of DNA distribution data. This is a powerful tool, as it requires no prior knowledge about the state of the cells in the population except their DNA content over time. As *Prochlorococcus* populations are extremely well phased in their divisions cycles (Jacquet et al. 2001, Binder & DuRand 2002), they are an excellent candidate for this approach.

Indeed, the Carpenter and Chang approach has been applied to *Prochlorococcus* in numerous studies, (e.g. Liu et al. 1997, Shalapyonok et al. 1998, Mann & Chisholm 2000, Worden & Binder 2003). However, the approach has not truly been tested, and the authors themselves pointed to possible weaknesses in the method and potential improvements (Carpenter & Chang 1988, Chang & Carpenter 1988, Antia et al. 1990, Chang & Carpenter 1990, 1991). Furthermore, very little information about the diel dynamics of *Prochlorococcus* growth and grazing has been extracted from such cell cycle data, although this information is imbedded in that data. My dissertation research is aimed at critically examining the Carpenter and Chang methodology as applied to *Prochlorococcus*, and at developing a numerical model to accurately calculate time varying growth and loss rates of *Prochlorococcus* and to predict changes in in-situ concentrations in the presence and absence of loss factors (grazing, viral lysis, sinking, etc.).

Dissertation Introduction

The main goal of my dissertation is to gain a clearer understanding of the diel dynamics of *Prochlorococcus* and *Synechococcus*, and how these patterns affect the ecology of their populations in the Sargasso Sea. In this context, I am interested in the seasonal differences these populations exhibit, as well as differences in diel population dynamics with regards to depth and location in the western Sargasso Sea. The main questions I intend to address are:

What are the diel dynamics of *Prochlorococcus* and *Synechococcus* in the Western Sargasso Sea? While a considerable amount of data is available regarding the large-scale seasonal dynamics of *Prochlorococcus* and *Synechococcus* in the Sargasso, their diel dynamics have not been well-studied. The variability of these dynamics from season to season, and within the water column is unknown at present. To gain a clear picture of these diel cycles, I will be utilizing in-situ sampling experiments, along with corresponding diel bottle incubations. These

data will allow me to examine the natural dynamics in the water column, and compare those results to a more controlled set of bottle experiment data.

Can we develop a cell-cycle based model to accurately calculate growth and loss parameters of *Prochlorococcus* and *Synechococcus*? In a 1990 paper, Chang and Carpenter recommended a method of data-smoothing to be used in conjunction with their cell cycle approach for growth rate estimation. This method has not been widely employed, but my initial evaluations (and those of Chang and Carpenter 1990) show that it lessens the error introduced when determining the timing of cell cycle events, and yields a more accurate measure of growth rate than the original method. Although promising, there are some issues (primarily involving the magnitude of variation of the fitted curves with the data, and more importantly, a frequent mismatch of the timing of the peaks in the fitted curve and the data) with this approach as applied to our data that need to be addressed. I will do so by constructing a diel cell cycle model and using it to interpret observed diel patterns. This model would be easily expandable to encompass population dynamics and time-dependent grazing. My goal is to develop a simple, accurate way of calculating time-resolved growth and grazing mortality rates from diel cell cycle measurements.

Chapter 2 – *In situ* Diel Cycles

As part of ongoing research, our lab has conducted diel, lagrangian water column sampling events in the Sargasso Sea. The purpose of these investigations is to examine the growth and loss parameters of *Prochlorococcus sp.* and *Synechococcus sp.* over a 24-48 hour period. For each experiment, a holey-sock type drogue was deployed and samples collected in its vicinity every 60 - 90 minutes at four depths. One of the sampling depths corresponded to the simulated depth in an on-deck incubator experiment (see below).

Samples from these experiments were stained with a DNA-specific Hoechst dye, and analyzed flow-cytometrically for *Prochlorococcus sp.* and *Synechococcus sp.* abundance, and *Prochlorococcus sp.* DNA distribution (e.g. Binder et al. 1996). These data will allow for the calculation of in-situ growth rates (and by inference, grazing rates) for *Prochlorococcus*.

In the present work, we have analyzed diel cell cycle data from four research cruises between 2001 and 2002 in the Western Sargasso utilizing the traditional "manual" method of calculating growth rates for *Prochlorococcus* populations, as well as the curve-fitting approach put forth by Chang and Carpenter (1990). Results from both methods are compared in order to discern whether one or the other yields a more robust estimate of in-situ growth rate. Diel variations in *Prochlorococcus* abundance and cellular characteristics are also reported and compared between depth and season.

The main goal for these analyses is to gain a greater understanding of the diel dynamics of cellular characteristics, abundance, and growth among *Prochlorococcus* and *Synechococcus* in-situ. In so doing, we hope to learn how *Prochlorococcus* and *Synechococcus* populations are affected by changes in water column structure (with seasons), depth (between 15 and 100m), and location (at varied sampling stations in the western Sargasso). These comparisons should provide a greater knowledge of the factors that primarily control the dynamics of *Prochlorococcus* and *Synechococcus* in the field.

Chapter 3 – Diel Bottle Experiments

On-deck incubations were run in tandem with the in-situ sampling described above. These diel incubation experiments were carried out at a light level corresponding to one of the 4 experimental depths of each in-situ profile. This chapter will discuss data from 7 diel incubation

experiments which (as stated above) correspond directly to 7 of the 18 in-situ diel time-series. All analyses on these samples were run following the same protocols as the in-situ experiments

These bottle experiments will allow for a better estimation of time-resolved growth and loss rates for *Prochlorococcus*, as uncertainties about sampling the same population over time are eliminated. These experiments will also serve as a direct comparison to the in-situ experiments, providing validation of the results of the in-situ experiments.

Chapter 4 – Diel Cell Cycle Model

Using the model of Chang and Carpenter (1990) as a starting point, we have developed a diel cell cycle model. This model will have multiple purposes. The first of these is to test the sensitivity of cell cycle based growth rate calculations to deviations from their underlying assumptions. By developing and utilizing an optimized growth rate calculation model, we will be able to better ensure that estimates of growth rates in our study populations are as accurate as possible.

Another function of this model is to combine the calculated growth rates with observed diel variation in cell number to accurately model the dynamics of the population. This will allow us to make inferences about the magnitude and diel variation of factors controlling *Prochlorococcus* abundance in the field.

The development of this model will be applicable to all studies of growth rates in similar populations, and potentially lead to a more uniform and precise method of calculating growth rates. This could be an important step forward, as accurately measuring the growth of the major producers in any ecosystem is an important first step in understanding how that system functions and changes over time.

References

Antia AN, Carpenter EJ, Chang J (1990) Species-Specific Phytoplankton Growth-Rates via Diel DNA-Synthesis Cycles .3. Accuracy of Growth-rate Measurement in the Dinoflagellate Prorocentrum-minimum. Mar. Ecol.-Prog. Ser. 63:273-279

Binder BJ, Chisholm SW (1995) Cell-Cycle Regulation in Marine Synechococcus Sp Strains. Appl. Environ. Microbiol. 61:708-717

Binder BJ, Chisholm SW, Olson RJ, Frankel SL, Worden AZ (1996) Dynamics of picophytoplankton, ultraphytoplankton and bacteria in the central equatorial Pacific. Deep-Sea Res. Part II-Top. Stud. Oceanogr. 43:907-931

Binder BJ, DuRand MD (2002) Diel cycles in surface waters of the equatorial Pacific. Deep-Sea Res. Part II-Top. Stud. Oceanogr. 49:2601-2617

Campbell L, Nolla HA, Vaulot D (1994) The Importance of Prochlorococcus to Community Structure in the Central North Pacific-Ocean. Limnol. Oceanogr. 39:954-961

Carpenter EJ, Chang J (1988) Species-Specific Phytoplankton Growth-Rates via Diel DNA-Synthesis Cycles. 1. Concept of the Method. Mar. Ecol.-Prog. Ser. 43:105-111

Chang J, Carpenter EJ (1988) Species-Specific Phytoplankton Growth-Rates via Diel DNA-Synthesis Cycles.2. DNA Quantification and Model Verification in the Dinoflagellate Heterocapsa-triquetra. Mar. Ecol.-Prog. Ser. 44:287-296

Chang J, Carpenter EJ (1990) Species-Specific Phytoplankton Growth-Rates via Diel DNA-Synthesis Cycles.4. Evaluation of the Magnitude of Error with Computer-Simulated Cell-Populations. Mar. Ecol.-Prog. Ser. 65:293-304

Chang J, Carpenter EJ (1991) Species-Specific Phytoplankton Growth-Rates via Diel DNA-Synthesis Cycles .5. Application to Natural Populations in Long Island Sound. Mar. Ecol.-Prog. Ser. 78:115-122

Chisholm SW, Olson RJ, Zettler ER, Goericke R, Waterbury JB, Welschmeyer NA (1988) A Novel Free-Living Prochlorophyte Abundant in the Oceanic Euphotic Zone. Nature Harvard Univ,Cambridge,Ma 02138. 334:340-343

DuRand MD, Olson RJ, Chisholm SW (2001) Phytoplankton population dynamics at the Bermuda Atlantic Time-series station in the Sargasso Sea. Deep Sea Research Part II: Topical Studies in Oceanography 48:1983-2003

Jacquet S, Partensky F, Lennon JF, Vaulot D (2001a) Diel patterns of growth and division in marine picoplankton in culture. J. Phycol. 37:357-369

Jacquet S, Partensky F, Marie D, Casotti R, Vaulot D (2001b) Cell cycle regulation by light in Prochlorococcus strains. Appl. Environ. Microbiol. 67:782-790

Johnson PW, Sieburth JM (1979) Chroococcoid Cyanobacteria in the Sea - Ubiquitous and Diverse Phototropic Biomass. Limnol. Oceanogr. 24:928-935

Johnson ZI, Zinser ER, Coe A, McNulty NP, Woodward EMS, Chisholm SW (2006) Niche partitioning among Prochlorococcus ecotypes along ocean-scale environmental gradients. Science 311:1737-1740

Li WKW (1994) Primary Production of Prochlorophytes, Cyanobacteria, and Eucaryotic Ultraphytoplankton: Measurements from Flow Cytometric Sorting. Limnol. Oceanogr. 39:169-175

Liu H, Campbell L, Landry MR, Nolla HA, Brown SL, Constantinou J (1998) Prochlorococcus and Synechococcus growth rates and contributions to production in the Arabian Sea during the 1995 Southwest and Northeast Monsoons. Deep-Sea Res. Part II-Top. Stud. Oceanogr. 45:2327-2352

Liu HB, Nolla HA, Campbell L (1997) Prochlorococcus growth rate and contribution to primary production in the equatorial and subtropical North Pacific Ocean. Aquat. Microb. Ecol. 12:39-47

Moore LR, Post AF, Rocap G, Chisholm SW (2002) Utilization of different nitrogen sources by the marine cyanobacteria Prochlorococcus and Synechococcus. Limnol. Oceanogr. 47:989-996

Moore LR, Rocap G, Chisholm SW (1998) Physiology and molecular phylogeny of coexisting Prochlorococcus ecotypes. Nature 393:464-467

Partensky F, Hess WR, Vaulot D (1999) Prochlorococcus, a marine photosynthetic prokaryote of global significance. Microbiol. Mol. Biol. Rev. 63:106-+

Rocap G, Distel DL, Waterbury JB, Chisholm SW (2002) Resolution of Prochlorococcus and Synechococcus ecotypes by using 16S-23S ribosomal DNA internal transcribed spacer sequences. Appl. Environ. Microbiol. 68:1180-1191

Rocap G, Larimer FW, Lamerdin J, Malfatti S, Chain P, Ahlgren NA, Arellano A, Coleman M, Hauser L, Hess WR, Johnson ZI, Land M, Lindell D, Post AF, Regala W, Shah M, Shaw SL, Steglich C, Sullivan MB, Ting CS, Tolonen A, Webb EA, Zinser ER, Chisholm SW (2003) Genome divergence in two Prochlorococcus ecotypes reflects oceanic niche differentiation. Nature 424:1042-1047

Shalapyonok A, Olson RJ, Shalapyonok LS (1998) Ultradian growth in Prochlorococcus spp. Appl. Environ. Microbiol. 64:1066-1069

Waterbury JB, S. W. Watson, F. W. Valois and D. G. Franks (1986) Biological and Ecological Characterization of the Marine Unicellular Cyanobacterium Synechococcus. In: Li TPaW (ed) Photosynthetic Picoplankton, Vol 214. Can. J. Fish. Aquat. Sci. Bull, p 71-120

Waterbury JB, Watson SW, Guillard RRL, Brand LE (1979) Widespread Occurrence of a Unicellular, Marine, Planktonic, Cyanobacterium. Nature 277:293-294

Worden AZ, Binder BJ (2003) Application of dilution experiments for measuring growth and mortality rates among Prochlorococcus and Synechococcus populations in oligotrophic environments. Aquat. Microb. Ecol. 30:159-174

Zinser ER, Coe A, Johnson ZI, Martiny AC, Fuller NJ, Scanlan DJ, Chisholm SW (2006) Prochlorococcus ecotype abundances in the North Atlantic Ocean as revealed by an improved quantitative PCR method. Appl. Environ. Microbiol. 72:723-732

CHAPTER 2

A CRITICAL ANALYSIS OF THE CELL CYCLE METHOD FOR CALCULATING *IN SITU* GROWTH RATES IN *PROCHLOROCOCCUS* POPULATIONS[1]

[1] Blythe, BJ and Binder, B. To be submitted to *Phycology*

Introduction

Prochlorococcus is a ubiquitous marine pico-cyanobacterium that contributes significantly to photosynthetic standing stock and primary production in tropical and temperate oceans (Waterbury 1986, Liu et al. 1997, Zubkov et al. 2000, DuRand et al. 2001, Maranon et al. 2003). *Prochlorococcus* exhibits strong diel patterns of cell growth and division (see reviews in Jacquet et al. 2001b, Binder and DuRand 2002). Cell division in populations of this organism is tightly phased, with all members of the population that are going to divide on a given day entering into the division cycle a few hours after "local noon," and finally dividing at night. Cellular characteristics also exhibit strong daily cycles: both flow cytometrically measured light scatter (a proxy for size) and chlorophyll fluorescence increase during the early day until cells begin dividing, at which point these properties begin to decrease until sunrise the next day (Jacquet et al. 2001a, Jacquet et al. 2001b, Binder and DuRand 2002).

The strongly phased division cycle of *Prochlorococcus* can be useful in evaluating the processes that control the dynamics of natural *Prochlorococcus* populations. By assessing diel changes in the distribution of per-cell DNA, growth rates (and by inference, mortality rates) for *Prochlorococcus* populations in the field can be estimated (Vaulot et al. 1995, Binder et al. 1996, Liu et al. 1997, Shalapyonok et al. 1998, Mann and Chisholm 2000, Worden and Binder 2003).

The theory underlying the cell cycle-based approach for calculating growth rates was first developed by McDuff & Chisholm (1982) in the context of their clarification of the "frequency of dividing cells" method. The approach relies on estimating both the fraction of cells in the process of division over the course of the day, and the duration of the division phase in any given cell. Estimation of the latter is the main source of error for these calculations. Carpenter and Chang (1988) expanded this approach by introducing the concept of a generalized "terminal

event," which can be any cell cycle stage or combination of stages that ends in cell division. They used the combined cell cycle phases S+G2 as the terminal event and showed that the duration of this event can be estimated as twice the time separating the peaks of cells in the S and G2 phases, based upon a time-series of population DNA distributions. This is a powerful tool, as it requires no prior knowledge about the state of the cells in the population or the duration of S + G2 within those cells. As *Prochlorococcus* populations are extremely well-phased in their division cycles (see above), they are excellent candidates for this approach.

Indeed, the Carpenter and Chang approach has been applied to *Prochlorococcus* in numerous studies (e.g. Valout et al. 1995, Liu et al. 1997, Shalapyonok et al. 1998, Mann & Chisholm 2000, Worden & Binder 2003). However, the approach has not been critically examined in the specific context of *Prochlorococcus,* despite possible weaknesses and potential improvements in the method pointed out by Carpenter and co-workers (Carpenter and Chang 1988, Chang and Carpenter 1988, Antia et al. 1990, Chang and Carpenter 1990, 1991). In particular, Chang and Carpenter (1990) recommended fitting a periodic function to reduce the error associated with non-continuous sampling (which may not accurately capture the timing of S and G2 maxima), but this approach has not been taken in studies of *Prochlorococcus* to date.

In the present work, we have analyzed diel cell cycle data from three research cruises between 2001 and 2002 in the Western Sargasso utilizing the traditional "manual" method of calculating growth rates for *Prochlorococcus* populations (see below), as well as the curve-fitting approach put forth by Chang and Carpenter (1990). Results from both methods are compared in order to discern whether one or the other yields a more robust estimate of *in situ* growth rate. Diel variations in *Prochlorococcus* abundance and cellular characteristics are also reported and compared between depth and season.

Methods

Samples were collected at various locations in the Sargasso Sea in the spring and fall of 2001, and the spring of 2002 (Table 2.1). Lagrangian time series observations lasting 24-36 h were conducted by sampling in the vicinity of a holey-sock type drogue deployed at the start of the experiment. Water was collected from 4 pre-determined depths every 60-90 min. using a Niskin bottle rosette. At the same time, samples were collected from duplicate 1-liter on-deck incubations established at the start of each time series from water at the depth of the drogue (see details in Chapter 3). Light levels in the incubations were matched as closely as possible to the *in situ* light level at this depth using neutral density screening, and temperature was controlled by the ship's running seawater.

All samples were preserved with paraformaldehyde (0.2% final conc.) for 15 minutes in the dark before transfer to liquid nitrogen. Upon return to the laboratory, samples were stored at -85ºC until analysis.

For flow cytometry, samples were thawed and stained with Hoechst 33342 (0.5µg ml^{-1} final concentration) and analyzed using a modified dual-beam EPICS 753 flow-cytometer (Beckman Coulter, Fullerton CA, USA) as described in Binder et al. (1996). Cell concentration and cellular light scatter, chlorophyll and phycobiliprotein fluorescence, and DNA content (as Hoechst fluorescence) were collected. Analysis of list-modes was performed using WinList software (Verity Software House, Topsham ME, USA); cellular DNA frequency distributions were de-convoluted into G1, S, and G2 subpopulations with Modfit (Verity Software House, Topsham ME, USA).

Growth rate was calculated as:

$$\mu = \frac{1}{t_d}\left(\frac{1}{24}\sum_{t=0}^{24}\left(\Delta t_i \cdot \ln\left(1+f_i\right)\right)\right) \quad \text{(Eq. 2.1)},$$

where Δt_i is the length of a given sampling interval, f_i is the fraction of cells in the terminal event for that interval, and t_d is the estimated duration of the terminal event (McDuff and Chisholm 1982). The time between S and G2 peaks was doubled to give the estimate of t_d (the time it takes cells to traverse the S and G2 phases) as per Chang and Carpenter (1990). For the "manual" approach, the timing of the maxima for S and G2 are selected from the available sampling time points, which are assumed to accurately match the timing of the true peaks in S and G2 in the population. In contrast to this "manual" approach, a curve-fitting model based on Chang and Carpenter (1990) was implemented in "R" (R Foundation for Statistical Computing 2007, Vienna Austria) to fit the diel behavior of S and G2. In this case, the S and G2 maxima were chosen from the maximum values of the fitted curves. These data were then used to calculate growth rate as described above, and compared to the traditional "manual" calculation method of cell-cycle analysis for all data-sets. The periodic fitting function we employed is as follows:

$$y(t) = a_0 + \left(a_1 \cdot cos\left(\frac{2\pi}{24}\right)\right) + \left(a_2 \cdot sin\left(\frac{2\pi}{24}\right)\right)t + \left(b_1 \cdot cos\left(\frac{2\pi}{12}\right)\right)t + \left(b_2 \cdot sin\left(\frac{2\pi}{12}\right)\right)t \quad \text{(Eq. 2.2)},$$

where y_t is the fitted phase fraction, a_1, a_2, b_1, and b_2 are fitting parameters, and t is time.

Mortality rates were calculated using the estimates of μ and the observed change in cell number using the equation: $g = \mu - ln\left(\frac{N_f}{N_i}\right)$ (Eq. 2.3), where N_i and N_f are the *Prochlorococcus* concentrations based on averaged FCM counts from the first and last two time-points in a 24 h period, respectively.

Results and Discussion

Water Column Conditions

Seasonal differences in temperature, nitrate, chlorophyll and *Prochlorococcus* and *Synechococcus* profiles were obvious, and were generally consistent with previously described seasonal cycles in the Sargasso (DuRand et al. 2001, Steinberg et al. 2001). At the fall stations the water column was well-stratified, with surface mixed layers extended to 20 – 50 m (Fig. 2.1). Nitrate concentrations in the top 60 m were generally below 50 nM, except for Fall-3, where they averaged 80 nM. Nitraclines occurred at approximately 100 m, which corresponded well with the base of the deep chlorophyll maximum (DCM) (Fig. 2.1). *Prochlorococcus* showed a subsurface maximum at all fall stations, occurring at depths shallower than the DCM.

In the spring of 2002, the water column was generally well mixed, as expected (Fig. 2.1, Spring 1, 2). Profiles show a surface mixed layer extending to approximately 125 m and 175 m respectively. The water column was more stratified at the single spring 2001 station, which was later in the year (Fig. 2.1, Spring 3). Nevertheless, *Prochlorococcus* depth distribution was relatively uniform at all spring stations, with no significant subsurface maxima. *Synechococcus* concentrations were much higher in the spring than in the fall, as expected (DuRand et al. 2001). Nitrate concentrations averaged 100-250 nM in the top 60 m in Spring-1 and -2 (data not available for Spring-3).

Diel Cell Cycle Dynamics

The *in situ* diel cell cycle patterns observed here were similar to those reported previously for *Prochlorococcus* in oceanic environments (Jacquet et al. 2001a, Binder and DuRand 2002). *Prochlorococcus* populations showed a peak in S-phase cells that corresponded very closely to local dusk, except that in the time series from the deepest stations (95 and 100 m depth) this

timing appeared to be shifted earlier by approximately 60 - 90 minutes (Fig. 2.2). Similar depth-related shifts have been observed previously, and were hypothesized to reflect a strategy by shallower populations to avoid UV damage during chromosome replication (Jacquet et al. 1998, Vaulot and Marie 1999, Jacquet et al. 2001a, Binder and DuRand 2002). The peak in G2 cells occurred 4 -5 hours after the S-peak; by dawn the *Prochlorococcus* populations were comprised almost exclusively of G1 cells again (Fig. 2.2). There was no apparent difference in these patterns between spring and fall.

Prochlorococcus populations in the bottle incubations generally displayed comparable diel cell cycle patterns (data not shown). The single exception was the "Spring 2" experiment, in which the population appeared to arrest in G2 (i.e. G2 cells persisted throughout the second half of the incubation – see Chapter 3 for details). Under these circumstances, estimating growth rate by either approach is inappropriate; results from this experiment were therefore excluded from further statistical analysis and discussion.

Calculating Growth Rate from Cell Cycle Data

There are two pieces of information necessary to calculate growth rate from cell-cycle data: the time-integrated fraction of the population within a given "terminal event" prior to cell division, and the duration (t_d) of that event (McDuff and Chisholm 1982). Following Chang and Carpenter (1990), we used the combination of S and G2 cell cycle phases as the terminal event in the present study. Growth rate was calculated as described in Methods.

Sampling discrete time-points (as opposed to continuous observation) necessarily leads to uncertainty in the estimation of t_d. The sampling interval employed here (1 - 1.5 h) was as short as possible within the constraints of recovering and processing samples from different depths at sea. Nevertheless, the remaining uncertainty in the precise timing of the S and G2 peaks could

lead to significant errors in t_d estimates, and therefore in calculated growth rates (see below). As discussed above, Chang and Carpenter (1990) showed that by fitting a periodic function to the time course of S and G2 phase fractions, these errors can be minimized. We therefore used two approaches for calculating μ from Eq. 2.1. In the standard "manual" approach, the raw cell cycle phase data are used; in the "curve-fit" approach, the data are fitted to a periodic function (see Methods), and the phase fractions and peak timing are then based on these fit curves.

Overall, the periodic function of Chang and Carpenter (1990) appeared to accurately describe the phase fraction curves from the *in situ* data (r^2 values ranged from 0.37 – 0.92 for S and 0.46 – 0.97 for G2, n = 16 - 21) (Fig. 2.2). Discrepancies worth noting are an inability to capture the apparent steep leading edge and peak values of the S-phase in many cases (less so for the G2 peak). When the fitted curves were combined to yield an "S + G2" curve, the result was generally a close fit to the measured S+G2 phase fractions (r^2 values ranged from 0.49 – 0.98, n = 16 - 21) (Fig. 2.3). Similar patterns were observed in the bottle incubations, with the single exception discussed above (data not shown here, see Chapter 3).

Parameter Estimates

As discussed above, accurate growth rate measurements depend upon accurate estimates of the duration of the terminal event on one hand, and the fraction of cells within that event, integrated over a 24h period on the other. This latter term is defined more precisely as $\Sigma\ \Delta t\ ln(1 + fi)$ (see Eq. 2.1), and for the sake of discussion will be referred to here as "Σ".

Proper estimation of t_d is critical, as much of the error associated with these calculations comes from errors in the estimation of this parameter, due to the multiplier in that term of the growth rate equation. In essence, any error in the estimation of the S or G2 peak position is doubled (e.g. a 0.5 h error in the estimation of the placement of the S-phase peak leads to an hour

over/underestimation of the length of t_d). Given that estimated t_d values generally range between approximately 7.5 and 15 h (see below), this magnitude of uncertainty is not insignificant.

When the results of the manual analysis are compared to those from the fit-curves, t_d estimates from the two methods are significantly correlated, though considerable variability is evident ($r = 0.66$, $p = 0.001$)(Fig. 2.4a). No clear pattern emerges with regard to over/underestimates by one method compared to the other ($p = 0.36$, pair-wise Wilcoxon signed rank test); the ratio of the two estimates ranged from 0.7 to 1.7. For the *in situ* data, neither method seems to yield significantly more consistent t_d estimates overall, although the overall variability in fit-based estimates was somewhat lower than the manual estimates (CV of t_d estimate = 28% and 19% for the manual and curve-fit approaches, respectively). There was also no statistically significant difference ($p > 0.05$) in the variances of the manual vs. curve-fit estimates of t_d, calculated for the replicate incubation bottles.

It is important to mention that the "variability" we are reporting is fundamentally different for the *in situ* and incubation results. For the *in situ* results, I am describing overall variability among all of the stations, while for the incubations variances are calculated among replicate bottles.

Estimation of Σ is generally subject to less error than t_d (Chang and Carpenter 1990). Comparison of estimates for Σ based on the manual analysis and curve fitting revealed a strong relationship for both in situ and incubation observations, with only relatively small deviations from a 1:1 relationship ($r = 0.90$, $p = 0.001$) (Fig. 2.4b). The Wilcoxon test shows again that the manual and curve-fit estimates are not significantly different ($p = 0.14$). My results suggest that any differences between the manual and curve-fit estimates of growth rates will come largely from differences in the estimation of t_d.

Growth Rate Estimates

Growth rate estimates based on the two methods were weakly (though significantly) correlated for the combined data set ($r = 0.51$, $p = 0.01$); again, I observed considerable differences between the two estimates (Fig. 2.4c). Consistent with the t_d and Σ data, there was no obvious trend for one method to over- or under-estimate growth rate when compared to the other ($p = 0.30$ pair-wise Wilcoxon signed rank test).

Sources of Variability in *in situ* Growth Rate Estimates

In order to identify the source of the variability among calculated growth rates (variability in t_d, Σ, or both), I examined the relationship between growth rate and each of these parameters, for both estimation methods. Variation in growth rate estimates depends heavily on variation in t_d (Figs. 2.5a, b): changes in $1/ t_d$ (used as a more direct comparison than t_d, see Eq. 2.1) explains 79% and 83% of the observed variability in growth rate for curve-fit and manual analysis respectively. For the curve-fit calculations, similar variability in growth rate (59%) could be explained by changes in Σ (Fig. 2.6b). In contrast, for the manual calculations changes in Σ explained a very small proportion (29%) of the variability in growth rate (Fig. 2.6a). In neither case were Σ and t_d significantly related (not shown). Thus, if the manual approach is to be believed, changes in growth rate in the field are driven largely by changes in t_d; i.e. by changes in the speed of cell cycle progression as opposed to changes in the time-integrated fraction of the population found in S+G2 on a given day. In contrast, according to the curve-fit analysis, changes in both the duration of S+G2 and the integrated fraction of the population in those stages underlie observed changes in growth rate.

Constraining Growth Rates: Minimum Estimates

As a check of the validity of these growth rate estimates, I calculated minimum growth rates, using the f-max approach (Antia et al. 1990);

$\mu_{min} = ln(1 + fmax)$ (Eq. 2.4),

where f_{max} is the maximum fraction of cells in S + G2 (for this analyses) observed in a 24 hour period. These calculated μ_{min} values were generally less than or equal to the fitted or manual growth rate calculations, as would be expected (Fig. 2.7). Of the two cases, the curve-fit calculation yielded a more consistent relationship of $\mu_{min} < \mu$. For the manual calculation, 7 of the 27 data points fell below the 1:1 line (i.e. μ_{min} was greater than μ in 26% of the cases), whereas for the curve-fit calculations only 2 data points (7%) did so. While this difference is perhaps not dramatic, it suggests that curve-fitting results in more robust calculations of *in situ* growth rates for these types of data sets.

FALS ratio vs. μ

Diel patterns in forward angle light scatter (FALS) were consistent with cell growth during the day and division at night (Fig. 2.11), as has been observed previously (Jacquet et al. 1998, Vaulot and Marie 1999, Jacquet et al. 2001a, Binder and DuRand 2002). A positive relationship between the magnitude of these diel FALS changes and growth rate has been reported in a number of studies (Binder et al. 1996, Mann and Chisholm 2000, Jacquet et al. 2001a). There was a significant relationship between μ and dusk/dawn FALS ratio for the incubation data in the case of the curve-fit, but not manual calculations ($r=0.90$, $p=0.016$ and $r=0.56$, $p=0.25$ respectively) in the present study. However, there was no significant relationship between FALS ratio and μ for the *in situ* observations ($r^2=0.001$, $p=0.95$ and $r^2=0.25$, $p=0.25$ for manual and curve-fit estimates respectively) (Fig. 2.12). When the entire data set was considered, a weak, but significant relationship was found for the curve-fit analysis ($r = 0.52$, $p =$

0.008). There was no significant relationship for the manual analysis ($r = 0.39$, $p = 0.06$). The reasons for the disparity between these results and previous studies are unknown at present. In those previous studies, FALS varied over a ~4-6 fold range (Binder et al. 1996, Mann and Chisholm 2000), while my data showed only a ~2.5 fold range. This may be due to differences in the FALS detection geometry in the different studies.

Depth Profiles

While no clear systematic differences have been noted between the two calculation methods thus far, very different pictures of the depth dependence of growth rate emerge from the application of the two methods. The "Fall 1" profile is the most markedly different when the two methods are compared (Figs. 2.8, 2.9). The manual method shows a large range of growth rates (0.35 - 0.68 day^{-1}), with a minimum at 15 m, and a maximum at 40 m, while the curve-fit data shows a much narrower range (0.45 - 0.54 day^{-1}), with a maximum at 15 m, and a minimum at 100 m (Fig. 2.8). These differences are reflected in the depth profiles of t_d as well (Fig. 2.9): while t_d is at its maximum at 15 m for the manual calculation, it is at a minimum at this depth for the curve-fit calculation. Similar contrasts are evident in other profiles. Overall, the curve-fit calculations showed less variation within a given depth profile than the manual calculations for both t_d (mean S^2 [within profile] = 3.8, 1.4 for manual and fit respectively, $P=0.04$) and μ (mean S^2 [within profile] = 9.9×10^{-3}, 3.3×10^{-3} for manual and fit respectively, $P=0.028$).

These results highlight the need for further development and validation of growth rate estimates based on cell cycle analysis. To date, studies have generally employed the "manual" approach for estimating *in situ Prochlorococcus* growth rates. If the curve fit approach is in fact more accurate, as theoretical studies suggest it should be (Chang and Carpenter 1990), the results

from these earlier studies may need to be re-evaluated given the significant differences we observed between depth profiles generated by the two approaches.

***Prochlorococcus* Mortality**

Prochlorococcus mortality rates can be calculated from estimates of μ and the observed change in cell number over a 24-hour period using Eq. 2.3 (see Methods). In contrast to the trends in μ vs. depth, mortality rates showed relatively little sensitivity to the μ calculation method (r = 0.86 for *in situ* data), despite being partially dependent on the μ estimates (Fig. 2.10). This indicates that the calculated mortality rates were more dependent on cell number changes than on the growth rates of the prey population in this study. As seen for μ and t_d, there were no consistent trends in mortality with depth, nor did data from fall and spring cluster as distinct seasons.

Seasonal differences

For the fall cruises, where *Prochlorococcus* exhibited a deep (~60 m) maximum, neither the manual nor curve-fit calculations showed a peak in growth or mortality at these depths. For the spring data, on the other hand, when *Prochlorococcus* is distributed evenly through the mixed layer, growth rates nevertheless varied with depth, although the range of values for any given profile was small relative to individual fall profiles (Fig. 2.8). Interestingly, the Spring-3 profile, where the highest spring *Prochlorococcus* cell numbers are observed, exhibited the lowest calculated growth rates in these experiments. When seasons are compared, the total variation in growth rate at all depths was comparable regardless of the method employed. Based on the current data, it is not possible to draw conclusions about major differences in *Prochlorococcus* in-situ dynamics on a seasonal time frame in the western Sargasso. My data

shows estimates of μ, g and t_d that do not cluster together by season or location, and any seasonal trends that might exist are masked by the overall variability of these parameters.

Conclusions

Based on previous theoretical studies (Carpenter and Chang, 1990), we expected the curve-fitting approach to provide more accurate and reproducible estimates of growth rate than the standard, manual approach. However, my results with *Prochlorococcus* show that the growth rates calculated by these two approaches were not drastically different (Figs. 2.4c, 2.8). I am unable to show that one method is clearly better than the other for these data, although the resultant growth rate estimates can differ considerably. The curve-fit calculation did result in lower within-profile variability in growth rate (and t_d), but it is difficult to know whether this reduced variability is in fact a better reflection of the actual growth rates of the *in situ* populations.

My sampling intervals (1 to 1.5h) were as short as we could manage, given the time it takes to collect and preserve samples. Chang and Carpenter (1990) showed that curve-fitting yielded improvements in estimates of μ only in cases when the sampling interval was greater than 2 hours. In that light, it is perhaps not surprising that variability in my manual and curve-fit estimates are comparable. The fact remains, however, that these two methods do yield different individual estimates of μ, Σ and t_d. Therefore, I urge caution when interpreting depth-related estimates of μ, as trends in such estimates may be very different depending on the method employed.

The curve-fit approach might be improved by incorporating a function that can better fit the steep leading edge of the phase fraction curves (especially the S-phase). Ultimately, independent measurements of growth rate, in the field and/or in laboratory cultures, may be

necessary to determine the most accurate and robust approach for estimating *Prochlorococcus* growth rates from cell cycle data.

References:

Antia, A. N., E. J. Carpenter, and J. Chang. 1990. Species-Specific Phytoplankton Growth-Rates via Diel DNA-Synthesis Cycles .3. Accuracy of Growth-rate Measurement in the Dinoflagellate Prorocentrum-minimum. Marine Ecology-Progress Series **63**:273-279.

Binder, B. J., S. W. Chisholm, R. J. Olson, S. L. Frankel, and A. Z. Worden. 1996. Dynamics of picophytoplankton, ultraphytoplankton and bacteria in the central equatorial Pacific. Deep-Sea Research Part Ii-Topical Studies in Oceanography **43**:907-931.

Binder, B. J. and M. D. DuRand. 2002. Diel cycles in surface waters of the equatorial Pacific. Deep-Sea Research Part Ii-Topical Studies in Oceanography **49**:2601-2617.

Carpenter, E. J. and J. Chang. 1988. Species-Specific Phytoplankton Growth-Rates via Diel DNA-Synthesis Cycles. 1. Concept of the Method. Marine Ecology-Progress Series **43**:105-111.

Chang, J. and E. J. Carpenter. 1988. Species-Specific Phytoplankton Growth-Rates via Diel DNA-Synthesis Cycles.2. DNA Quantification and Model Verification in the Dinoflagellate Heterocapsa-triquetra. Marine Ecology-Progress Series **44**:287-296.

Chang, J. and E. J. Carpenter. 1990. Species-Specific Phytoplankton Growth-Rates via Diel DNA-Synthesis Cycles.4. Evaluation of the Magnitude of Error with Computer-Simulated Cell-Populations. Marine Ecology-Progress Series **65**:293-304.

Chang, J. and E. J. Carpenter. 1991. Species-Specific Phytoplankton Growth-Rates via Diel DNA-Synthesis Cycles .5. Application to Natural Populations in Long Island Sound. Marine Ecology-Progress Series **78**:115-122.

DuRand, M. D., R. J. Olson, and S. W. Chisholm. 2001. Phytoplankton population dynamics at the Bermuda Atlantic Time-series station in the Sargasso Sea. Deep Sea Research Part II: Topical Studies in Oceanography **48**:1983-2003.

Jacquet, S., J. F. Lennon, D. Marie, and D. Vaulot. 1998. Picoplankton population dynamics in coastal waters of the northwestern Mediterranean Sea. Limnology and Oceanography **43**:1916-1931.

Jacquet, S., F. Partensky, J. F. Lennon, and D. Vaulot. 2001a. Diel patterns of growth and division in marine picoplankton in culture. Journal of Phycology **37**:357-369.

Jacquet, S., F. Partensky, D. Marie, R. Casotti, and D. Vaulot. 2001b. Cell cycle regulation by light in Prochlorococcus strains. Applied and Environmental Microbiology **67**:782-790.

Liu, H. B., H. A. Nolla, and L. Campbell. 1997. Prochlorococcus growth rate and contribution to primary production in the equatorial and subtropical North Pacific Ocean. Aquatic Microbial Ecology **12**:39-47.

Mann, E. L. and S. W. Chisholm. 2000. Iron limits the cell division rate of Prochlorococcus in the eastern equatorial Pacific. Limnology and Oceanography **45**:1067-1076.

Maranon, E., M. J. Behrenfeld, N. Gonzalez, B. Mourino, and M. V. Zubkov. 2003. High variability of primary production in oligotrophic waters of the Atlantic Ocean: uncoupling from phytoplankton biomass and size structure. Marine Ecology-Progress Series **257**:1-11.

McDuff, R. E. and S. W. Chisholm. 1982. The Calculation of Insitu Growth-Rates of Phytoplankton Populations from Fractions of Cells Undergoing Mitosis - a Clarification. Limnology and Oceanography **27**:783-788.

Shalapyonok, A., R. J. Olson, and L. S. Shalapyonok. 1998. Ultradian growth in Prochlorococcus spp. Applied and Environmental Microbiology **64**:1066-1069.

Steinberg, D. K., C. A. Carlson, N. R. Bates, R. J. Johnson, A. F. Michaels, and A. H. Knap. 2001. Overview of the US JGOFS Bermuda Atlantic Time-series Study (BATS): a decade-scale look at ocean biology and biogeochemistry. Deep Sea Research Part II: Topical Studies in Oceanography **48**:1405-1447.

Vaulot, D. and D. Marie. 1999. Diel variability of photosynthetic picoplankton in the equatorial Pacific. Journal of Geophysical Research-Oceans **104**:3297-3310.

Vaulot, D., D. Marie, R. J. Olson, and S. W. Chisholm. 1995. Growth of Prochlorococcus, A Photosynthetic Prokaryote, In the Equatorial Pacific Ocean. Science **268**:1480-1482.

Waterbury, J. B., S. W. Watson, F. W. Valois and D. G. Franks. 1986. Biological and Ecological Characterization of the Marine Unicellular Cyanobacterium Synechococcus. Pages 71-120 *in* T. P. a. W. Li, editor. Photosynthetic Picoplankton. Can. J. Fish. Aquat. Sci. Bull.

Worden, A. Z. and B. J. Binder. 2003. Application of dilution experiments for measuring growth and mortality rates among Prochlorococcus and Synechococcus populations in oligotrophic environments. Aquatic Microbial Ecology **30**:159-174.

Zubkov, M. V., M. A. Sleigh, P. H. Burkill, and R. J. G. Leakey. 2000. Picoplankton community structure on the Atlantic Meridional Transect: a comparison between seasons. Progress in Oceanography **45**:369-386.

Table 1.1. Start dates and locations of time series used in this study.

Time Series	Cruise	Start Date	Location
Fall 1	EN360	9/21/2001	34.5154 ºN 72.0268 ºW
Fall 2	EN360	9/24/2001	34.4169 ºN 73.1523 ºW
Fall 3	EN375	8/28/2002	33.2264 ºN 64.8690 ºW
Fall 4	EN375	8/31/2002	33.2184 ºN 64.8852 ºW
Spring 1	OC374	3/6/2002	31.6599 ºN 64.2092 ºW
Spring 2	OC374	3/9/2002	33.2173 ºN 64.8854 ºW
Spring 3	EN351	4/4/2001	31.8273 ºN 64.1767 ºW

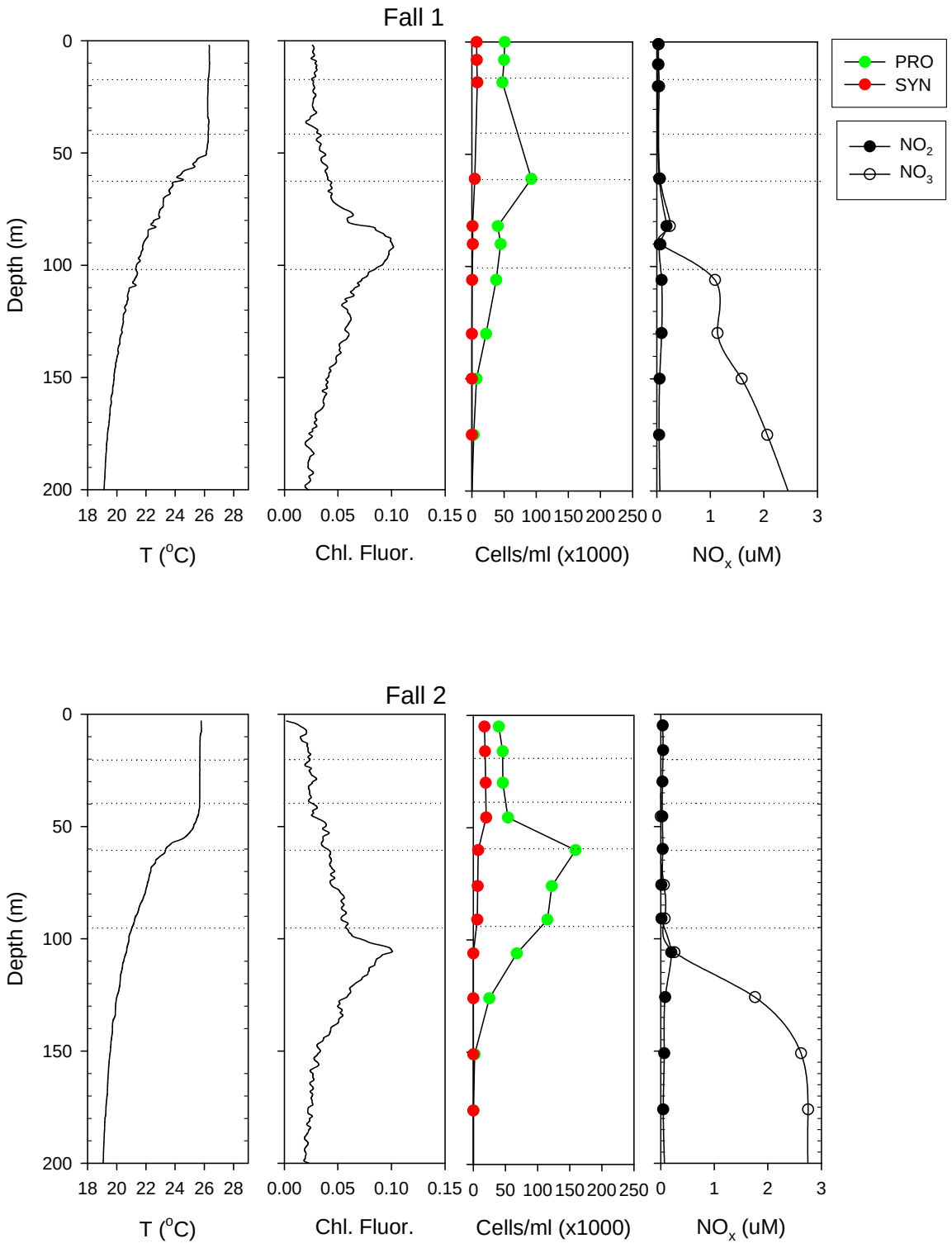

Fig. 2.1. Depth profiles of temperature, chlorophyll fluorescence, *Prochlorococcus* and *Synechococcus* cell concentrations, and nitrate and nitrate concentrations. Horizontal lines denote depths sampled for time-series experiments.

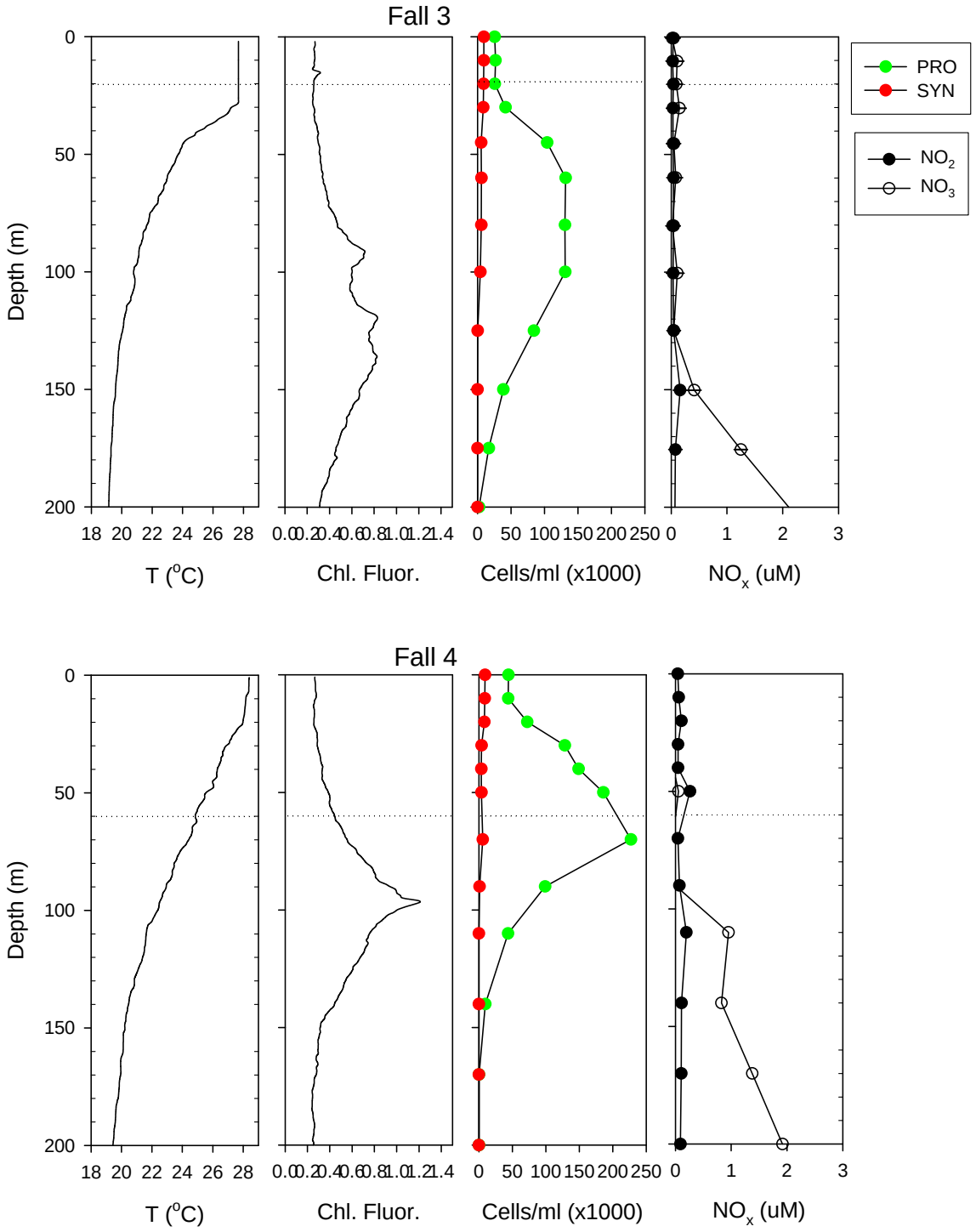
Fall 3
Depth (m)
0
50
100
150
200
18 20 22 24 26 28
T (°C)
0.0 0.2 0.4 0.6 0.8 1.0 1.2 1.4
Chl. Fluor.
0 50 100 150 200 250
Cells/ml (x1000)
0 1 2 3
NOx (uM)
PRO
SYN
NO2
NO3
Fall 4
Depth (m)
0
50
100
150
200
18 20 22 24 26 28
T (°C)
0.0 0.2 0.4 0.6 0.8 1.0 1.2 1.4
Chl. Fluor.
0 50 100 150 200 250
Cells/ml (x1000)
0 1 2 3
NOx (uM)

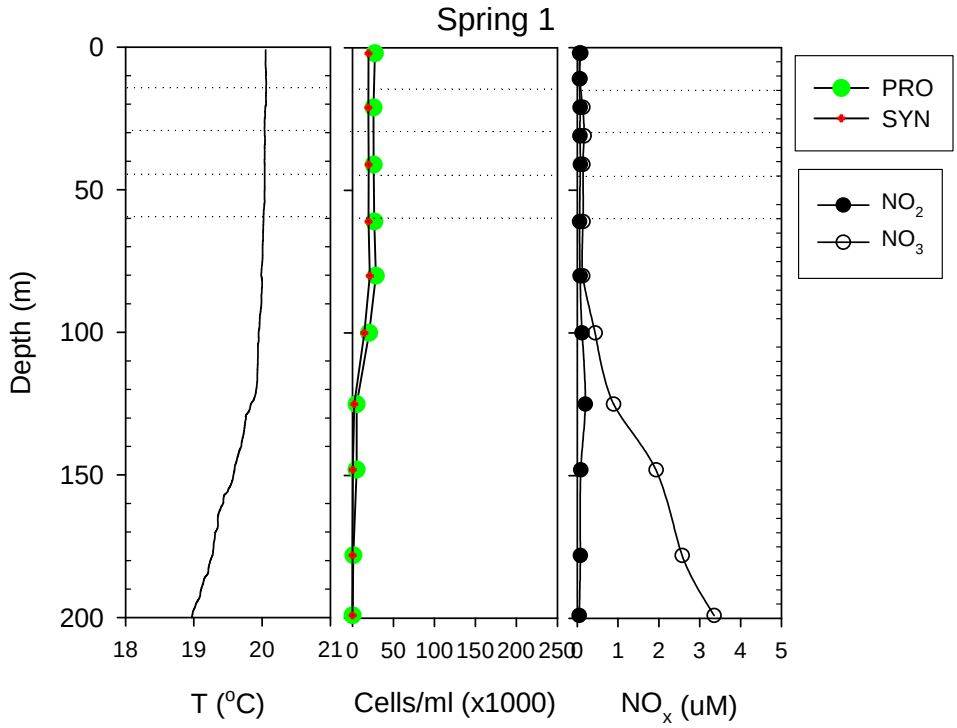
Spring 1
Depth (m)
0
50
100
150
200
18
19
20
21
T (°C)
0
50
100
150
200
250
Cells/ml (x1000)
0
1
2
3
4
5
NOx (uM)
PRO
SYN
NO2
NO3

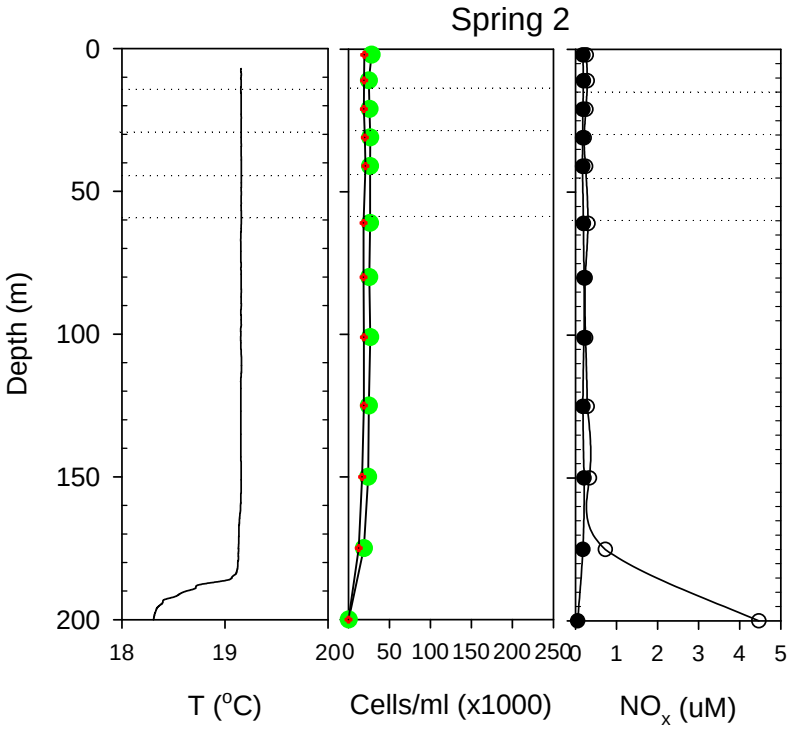
Spring 2
Depth (m)
0
50
100
150
200
18
19
200
T (°C)
50
100
150
200
250
Cells/ml (x1000)
0
1
2
3
4
5
NOx (uM)

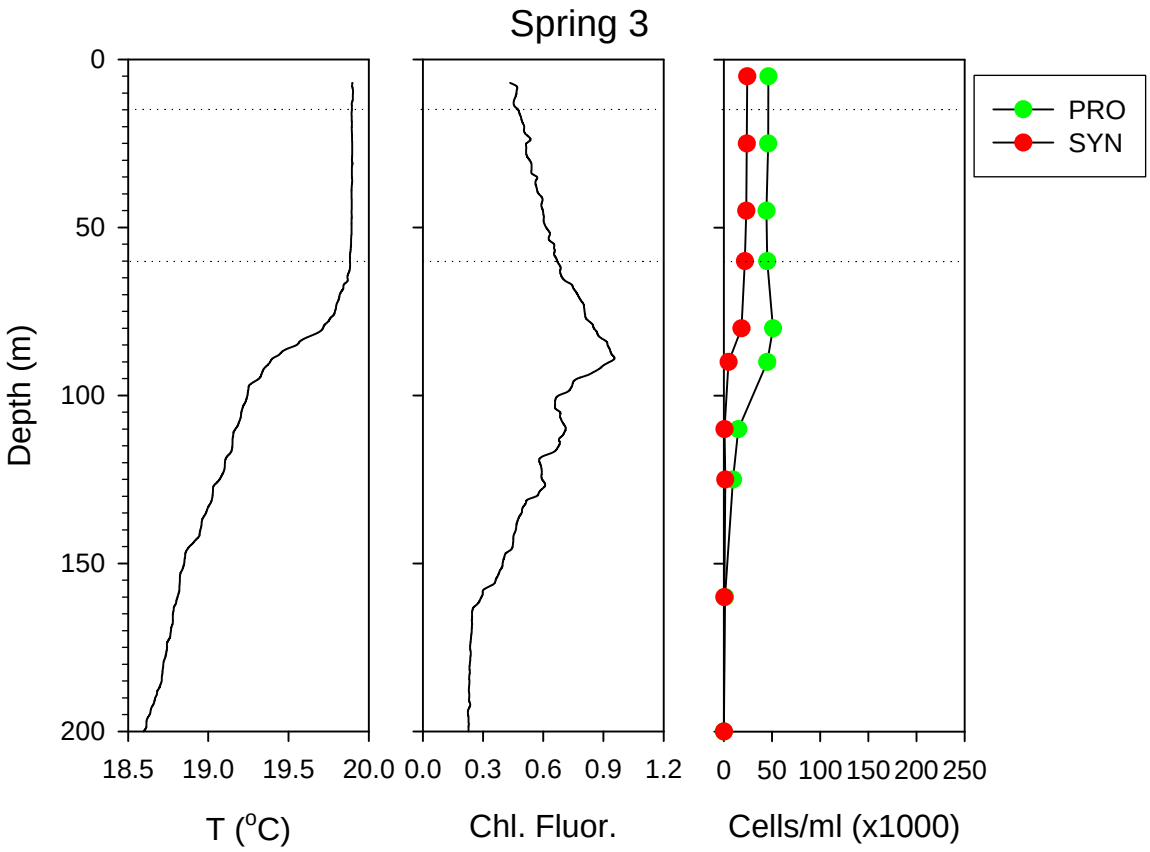
Spring 3
Depth (m)
0
50
100
150
200
18.5
19.0
19.5
20.0
T (°C)
0.0
0.3
0.6
0.9
1.2
Chl. Fluor.
0
50
100
150
200
250
Cells/ml (x1000)
PRO
SYN

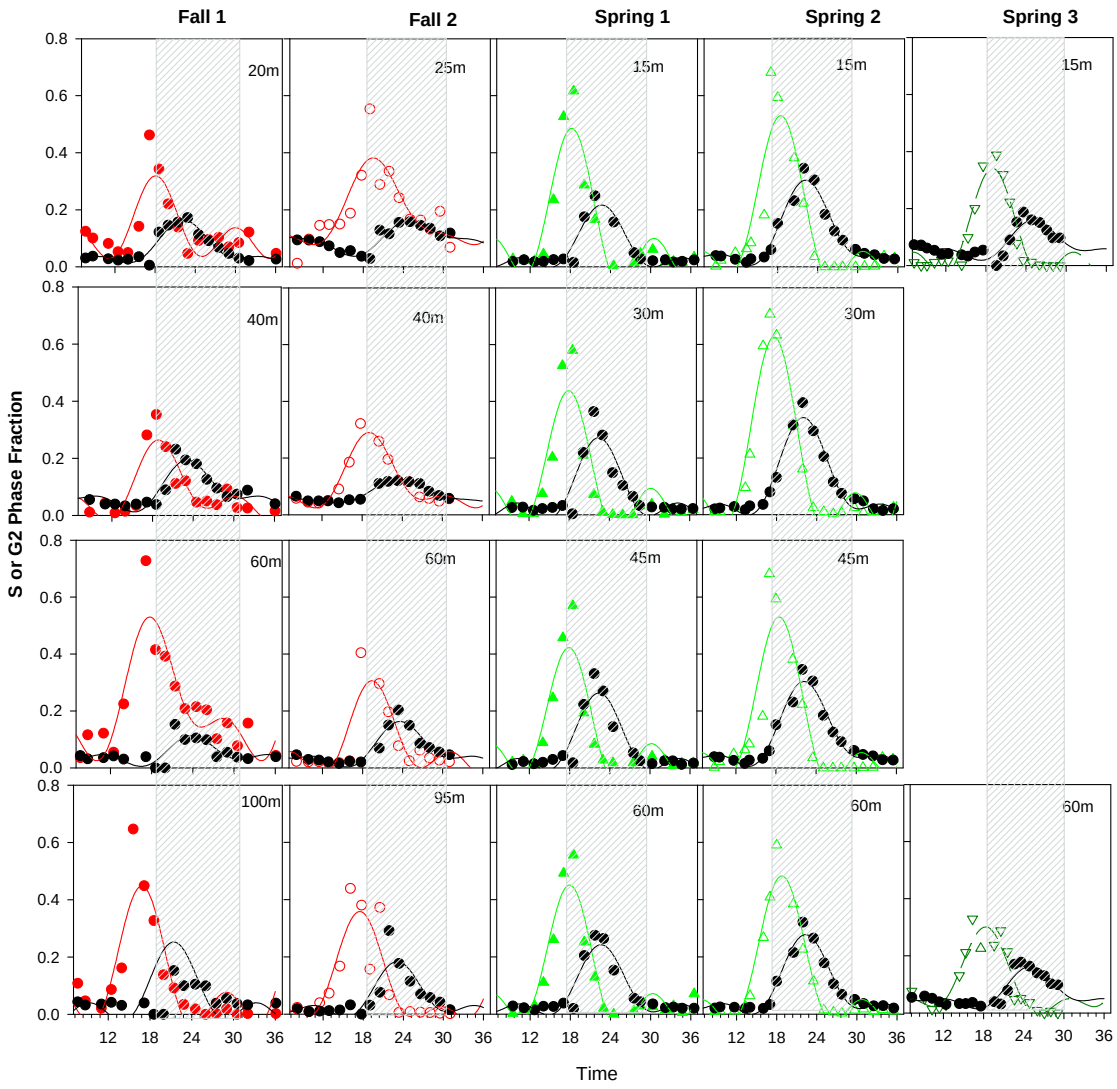

Fig. 2.2. Time series of percent of population in S (color) and G2 (black) cell cycle phases for the *in situ Prochlorococcus* populations as determined by flow cytometry. Hatched areas indicate local night. Solid lines are fitted periodic functions (see text), symbols are measured data points. Colors and symbols correspond to later figures. X-axis is local time.

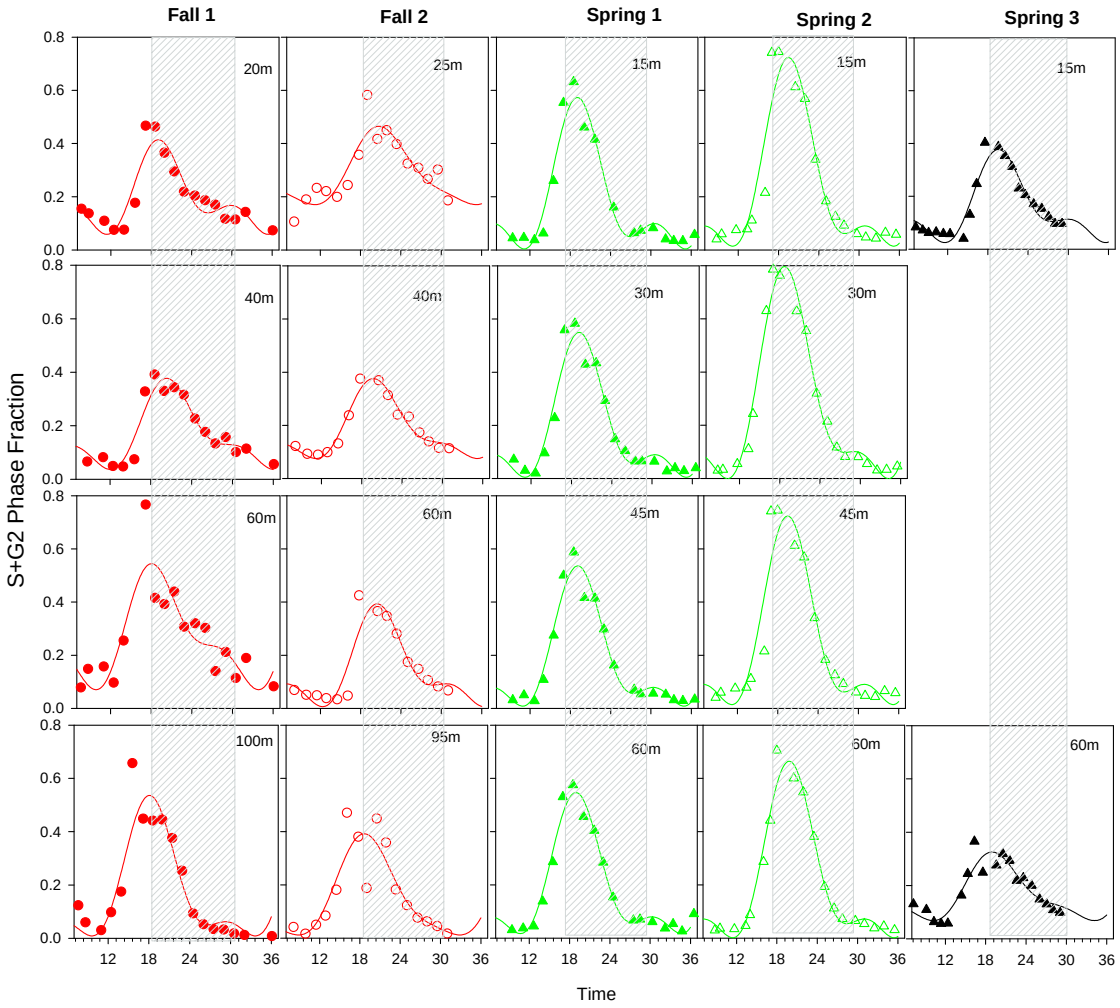

Fig. 2.3. Time series of the sums of the percent of population in S +G2 cell cycle phase for the *in situ Prochlorococcus* populations as determined by flow cytometry. Hatched areas indicate local night. Solid lines are fitted periodic functions (see text), symbols are measured data points. X-axis is local time.

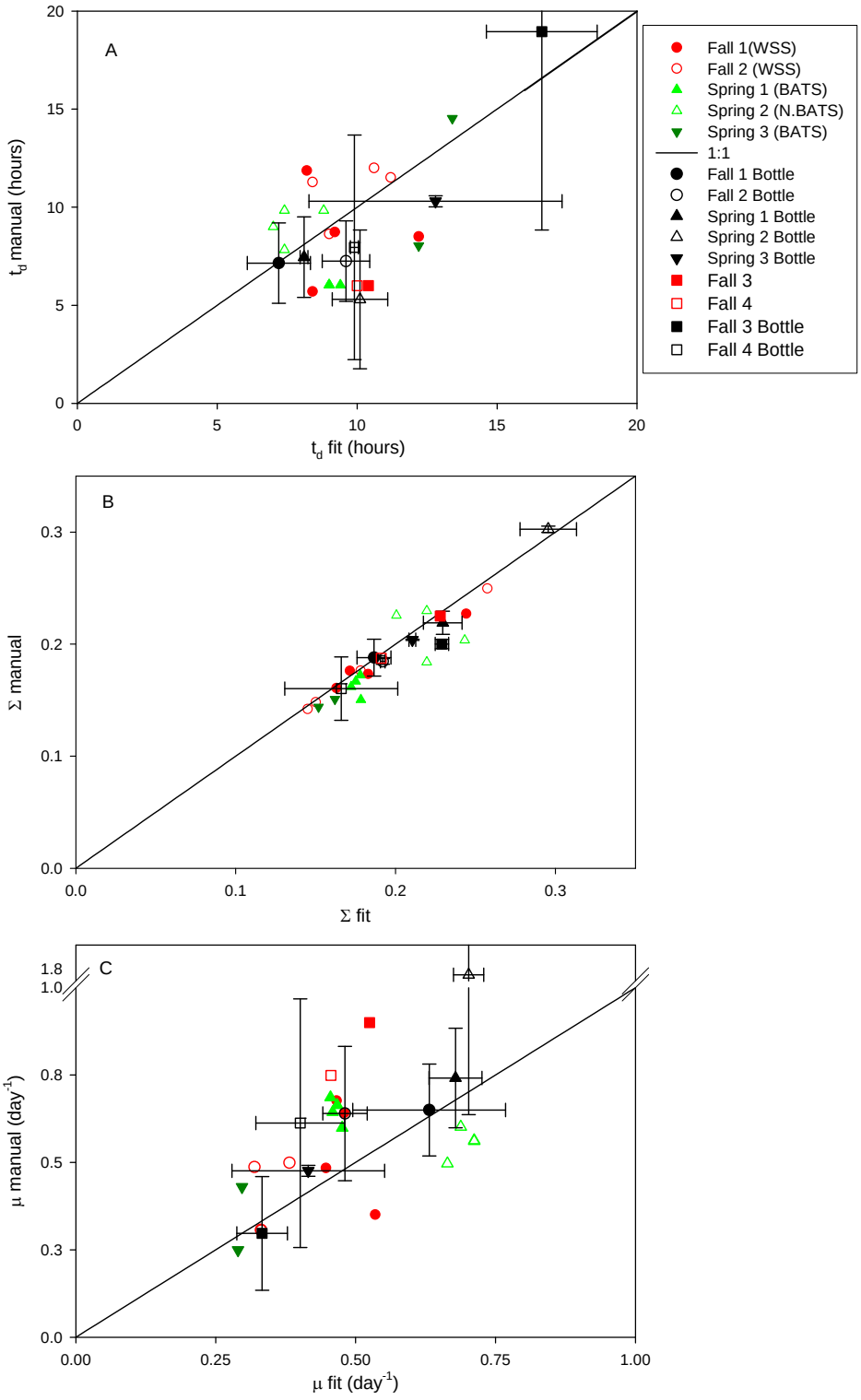

Fig. 2.4. Comparison of manual vs curve fit estimates of (a) t_d , (b) Σ and (c) μ. Bars on incubation data are ± 1 SD. Lines indicate 1:1 relationships.

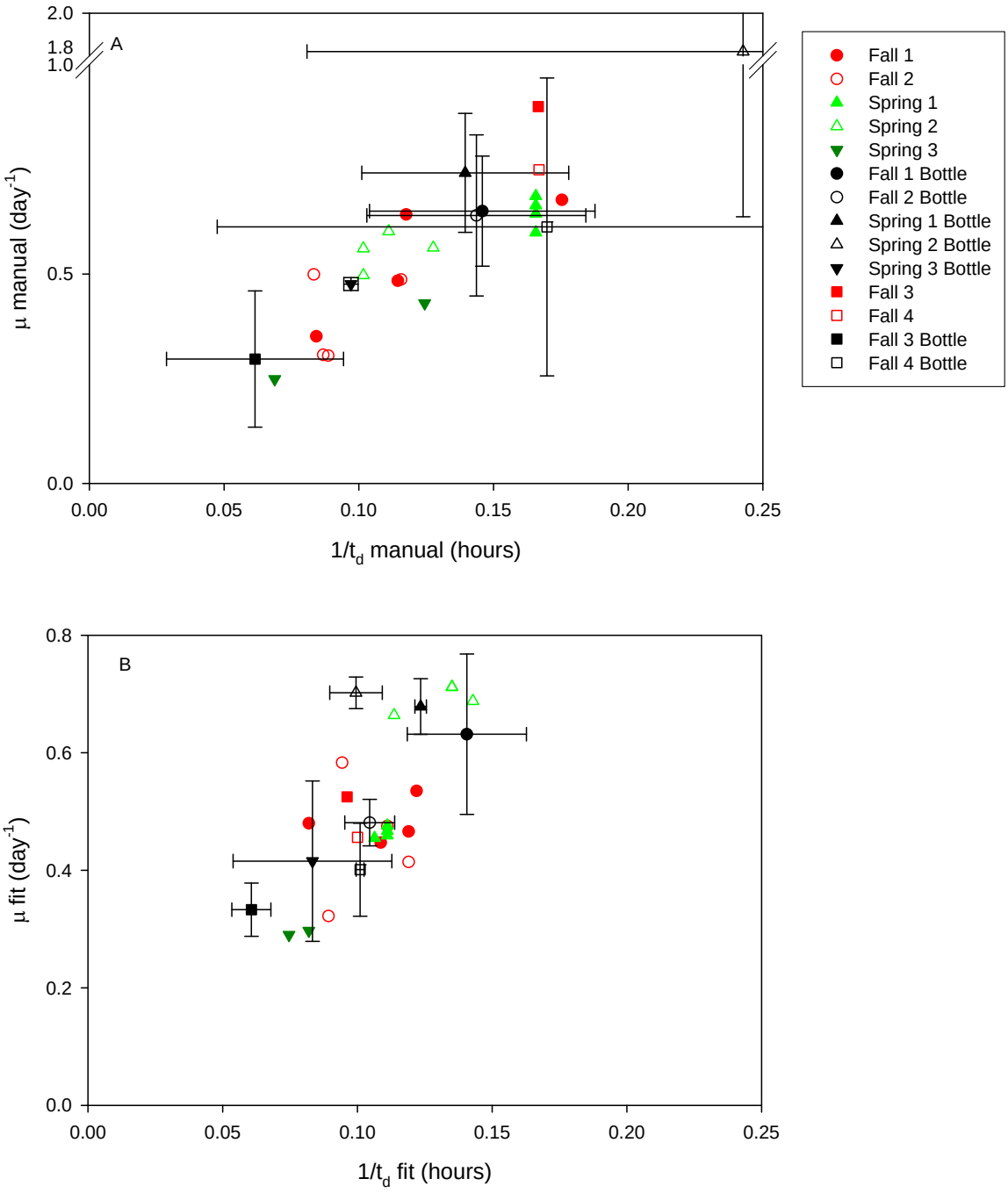

Fig. 2.5. Relationship between μ and 1/ t_d for manual (a) and curve fit analysis (b). Symbols as in Fig. 2.4.

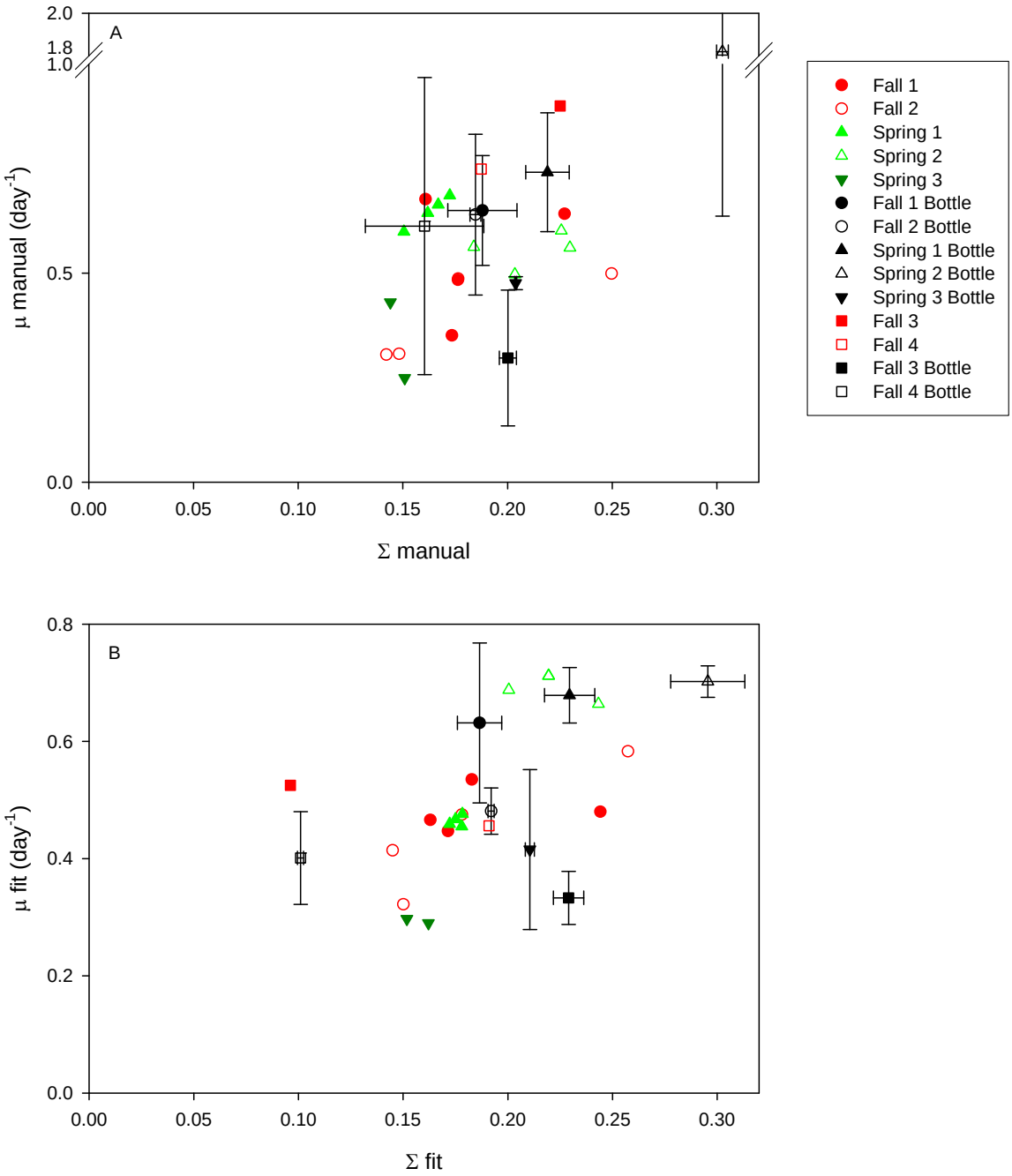

Fig. 2.6. Relationship between μ and Σ for manual (a) and curve fit analysis (b). Symbols as in Fig. 2.4.

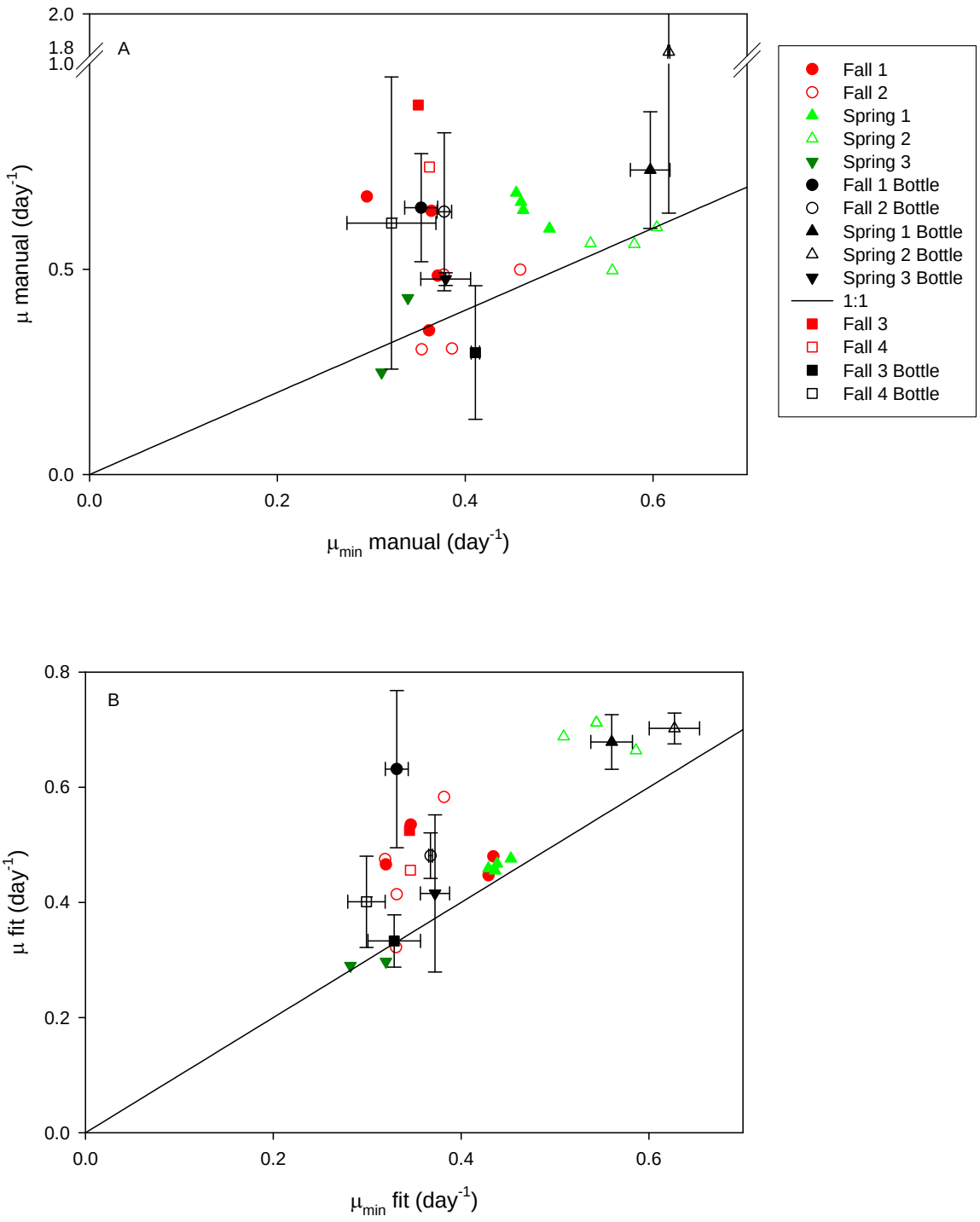

Fig. 2.7. Relationship between μ and minimum estimates of μ (see text) for manual (a) and curve fit analysis (b). Symbols as in Fig. 2.4.

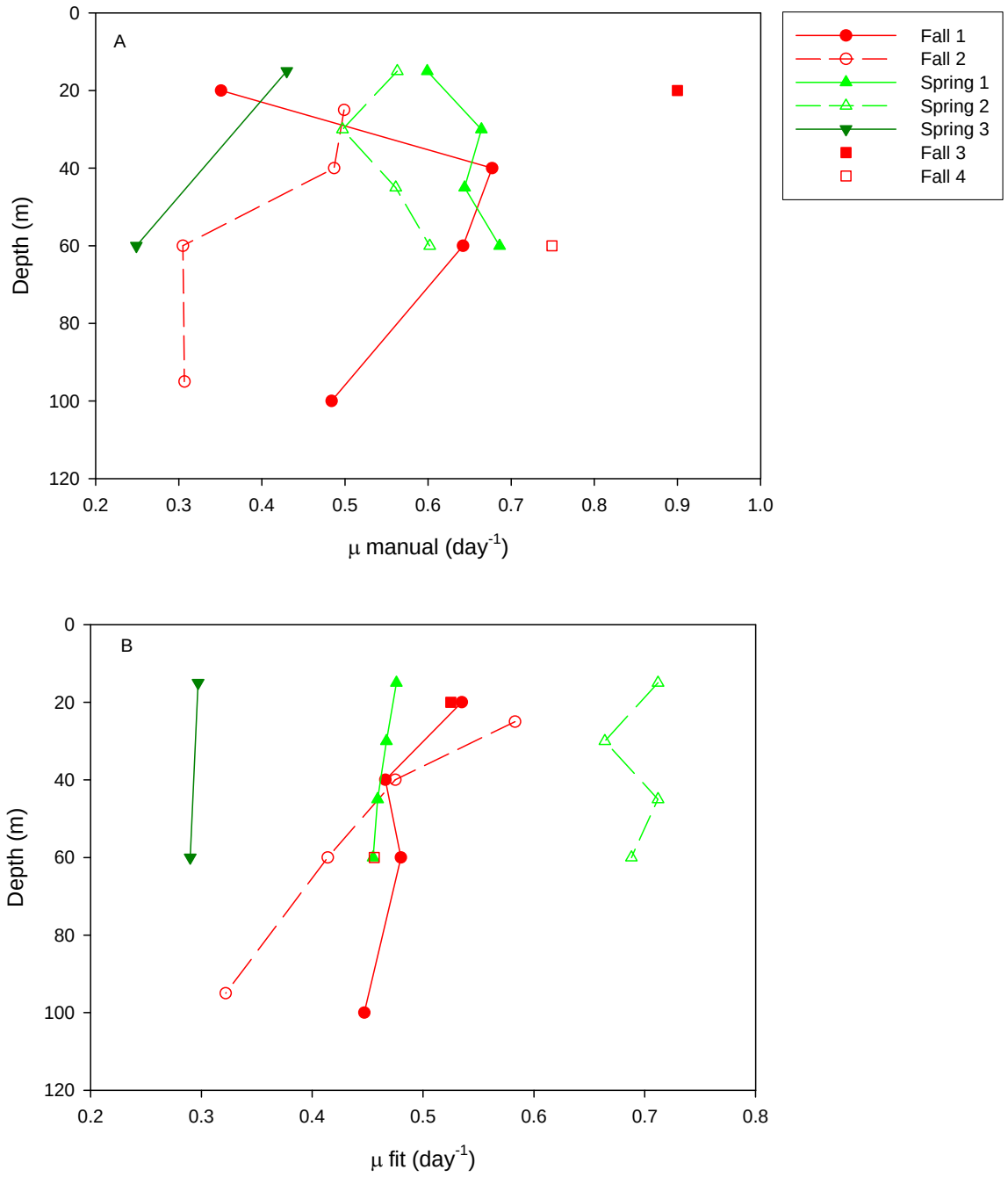

Fig. 2.8. Depth profiles of μ for manual (a) and curve-fit approach (b) for Fall (red) and Spring (green).

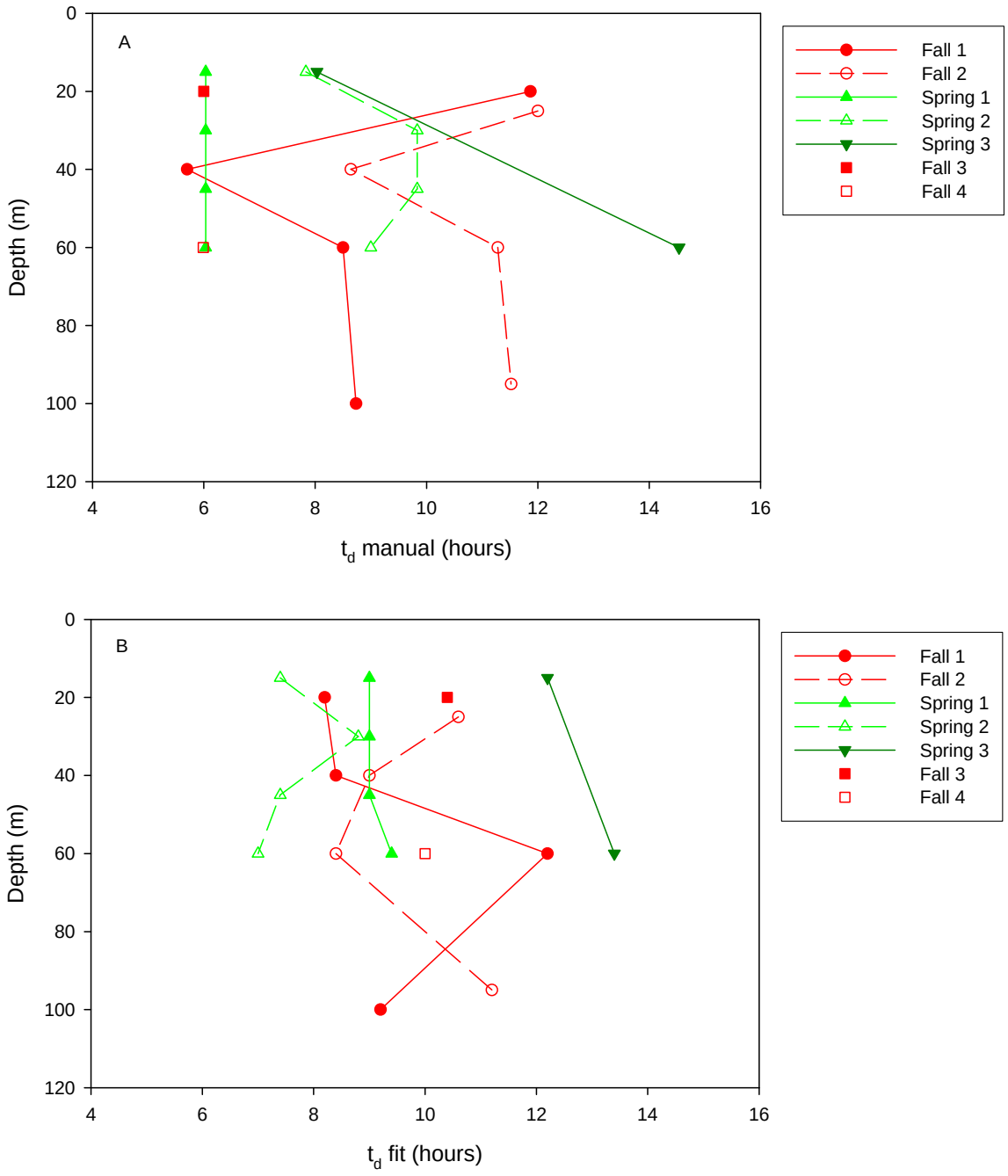

Fig. 2.9. Depth profiles of t_d for manual (a) and curve-fit analysis (b) for Fall (red) and Spring (green).

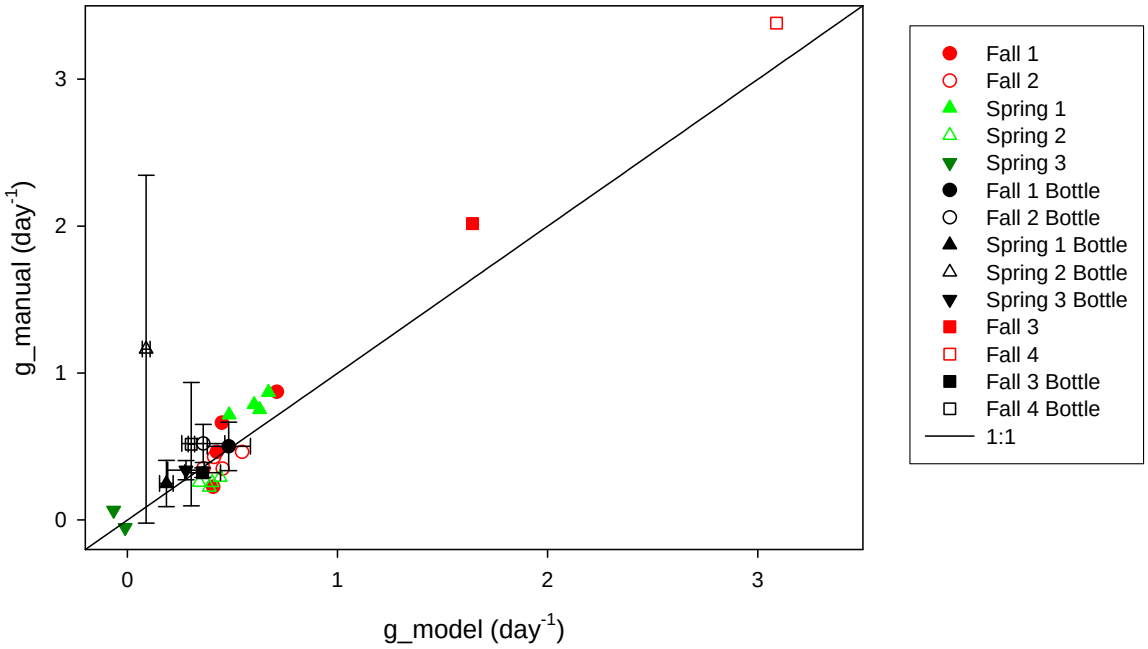

Fig. 2.10. Comparison of *Prochlorococcus* loss rates (g) (day^{-1}) calculated using manual vs. curve-fit estimates of μ (see text).

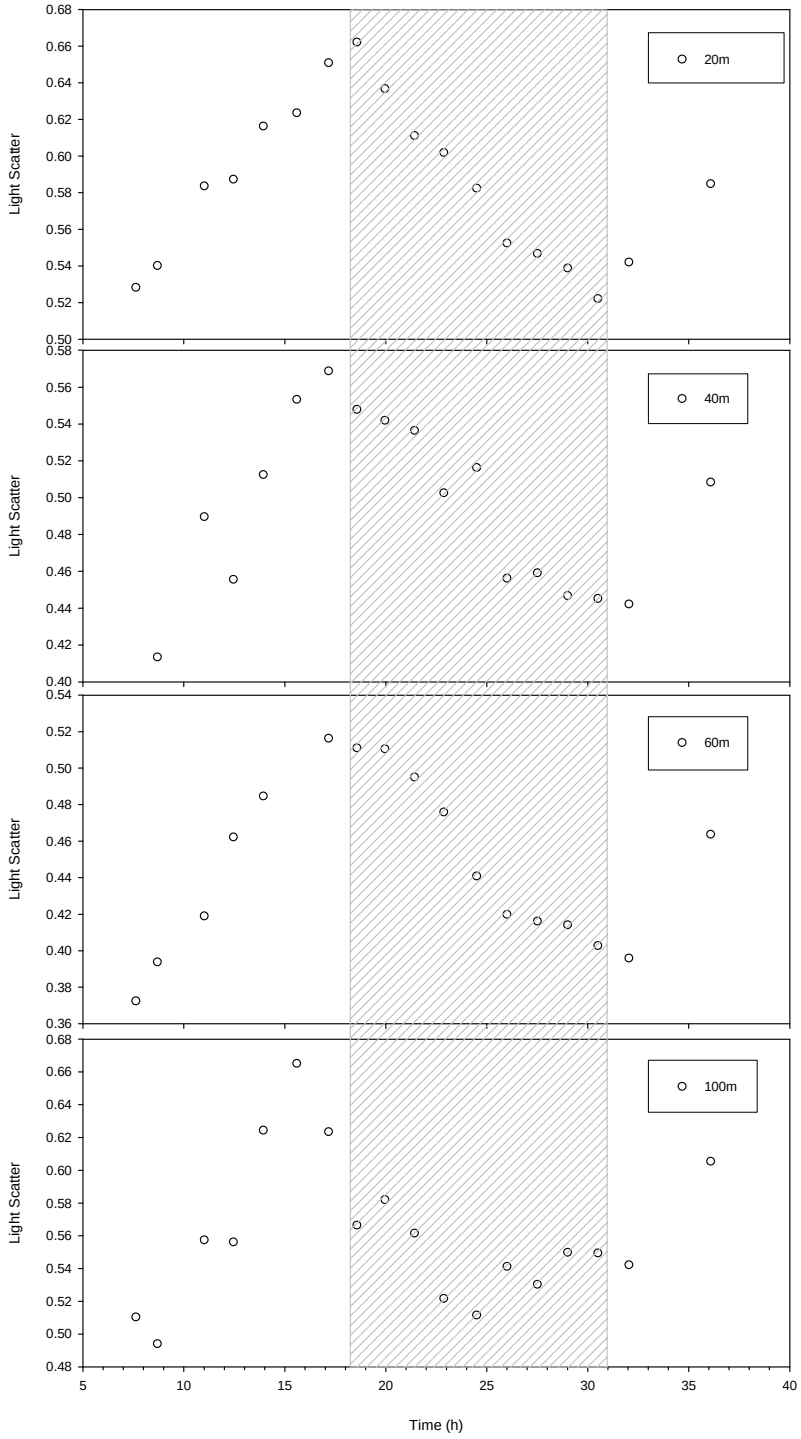

Fig. 2.11. Example of the diel pattern of forward angle light scatter (FALS) at 4 depths (Data are from the "Fall 1" station). Y-axes compressed and variable to show patterns more clearly. Hatched area denotes local night.

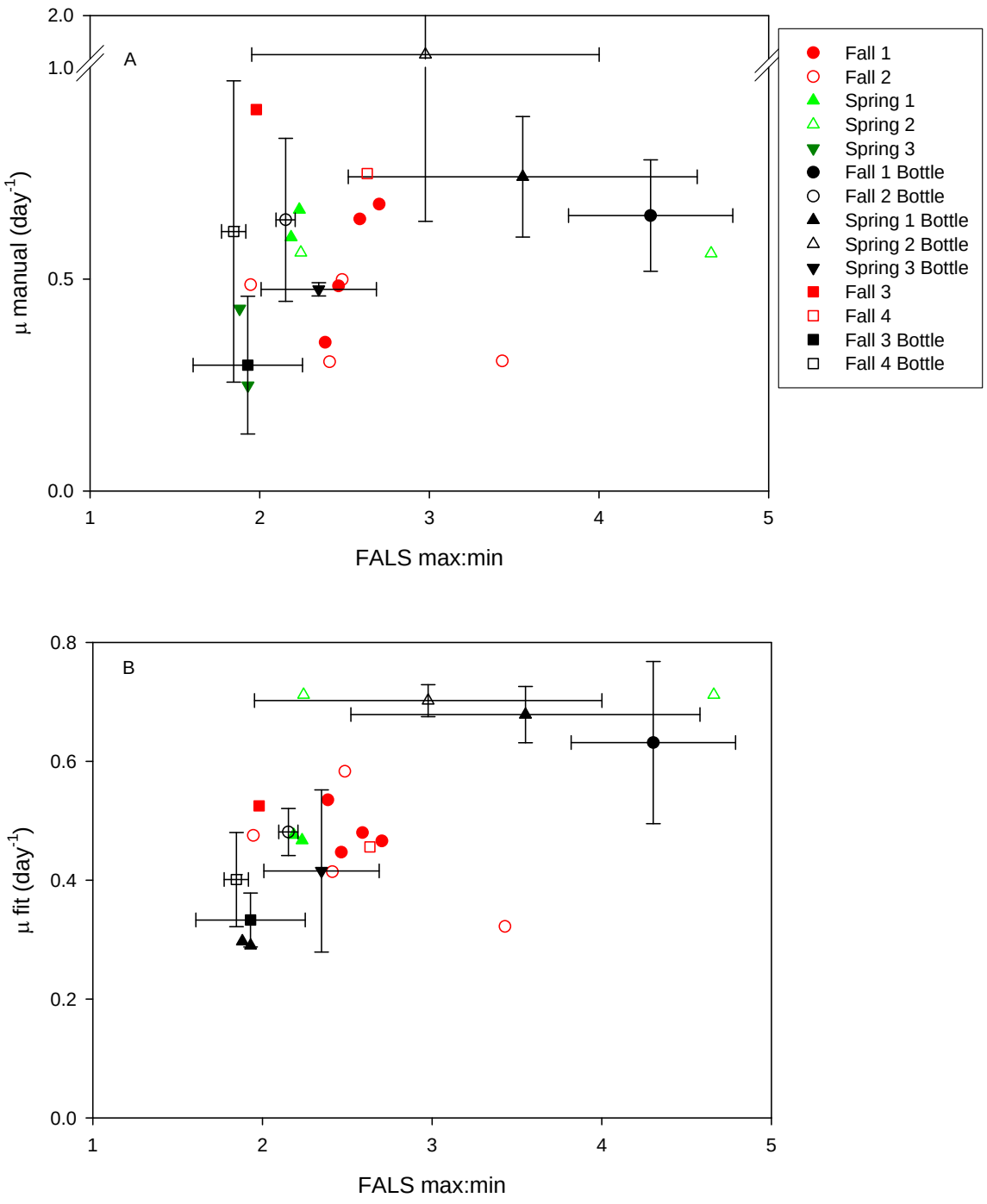

Fig 2.12. Relationship between the daily FALS ratio (max:min) and calculated μ values for manual (a) and curve-fit (b) analyses. Symbols as in Fig. 2.7.

CHAPTER 3

PROCHLOROCOCCUS GROWTH AND MORTALITY IN THE WESTERN SARGASSO SEA: DIEL OBSERVATIONS FROM COUPLED *IN SITU* AND INCUBATION STUDIES[1]

[1] Blythe, BJ and Binder, B. To be submitted to *Limnology and Oceanography*

Introduction

Bottle incubations are widely used for assessing activity in planktonic communities. These methods can be highly useful for teasing apart trophic interactions that are generally difficult to study *in situ*, as well as for assessing nutrient dynamics, primary production, and a host of other processes. Bottle incubations are not without complications however. "Bottle effects" such as exclusion of and/or physical damage to grazers, alteration of nutrient and turbulence regimes, and toxicity have been well documented (Venrick *et al.*, 1977, Roman M. & Rublee, 1980, Fitzwater *et al.*, 1982), and much effort has been put into their minimization.

Despite these complications, bottle incubations remain a useful tool for oceanographers. The controlled nature of incubations makes it possible to observe one aspect of the ecology of a system independently of other potential environmental or trophic interactions. In addition to measurements of primary production and nutrient uptake rates, bottle incubations have been used to investigate trophic interactions (Landry *et al.*, 1995, Verity *et al.*, 1996, Calbet *et al.*, 2001, Quevedo & Anadon, 2001, Stelfox-Widdicombe *et al.*, 2000), nutrient limitation (Mann & Chisholm, 2000, Moore, 2008, Van Mooy, 2008), trace metal toxicity (Mann *et al.*, 2002), light and temperature effects, and a host of other issues in the field.

At the heart of these studies is the assumption that the behavior of the system enclosed within bottles reasonably reflects the *in situ* system. This assumption is typically difficult to test directly, however. *Prochlorococcus* presents a unique opportunity to compare the behavior of picoplankton in bottle incubations relative to the natural system, as it is possible to use cell cycle analysis to estimate *Prochlorococcus* growth rates in both situations contemporaneously (McDuff & Chisholm, 1982, Carpenter & Chang, 1988). For this analysis, DNA frequency distributions of the population of interest are obtained periodically by flow-cytometry, and each

of these distributions are de-convoluted into G1, S, and G2 subpopulations. The time course of %S and %G2 are then used to calculate the growth rate of the population (see Methods for a detailed description).

While there have been many studies examining *Prochlorococcus* and *Synechococcus* dynamics *in situ* (see reviews in Jacquet *et al.*, 2001 and Binder & DuRand, 2002) and in incubation experiments (e.g. Llabres & Agusti, 2006, Timmermans *et al.*, 2005, Worden & Binder, 2003) there have been no studies to date that have directly compared the two approaches.

In the present study, estimates of growth and grazing for *Prochlorococcus* in concurrent on-deck, bottle incubations and in the water column are compared during four research cruises between 2001 and 2002 in the Western Sargasso. Observations of cell densities, cellular fluorescence and cell cycle parameters were made at each station at approximately 1 hour intervals for 24- 36 hours. Growth rates (μ) were calculated using the cell cycle approach described above, and are considered insensitive to grazing pressure. Estimates of mortality are based on these estimates of μ and the difference in observed cell number changes over the course of the time series.

Methods

Samples were collected at various locations and depths in the Sargasso Sea in the spring and fall of 2001, and the spring of 2002 (Table 3.1). Lagrangian time series observations lasting 24-36 h were conducted by sampling in the vicinity of a holey-sock type drogue deployed at the start of the experiment. Water was collected from a pre-determined depth every 60-90 min. using a Niskin bottle rosette. At the same time, samples were also collected from 1-liter on-deck incubations established at the start of each time series.

For the on-deck incubations, a 20 l acid-washed carboy was filled with water collected from a single depth using Teflon-lined Go-Flow bottles suspended on a non-metallic cable. Duplicate 1000 ml polycarbonate incubation bottles were filled with water from the carboy and placed randomly in a Plexiglas on-deck incubator. All sampling gear and incubation bottles were critically cleaned prior to use (Fitzwater et. al., 1992). Water transfers (from GoFlo to carboy, and carboy to incubation bottles) were made through Teflon and/or silicone tubing held beneath the water surface in the receiving vessel to minimize turbulence. Light levels in the incubators were matched as closely as possible to the *in situ* light level at the drogue depth using neutral density screening, and temperature was controlled by the ship's running seawater. Bottles were sampled at the same time-points as the water-column sampling, using custom sampling caps (Worden and Binder, 2003).

All samples were preserved with paraformaldehyde (0.2% final conc.) for 15 minutes in the dark before transfer to liquid nitrogen. Upon return to the laboratory, samples were stored at -85ºC until analysis.

Samples were analyzed using a modified dual-beam EPICS 753 flow-cytometer (Beckman Coulter, Fullerton CA, USA) as described in Binder *et al.* (1996). Samples were stained with Hoechst 33342 (see Ch. 2 for details), after which cellular red and orange fluorescence (from chlorophyll and phycobiliproteins, respectively), forward angle light scatter (FALS), and DNA content (as Hoechst fluorescence) were measured on a total of ~8000 *Prochlorococcus* and up to the same number of *Synechococcus* cells. In order to compare the incubation and *in situ* data, *in situ* FALS and red fluorescence were normalized to their respective initial values in the incubations. As noted previously, natural *Synechococcus*

populations stain poorly under these conditions (Vaulot *et al.*, 1996); cell cycle analysis was therefore confined to *Prochlorococcus* in this study.

Analysis of flow-cytometry data was performed using WinList software (Verity Software House, Topsham ME, USA); *Prochlorococcus* DNA frequency distributions were de-convoluted into G1, S, and G2 subpopulations with Modfit (Verity Software House, Topsham ME, USA), using a dual-trapezoid model for the S-phase.

A periodic function was fit to each time course of %S and %G2 (see Ch. 2), and these curves were used to calculate growth rate using the following equation:

$$\mu = \frac{1}{t_d} \sum_{t=0}^{24} (\Delta t_i \cdot \ln(1 + f_i)) \quad \text{(Eq. 3.1)}$$

where Δt_i is the sampling interval, f_i is the fraction of cells in S or G2 for that interval and t_d is the duration of S + G2 (McDuff & Chisholm, 1982). The latter term (t_d) was approximated as twice the interval between the S and G2 peaks, as per Carpenter and Chang (1988).

Prochlorococcus mortality rates were calculated using the estimates of μ and the observed change in cell number using the equation:

$$g = \mu - ln\left(\frac{N_f}{N_i}\right) \text{ (Eq. 3.2),}$$

where N_i and N_f are the *Prochlorococcus* concentrations based on averaged FCM counts from the first and last two time-points in a 24 h period, respectively.

Results

Cell Abundance

Our analysis of *Prochlorococcus* and *Synechococcus* concentrations were consistent with those observed in previous studies in the Sargasso Sea (Jacquet et al., 2001, Binder & DuRand, 2002). In fall when the water column is stratified, *Prochlorococcus* was found to be 1-2 orders of magnitude greater in abundance than *Synechococcus* (Fig. 3.1). In contrast, under well-mixed

spring conditions *Prochlorococcus* and *Synechococcus* were present in similar abundances (Fig. 3.2).

In general, replicate bottles were in very close agreement with regards to the time course of cell concentration (Figs. 3.1, 3.2), however these incubation time courses often varied systematically from the *in situ* time courses. Initial *Prochlorococcus* and *Synechococcus* concentrations in the bottles agreed with the *in situ* concentrations as would be expected, but over the course of the experiment, the incubation and *in situ* numbers often diverged. Cell abundances in the bottles were generally greater than or equal to the water-column, but the patterns of change varied.

In Fall-1 and -2, and in Spring-2 time-series, neither *Prochlorococcus* nor *Synechococcus* numbers changed significantly over the course of the experiment, both in the bottles and *in situ*. In Fall-3 and -4, *in situ Prochlorococcus* and *Synechococcus* numbers steadily declined during the daylight hours before stabilizing after dusk, while cell concentrations in the bottles were relatively constant during the day and constant or slightly increasing during the evening hours. In contrast, in Spring-1 and -3, the *in situ* cell abundances of *Prochlorococcus* and *Synechococcus* remained nearly constant throughout the course of the experiment, while the incubation populations show well replicated, significant increases in cell abundance after dusk (Figs. 3.1, 3.2).

We could find no specific environmental or experimental factor (e.g. temperature, light intensity, depth, ambient nutrient concentration, water column structure) that could explain the observed inter- and intra-seasonal differences in cell abundance trends in bottles versus *in situ*.

Cellular Characteristics

Trends in forward-angle light scatter of both *Prochlorococcus* and *Synechococcus* were generally well-replicated between bottles, although the magnitude of the diel variation differed in a few instances (Figs. 3.3, 3.4). FALS showed clear patterns of increase during daylight hours (reflecting cell growth), followed by a decrease at night (reflecting cell division).

The patterns observed in the bottles generally reflected the *in situ* patterns (Figs. 3.3, 3.4). The single significant exception was "Fall 1", in which *in situ* FALS peaked earlier and at lower FALS values than did the bottle populations; the reason for this discrepancy is not known.

Prochlorococcus and *Synechococcus* red (chlorophyll) fluorescence in the bottles increased during day-light hours and decreased at night, in a manner similar to FALS (Figs 3.5, 3.6). In this case, however, the diel pattern appeared to be overlaid on a general increase (in the spring) or decrease (in the fall) in fluorescence over the course of the experiment, suggesting photo-acclimation in the bottles, and leading to a divergence between the incubation and *in situ* trends (Figs. 3.5, 3.6). Replicate bottles for the incubations were in good agreement, as was seen for the FALS data.

Prochlorococcus Growth

In general, *Prochlorococcus* cell cycle patterns were well-replicated in our bottles, and for the most part these patterns reflected the *in situ* cell cycle dynamics observed at the corresponding depths (Figs. 3.7, 3.8). *Prochlorococcus* populations showed a peak in S-phase cells that corresponded very closely to local dusk. The peak in G2 cells occurred 4-5 hours after the S-peak; by dawn the *Prochlorococcus* populations were comprised almost exclusively of G1 cells again. There was no apparent difference in these patterns between spring and fall.

Calculated growth rates for both incubations and water-column reached a maximum near 1 doubling per day (range for $\mu_{in\ situ}$=0.46 - 0.66, and $\mu_{incubation}$=0.33 – 0.70). There was no systematic difference observed between bottle and *in situ* growth rate estimates. The ratio of the two estimates (bottle: *in situ*) averaged 1.08, and ranged from 0.64-1.54. Nevertheless, the two estimates were not significantly correlated (Fig. 3.9A).

Data from "Spring 2" was omitted from the above analysis as the populations in both bottles in this experiment apparently became arrested in the G2 phase, making growth rate estimates impossible. The cause of this behavior in the bottles is unknown; no such cell cycle arrest was observed *in situ*.

***Prochlorococcus* Mortality**

Prochlorococcus mortality rates were well-replicated between bottles (Fig. 3.9b). In contrast to our growth rate estimates, however, *in situ* mortality rates were systematically higher than the mortality rates in corresponding bottles (by a factor of ~2 to ~10). There was no relationship between the calculated incubation and *in situ* mortality rates, but in all cases mortality was greater *in situ* than in the bottles.

Discussion

Taken together, our data strongly suggest that *Prochlorococcus* and *Synechococcus* physiology (as reflected in growth rate) are reasonably unperturbed in bottle incubations of the sort used here. For both these groups, diel patterns in FALS (driven by cell growth and division) were very similar in bottles and *in situ* populations. Cell cycle patterns (in the case of *Prochlorococcus*) in bottle and natural populations were also generally the same: both the timing of the peaks and the magnitude of changes in S and G2 phase fractions were nearly identical in bottles versus *in situ* (with the exception of one Spring station, as discussed above,

and a delay in the G2 peak in Fall-3 (Fig. 3.7). Cell cycle-based growth rate estimates for bottle and *in situ Prochlorococcus* populations were therefore not significantly different (although they were also uncorrelated) (Fig. 3.9).

Patterns in red (chlorophyll) fluorescence were well replicated between replicate bottles in most cases, and generally matched the *in situ* patterns observed. There was however some evidence for photo-acclimation in some of the bottle experiments, despite our best efforts to match incubation light levels with *in situ* levels. Fall-1, -3, and -4 all appear to have an exaggerated increase in red fluorescence during the day when compared to the *in situ* data (Fig. 3.5). This would suggest that the cells in our bottles were experiencing a lower light intensity than the *in situ* populations and correspondingly increased their cellular chlorophyll content. The Spring-2 and -3 bottle data sets showed a well-replicated decrease in cellular chlorophyll content when compared to the *in situ* time series (Fig. 3.6). In contrast to the fall data, this would suggest that in our spring incubations, populations were acclimating to a higher level of light than that experienced *in situ*. Despite these apparent shifts in physiology, growth rates appeared to be largely unaffected over the 24 h time scale of our incubations, as discussed above.

Given the apparently unaltered growth rates of *Prochlorococcus* and *Synechococcus* populations in our incubation bottles, the dramatically different diel patterns in cell abundance between the bottles and water-column (Figs. 3.1, 3.2) suggest that grazing mortality was very different (lower) in many of the bottle treatments. The reasons for this apparent reduction in grazing mortality are not clear at present. Total protist numbers did not change appreciably over the course of our incubations (C. Burbage, pers.comm.), suggesting that reduced grazer activity (rather than grazer abundance) was responsible for this divergence. There are a number of potential factors that may have induced changes in grazer activity, including temperature shifts,

physical damage to grazer cells, and bottle toxicity (Venrick *et al.*, 1977, Roman M. & Rublee, 1980, Fitzwater *et al.*, 1982).

There was generally no significant difference between the incubation and *in situ* temperatures, as most experiments were carried out within the mixed layer. The exceptions were Fall-1 and Fall-4, where the incubations were ~1.5 and ~3ºC warmer than the *in situ* water, respectively. A strong shift in phytoplankton dynamics was observed in Fall-4, but not Fall-1, suggesting again that temperature was not the driving force for the reduced grazing pressure observed in our study. If there was a toxicity effect in our bottles, it was a consistent one, as replicate bottles behaved similarly, and reduced grazing pressure was observed in bottles from all cruises.

The apparently lowered mortality of *Prochlorococcus* and *Synechococcus* in our bottles allows for an interesting comparison of diel mortality patterns between seasons. In some cases (e.g. Fall-3 & 4), the data are consistent with fairly even grazing pressure over the entire diel cycle (Fig. 3.1). *In situ Prochlorococcus* and *Synechococcus* numbers decline steadily in the first half of the day (when cell cycle and FALS data indicate minimal cell division is occurring), and then stabilize when the cyanobacterial cells divide in the late afternoon and evening. Consistent with this scenario, our incubation data shows constant cell numbers during the early portion of the day (in the face of presumably reduced grazing activity, as discussed above), followed (in some cases) by a moderate increase in cell numbers as the cyanobacterial populations divide in the evening. These contrasting patterns (*in situ* vs. bottle) are consistent with grazing pressure that is relatively unchanged throughout the day. Complicating this interpretation, however, is the fact that non-steady state conditions seem to prevail *in situ* (at least over the 24 h experimental period) in the Fall-3 and -4 series, as cell numbers decrease

significantly during the first part of the day, but do not return to initial levels after cell division during the evening. It is possible that the *in situ* populations may reflect advection of different water into the vicinity of our drogue. However neither salinity nor temperature changed appreciably over the course of the experiment. Likewise, cell parameters show no changes that might be indicative of a different population.

Our spring results appear to show a different diel mortality pattern. In this case, cell numbers in the incubations and *in situ* are constant for the first half of the day, suggesting that grazing activity is low in both the bottles and *in situ* at this time. As cells are added through division in the late afternoon and evening, the patterns begin to diverge significantly in some cases. *In situ*, the cell numbers remain fairly constant despite the input of newly divided cells, suggesting increased grazing mortality during that portion of the day. At the same time, bottle populations show a moderate to significant increase in cell counts, reflecting cell division in the apparent absence of strong grazing. This pattern of increased grazing mortality during the portion of the day when cells are actively dividing has been hypothesized previously for *Prochlorococcus* based on similar sorts of observations, but has yet to be tested quantitatively (Liu *et al.*, 1997, Worden & Binder, 2003).

Based on our data, it appears that there may be seasonal differences in the diel pattern of grazing pressure faced by *Prochlorococcus* and *Synechococcus* in the western Sargasso Sea. These changes may be driven by changes in the grazer community composition or behavior from season to season as the water column changes from stratified to well-mixed conditions. Protistan counts in our experiments varied from 10^2 to 10^3 ml^{-1} in both spring and fall data sets (C. Burbage, pers.comm.), suggesting that changes in grazer density between seasons are not likely the source of the variability in mortality we observed. *Prochlorococcus* was generally found at

concentrations on the order of 10^4-10^5 cells ml^{-1} in spring and fall, while *Synechococcus* cell densities increased from ~10^3-10^4 cells ml^{-1} in the fall to ~10^4-10^5 cells ml^{-1} in the spring. Differences in cell density do not appear to be driving the changes in mortality patterns, as both groups of cyanobacteria exhibit similar diel patterns of abundance within seasons.

Taking all the data together, our comparison of bottle and *in situ* observations suggests that the implicit assumption of relatively unaltered system behavior in bottle incubations does not always hold true. While it is encouraging to find the physiology of *Prochlorococcus* and *Synechococcus* to be unperturbed, grazing mortality among these populations was obviously strongly altered in the bottles (Figs. 3.1, 3.2).

Based on these results, it appears that short-term (~24 h) bottle incubations are a reasonable way to examine the physiological traits of *in situ Prochlorococcus* and *Synechococcus*. There is, however, a real concern that must be addressed when using incubation studies to investigate the ecology of marine systems. As shown here and elsewhere (Venrick et al., 1977, Roman M. & Rublee, 1980), there can be significant alterations to the behavior or physiology of a particular group or groups in incubations that are not exhibited by other members of the planktonic assemblage. In this case, it becomes imperative to have at least some knowledge of the state of all groups that may affect or be affected by the group of interest. In our study in particular, knowing that cyanobacterial physiology was unaltered, and that grazer abundance was relatively constant, we can say with some certainty that grazing activity must have been reduced, presumably due to handling issues.

Care must obviously be taken when interpreting the results of incubation studies. Without a direct comparison to the *in situ* dynamics of the planktonic community as a whole,

observations based on bottle incubations may miss or incorrectly characterize important ecological phenomena and yet still show good replication and consistency between experiments.

References

Binder, B. J., Chisholm, S. W., Olson, R. J., Frankel, S. L. & Worden, A. Z. 1996. Dynamics of picophytoplankton, ultraphytoplankton and bacteria in the central equatorial Pacific. *Deep-Sea Res. Part II-Top. Stud. Oceanogr.* **43**:907-31.

Binder, B. J. & DuRand, M. D. 2002. Diel cycles in surface waters of the equatorial Pacific. *Deep-Sea Res. Part II-Top. Stud. Oceanogr.* **49**:2601-17.

Burbage, C. D. & Binder, B. J. 2007. Relationship between cell cycle and light-limited growth rate in oceanic *Prochlorococcus* (MIT9312) and *Synechococcus*(WH8103) (Cyanobacteria). *J. Phycol.* **43**:266-74.

Calbet, A., Landry, M. R. & Nunnery, S. 2001. Bacteria-flagellate interactions in the microbial food web of the oligotrophic subtropical North Pacific. *Aquat. Microb. Ecol.* **23**:283-92.

Carpenter, E. J. & Chang, J. 1988. Species-Specific Phytoplankton Growth-Rates via Diel DNA-Synthesis Cycles. 1. Concept of the Method. *Mar. Ecol.-Prog. Ser.* **43**:105-11.

Fitzwater, S. E., Knauer, G. A. & Martin, J. H. 1982. Metal Contamination and its Effect on Primary Production Measurements. *Limnol. Oceanogr.* **27**:544-51.

Jacquet, S., Partensky, F., Lennon, J. F. & Vaulot, D. 2001. Diel patterns of growth and division in marine picoplankton in culture. *J. Phycol.* **37**:357-69.

Landry, M. R., Constantinou, J. & Kirshtein, J. 1995. Microzooplankton Grazing in the Central Equatorial Pacific During February and August, 1992. *Deep-Sea Res. Part II-Top. Stud. Oceanogr.* **42**:657-71.

Liu, H. B., Nolla, H. A. & Campbell, L. 1997. Prochlorococcus growth rate and contribution to primary production in the equatorial and subtropical North Pacific Ocean. *Aquat. Microb. Ecol.* **12**:39-47.

Llabres, M. & Agusti, S. 2006. Picophytoplankton cell death induced by UV radiation: Evidence for oceanic Atlantic communities. *Limnol. Oceanogr.* **51**:21-29.

Mann, E. L., Ahlgren, N., Moffett, J. W. & Chisholm, S. W. 2002. Copper toxicity and cyanobacteria ecology in the Sargasso Sea. *Limnol. Oceanogr.* **47**:976-88.

Mann, E. L. & Chisholm, S. W. 2000. Iron limits the cell division rate of Prochlorococcus in the eastern equatorial Pacific. *Limnol. Oceanogr.* **45**:1067-76.

McDuff, R. E. & Chisholm, S. W. 1982. The Calculation of Insitu Growth-Rates of Phytoplankton Populations from Fractions of Cells Undergoing Mitosis - a Clarification. *Limnol. Oceanogr.* **27**:783-88.

Moore, C. M., Matthew M. Mills, Rebecca Langlois, Angela Milne, Eric P. Achterberg, Julie La Roche, and Richard J. Geider 2008. Relative influence of nitrogen and phosphorous availability on phytoplankton physiology and productivity in the oligotrophic sub-tropical North Atlantic Ocean *Limnol. Oceanogr.* **53**:291-305.

Quevedo, M. & Anadon, R. 2001. Protist control of phytoplankton growth in the subtropical north-east Atlantic. *Mar. Ecol.-Prog. Ser.* **221**:29-38.

Roman M. & Rublee, P. 1980. Containment effects in copepod grazing experiments: A plea to end the black box approach. *Limnol. Oceanogr.* **25**:982-90.

Stelfox-Widdicombe, C. E., Edwards, E. S., Burkill, P. H. & Sleigh, M. A. 2000. Microzooplankton grazing activity in the temperate and sub-tropical NE Atlantic: summer 1996. *Mar. Ecol.-Prog. Ser.* **208**:1-12.

Timmermans, K. R., van der Wagt, B., Veldhuis, M. J. W., Maatman, A. & de Baar, H. J. W. 2005. Physiological responses of three species of marine pico-phytoplankton to ammonium, phosphate, iron and light limitation. *Journal of Sea Research* **53**:109-20.

Van Mooy, B. A. S., and Allan H. Devol 2008. Assessing nutrient limitation of Prochlorococcus in the North Pacific subtropical gyre by using an RNA capture method. *Limnol. Oceanogr.* **53**:78-88.

Vaulot, D., LeBot, N., Marie, D. & Fukai, E. 1996. Effect of phosphorus on the Synechococcus cell cycle in surface Mediterranean waters during summer. *Appl. Environ. Microbiol.* **62**:2527-33.

Venrick, E. L., Beers, J. R. & Heinbokel, J. F. 1977. Possible consequences of containing microplankton for physiological rate measurements. *Journal of Experimental Marine Biology and Ecology* **26**:55-76.

Verity, P. G., Stoecker, D. K., Sieracki, M. E. & Nelson, J. R. 1996. Microzooplankton grazing of primary production at 140 degrees W in the equatorial Pacific. *Deep-Sea Res. Part II-Top. Stud. Oceanogr.* **43**:1227-55.

Worden, A. Z. & Binder, B. J. 2003. Application of dilution experiments for measuring growth and mortality rates among Prochlorococcus and Synechococcus populations in oligotrophic environments. *Aquat. Microb. Ecol.* **30**:159-74.

Table 3.1. Time series dates and locations used in this study.

Time Series	Cruise	Date	Location	Depth
Fall 1	EN360	9/21/2001	34.5154 ºN 72.0268 ºW	60 m
Fall 2	EN360	9/24/2001	34.4169 ºN 73.1523 ºW	25 m
Fall 3	EN375	8/28/2002	33.2264 ºN 64.8690 ºW	20 m
Fall 4	EN375	8/31/2002	33.2184 ºN 64.8852 ºW	60 m
Spring 1	EN351	4/4/2001	31.8273 ºN 64.1767 ºW	15 m
Spring 2	OC374	3/6/2002	31.6599 ºN 64.2092 ºW	30 m
Spring 3	OC374	3/9/2002	33.2173 ºN 64.8854 ºW	30 m

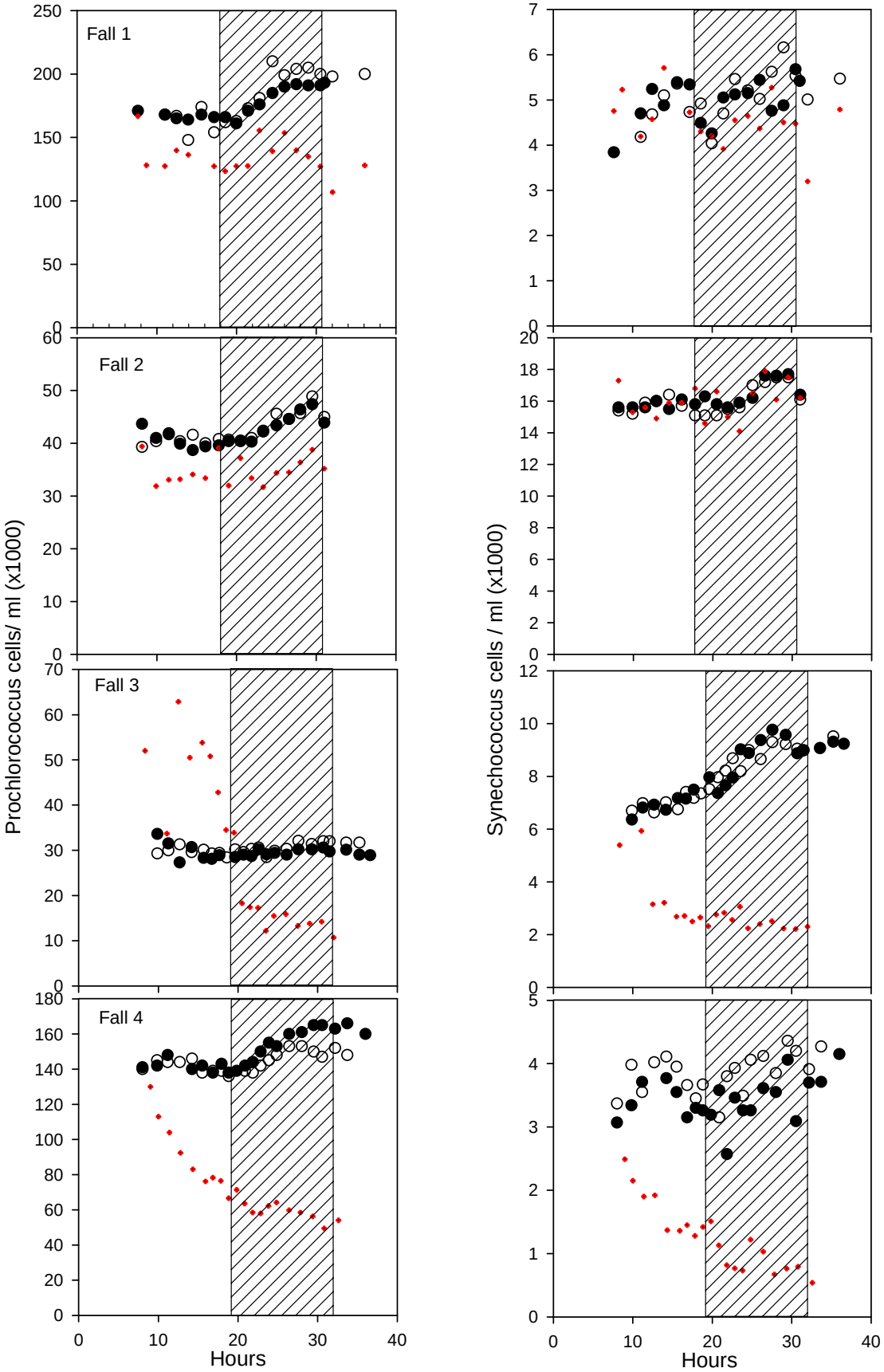

Fig. 3.1. Time series of Prochlorococcus and Synechococcus cell densities at fall stations in replicate bottles (filled and empty circles) and in situ (red dots). Hatched areas denote local night. X-axis is hours from midnight on day 1 of experiment.

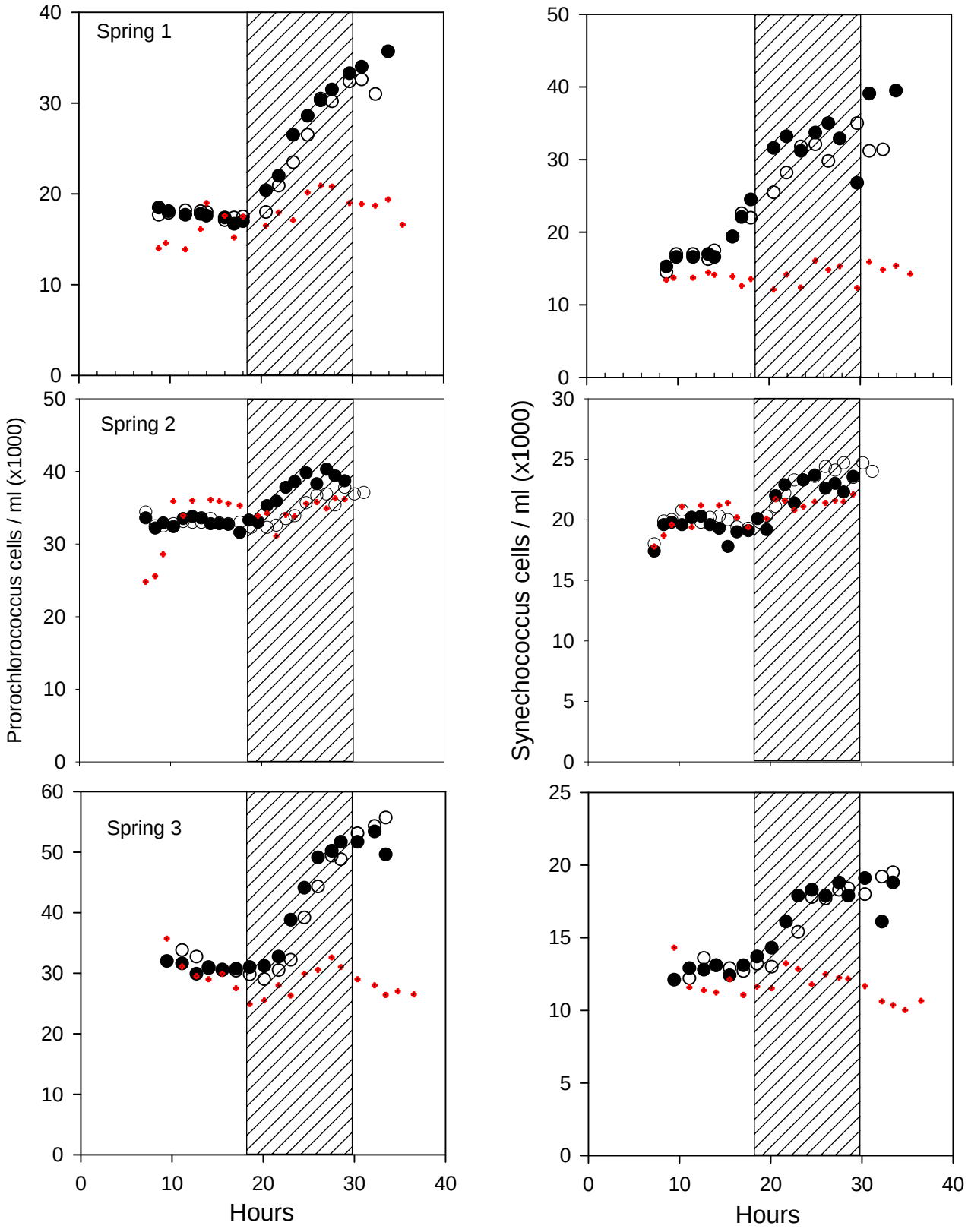

Fig. 3.2. Time series of Prochlorococcus and Synechococcus cell densities at spring stations in replicate bottles (filled and empty circles) and in situ (red dots). Hatched areas denote local night. X-axis is hours from midnight on day 1 of experiment.

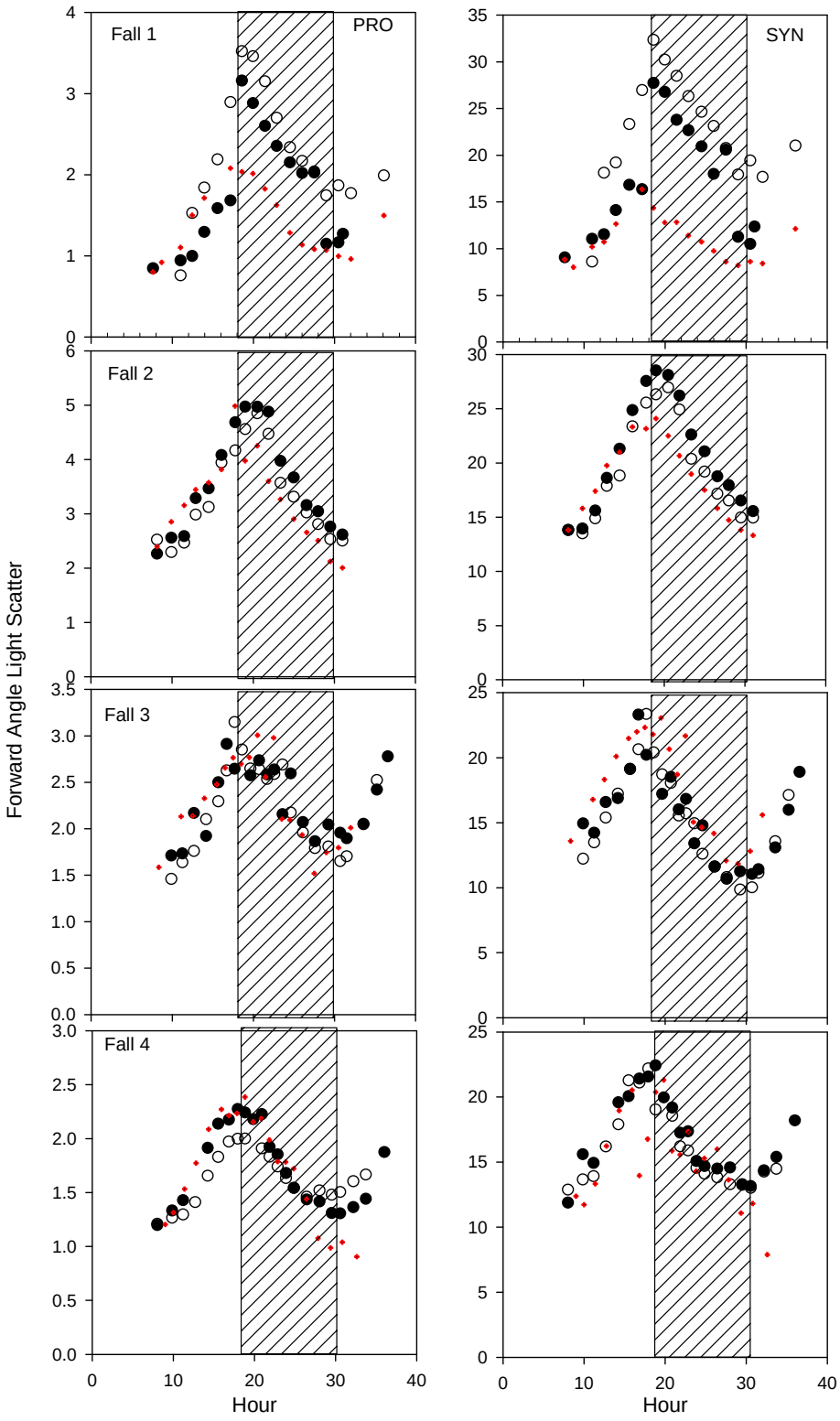

Fig. 3.3. Time series of Prochlorococcus forward angle light scatter at fall stations in replicate bottles (filled and empty circles) and in situ (red dots). Hatched areas denote local night. X-axis is hours from midnight on day 1 of experiment.

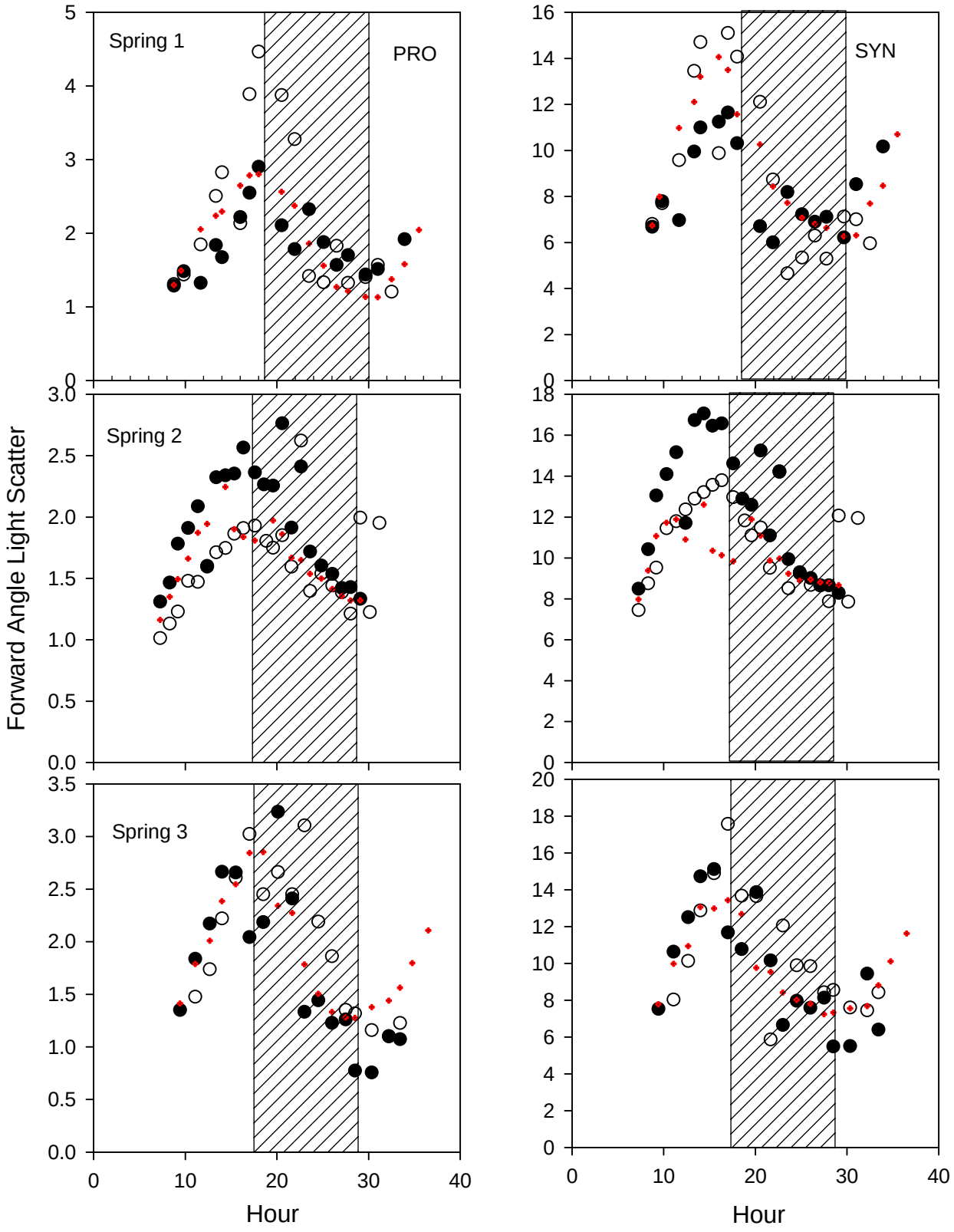

Fig. 3.4. Time series of Prochlorococcus forward angle light scatter at spring stations in replicate bottles (filled and empty circles) and in situ (red dots). Hatched areas denote local night. X-axis is hours from midnight on day 1 of experiment

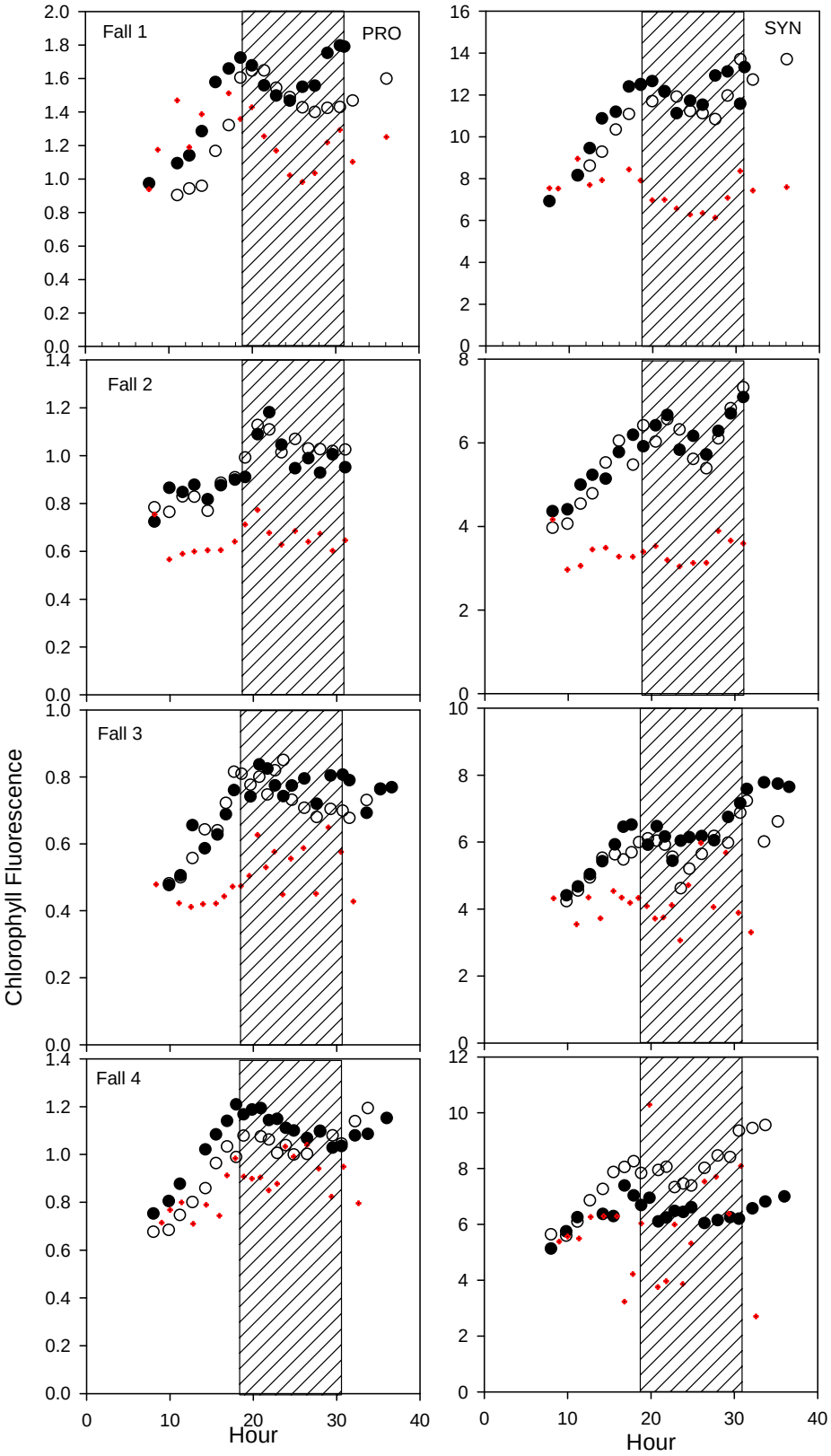

Fig. 3.5. Time series of Prochlorococcus chlorophyll fluorescence at fall stations in replicate bottles (filled and empty circles) and in situ (red dots). Hatched areas denote local night. X-axis is hours from midnight on day 1 of experiment.

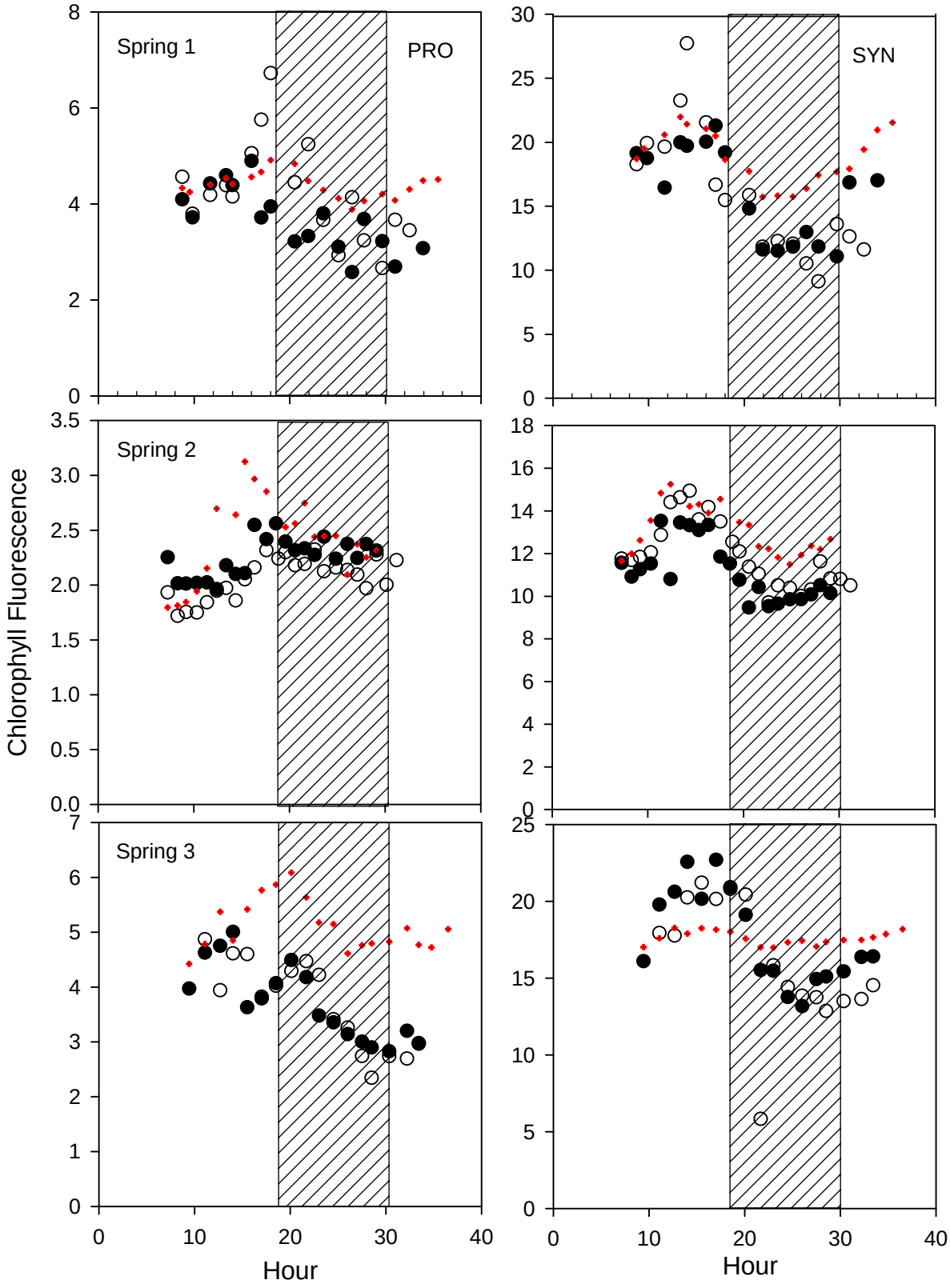

Fig. 3.6. Time series of Prochlorococcus and Synechococcus chlorophyll fluorescence at spring stations in replicate bottles (filled and empty circles) and in situ (red dots). Hatched areas denote local night. X-axis is hours from midnight on day 1 of experiment.

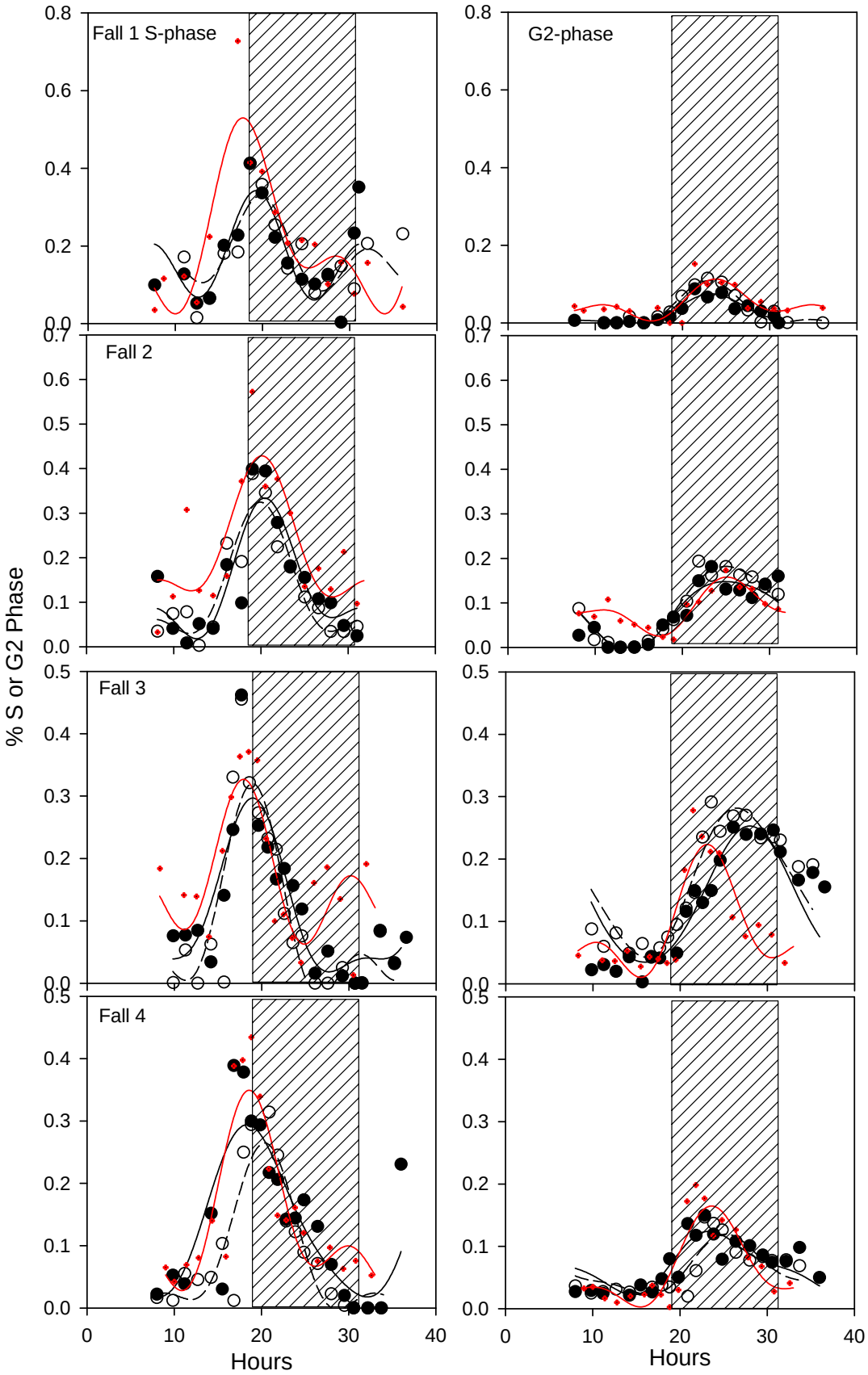

Fig. 3.7. Time series of percent of fall Prochlorococcus populations in S (left col.) and G2 (right col.) cell cycle phases in replicate bottles (filled and empty circles, solid and broken black lines) and in situ (red dots, red line). Symbols are measured data points, lines are fitted periodic functions (see text). Hatched areas indicate local night. X-axis is hours from midnight on day 1 of experiment.

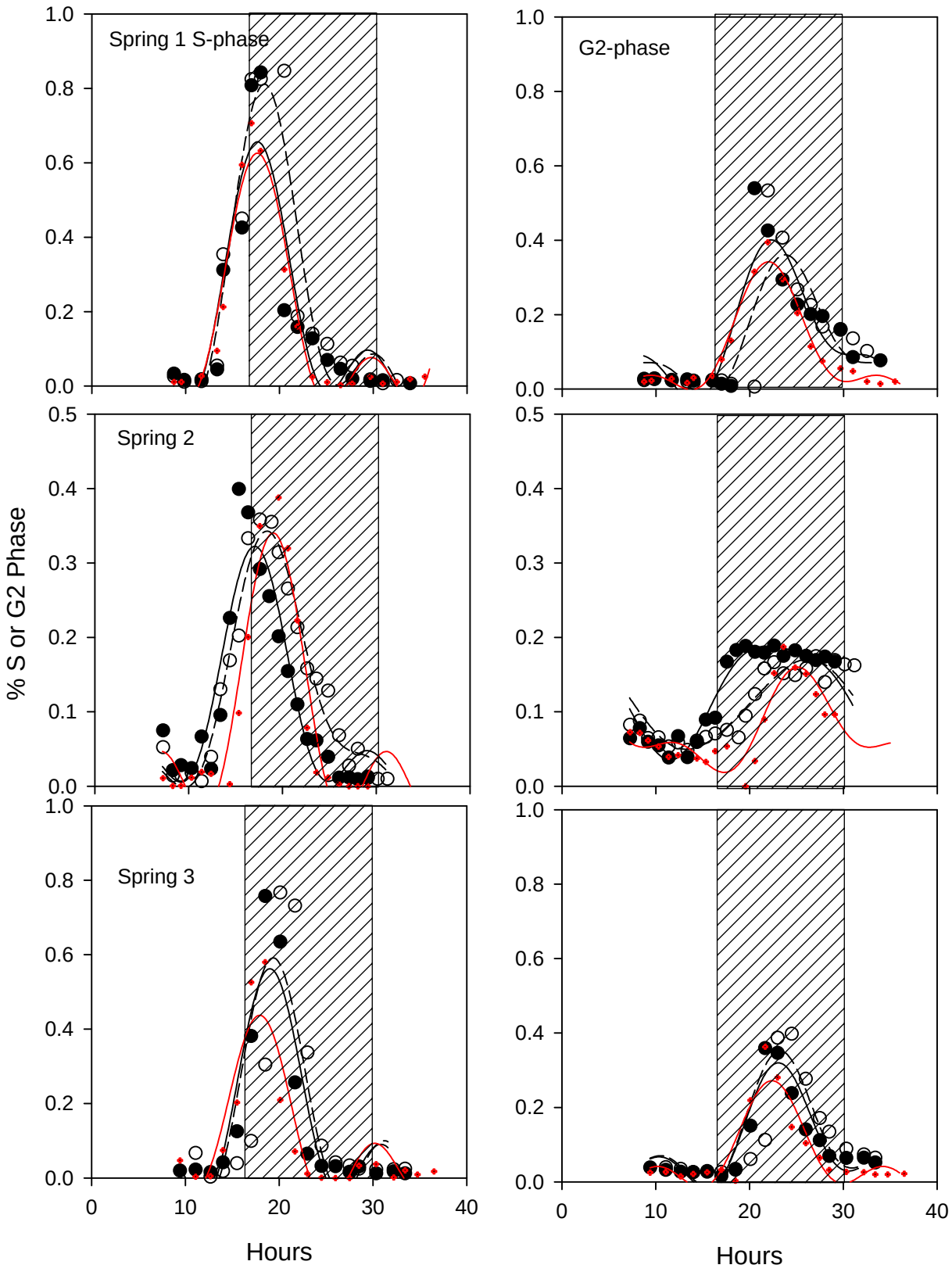

Fig. 3.8. Time series of percent of spring Prochlorococcus populations in S (left col.) and G2 (right col.) cell cycle phases in replicate bottles and in situ. Symbols and lines as in Fig. 7. X-axis is hours from midnight on day 1 of experiment.

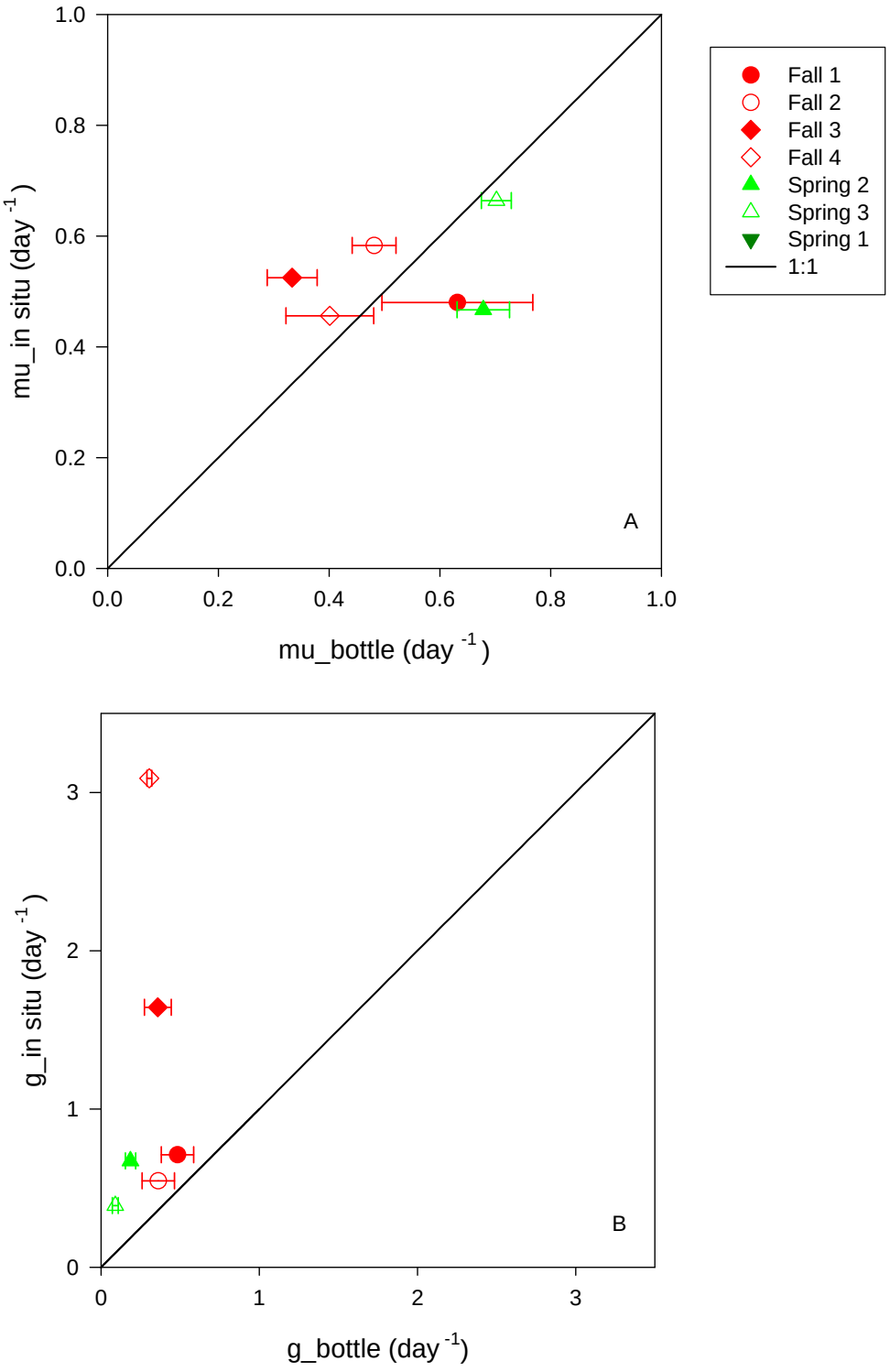

Fig. 3.9. Comparison of estimates of Prochlorococcus growth rates (A) and mortality rates (g, d-1) (B) in situ and in the incubation bottles. Red and green symbols correspond to fall and spring stations, respectively. Error bars indicate SD of replicate bottles. Solid lines indicate 1:1 relationship between the two estimates.

Chapter 4

AN INDIVIDUAL-BASED MODEL FOR THE ANALYSIS OF *PROCHLOROCOCCUS* DIEL CELL CYCLE BEHAVIOR[1]

[1] Blythe, BJ and Binder, B. To be submitted to *Limnology and Oceanography*

Introduction

Natural *Prochlorococcus* populations exhibit tightly timed diel growth and division cycles (Jacquet *et al.*, 2001a, Jacquet *et al.*, 2001b, Binder & DuRand, 2002). These cycles engender systematic variation in both cell size and abundance, and as such have the potential to influence interactions between *Prochlorococcus* and their protozoan grazers (Caron *et al.*, 1991, Christaki *et al.*, 1999, Guillou *et al.*, 2001, Christaki *et al.*, 2005). In addition, the strongly phased division cycle can be useful for evaluating the growth rate of natural *Prochlorococcus* populations, and assessing the processes that control the dynamics of these populations (Binder *et al.*, 1996, Liu *et al.*, 1997, Shalapyonok *et al.*, 1998, Worden & Binder, 2003). While cell cycle progression in natural *Prochlorococcus* populations can be tracked relatively easily using flow cytometry, teasing apart the factors affecting or driving the observed patterns can be difficult.

One way to explore the relationships between cell cycle progression, population growth, and grazing mortality is through the application of numerical models and simulations. To date, there have been only a few attempts at modeling diel cell cycle patterns in phytoplankton (Smith & Martin, 1973, Gotham & Frisch, 1981, Cooper, 1982, Vaulot & Chisholm, 1987, Hellweger & Kianirad, 2007, Hellweger, 2008), and these have all been primarily directed toward eukaryotic cell cycle behavior.

Smith and Martin (1973) proposed that the generation times observed in (eukaryotic) phytoplankton populations were driven by variability in the duration of the G1-phase. In their estimation, all cells had a probability of entering S-phase and this probability was driving the patterns of cell-densities observed. They postulated the existence of an "A-state" through which a cell must pass after mitosis (i.e. preceding the next round of DNA synthesis); the duration of

this “A-state” was dependent the probability described above. The “A-state” may encompass some or all of the G1 phase.

Gotham and Frisch (1981) took a slightly different approach, and proposed that cells need to accomplish certain “tasks” before they can begin chromosome replication. Essentially the completion of G1-specific tasks limits the entry of cells into S-phase. Likewise, certain other “marker events” must be completed before cells can undergo mitosis. The replication of chromosomal or nuclear DNA was viewed as one of these marker events, along with replication of chloroplast and mitochondrial DNA, and certain enzyme activities. According to this view, instead of a trigger for chromosome replication that leads inexorably to mitosis, chromosome replication is one of many processes that all need to be completed to create a cumulative mitosis trigger. Using this model, Gotham and Frisch (1981) were able to reasonably reproduce diel patterns in average cell biomass, but could not accurately match many of the other system behaviors (such as cell frequency distributions for their proposed marker events).

Vaulot and Chisholm (1987) invoked a single critical transition point, the position of which is not associated with any particular cell cycle stage. In this model, unspecified light-dependent and light-independent biochemical processes need to be completed before cells may pass the transition point and ultimately divide. The time required for the former was assumed to be dependent on the cumulative light exposure experienced by the cells. By varying the timing of the transition point (as well as other parameters), this model can qualitatively reproduce the timing of cell division over a diel L:D cycle in a number of eukaryotic algae.

The models discussed thus far were based on the eukaryotic cell cycle, which is traditionally thought to encompass phases (G1, S, G2 and M) during which specific processes must be completed. A different view of cell progression is generally held for prokaryotes, in

which phase-specific activities do not exist. This view is based largely on early experimental work with *E. coli* (see reviews in Clark & Maaløe, 1967, Cooper & Helmstetter, 1968, Helmstetter & Pierucci, 1976), and is formally described in Cooper's Continuum Model (Cooper, 1979, Cooper, 1982). In this model, no "G1-specific" activities are assumed to precede DNA replication. Instead, events that regulate cell division can take place at any time during the cell cycle, and thus a cell need not "wait" in G1 before DNA synthesis can occur. Cooper postulated that the accumulation of some initiator molecule controls the start of DNA replication ("S-phase," in eukaryotes). This initiator accumulates continuously, and when the ratio of initiator to chromosome origins reaches a critical value, DNA synthesis commences. The resultant increase in chromosome origins decreases the initiator: origin ratio and further rounds of DNA replication must await accumulation of more initiator. If it takes longer for the initiator to reach the critical level than it takes for a cell to complete DNA replication and cell division (the 'slow-growth' case of the model), a G1 phase is observed. Conversely, if the initiator accumulates rapidly enough, the critical level may be reached before the cell finishes its current round of DNA synthesis, allowing a second round of replication to commence (the 'fast-growth' case). In this case the daughter cells would be "born" in the process of DNA replication, and no G1 phase would occur. Thus, under this model the initiation of DNA replication plays a central role: cell division is only a terminal process that occurs some time after this initiation, and the duration of 'G1' (to the extent that it occurs at all) is a consequence of the interplay between initiator accumulation (or cell growth) and DNA replication rate, rather than a forcing mechanism within the cell cycle.

Recently, Hellweger (2008) constructed a model based on Cooper's continuum model that attempted to reproduce diel patterns of average cell size, cell concentration and cell cycle

phase distribution for well-phased phytoplankton populations. This model specifies that a critical "initiation mass" (analogous to Cooper's (1982) initiator) must be reached before DNA replication is initiated, and thus chromosome replication is tied intimately to the accumulation of cellular biomass. When an individual cell reaches this initiation mass, it progresses through S and G2-phases at a constant rate and then divides. This model was capable of recreating with reasonable accuracy diel changes in cell concentration and cell cycle distribution observed previously in a eukaryotic alga (*Euglena*). Interestingly, although the continuum model is based originally on the prokaryotic cell cycle, Hellweger's model was less successful at explaining the diel cell cycle progression of *Prochlorococcus*.

In the present study, a Matlab model was developed to simulate the diel patterns of *Prochlorococcus* cell growth, chromosome replication, and division tied to a light:dark cycle. The prokaryote-based continuum model described above serves as the foundation for this model, although some differences were incorporated to reflect our knowledge of cyanobacterial cell cycle behavior (see Model Description). I employ an "individual based" approach, which tracks the properties of individual cells over the course of the simulation (Hellweger & Kianirad, 2007, Hellweger, 2008). Population-level patterns ultimately emerge as the sum of the patterns of the individual cells within the entire population. This approach allows for the application of standard analyses of *Prochlorococcus* populations to our simulated populations, and investigation of the effects of varying the parameters thought to affect growth rates of natural populations of *Prochlorococcus*.

This model can also be used to test the methods employed in previous chapters to estimate *Prochlorococcus* growth in the field. Specifically, I will be able to directly test the validity of the widely used Carpenter and Chang approach (Carpenter & Chang, 1988, Chang &

Carpenter, 1988, Antia *et al.*, 1990, Chang & Carpenter, 1990) by comparing calculated growth rate estimates for simulated populations to the actual growth rate (as determined by the model run parameters).

Finally, I will compare simulation runs to our incubation data from the previous chapters. Significant deviations from those observations would indicate that the model does not accurately incorporate all the important factors affecting *Prochlorococcus* growth and diel behavior, and therefore would suggest that our current understanding of cell cycle regulation in this important group of organisms is incomplete.

Model Description

Purpose

I developed an "individual based" model using Matlab to simulate the diel cell cycle behavior of *Prochlorococcus* populations. The ultimate purpose of this model is to tease apart the main contributing factors that drive *Prochlorococcus* diel cellular and population dynamics in natural systems. The immediate goal was to develop a model that would produce realistic patterns of *Prochlorococcus* cell cycle phase fractions (%S and G2) and cellular biomass over a diel cycle. (Note that although the continuum model does not recognize S and G2 phases *per se*, for clarity this terminology will continue to be used to refer to cells that have DNA content between 1 and 2, and exactly 2 genome equivalents, respectively.)

State Variables

Each *Prochlorococcus* cell is represented by a structure of properties, which include size at creation (base-size), current biomass, current DNA content, and the growth rate (μ_i) applied at model initiation (which is equal for all cells in the population). Duration of S- and G2-, cell mass at initiation of DNA replication ($M_{ini.}$), rate of DNA accumulation, and the timing of the

circadian gate (see below) are all assumed constant for the entire population for any given run of the model. Light is treated as being "on" or "off" in our model (with a 12 hour cycle), and determines whether or not cell growth occurs in a given time step. Table 1 presents the values and ranges of values used for the model variables.

Resolution

The model was run at a temporal resolution of 50 time-steps per day, which is equivalent to a time-step of 28.8 minutes. This time-step size provides adequate resolution of population scale patterns while allowing a model run to complete in a reasonable amount of time. All simulations were run for 31 days, with data from days 28-30 serving as the reference days for comparison between model runs. The model spin-up period of 28 days allows for initial transient behavior to die down.

Model Process Overview

The main process simulated in this model is cell division, which is controlled by other lower level processes within the model (Fig. 4.1). Cells accumulate biomass during the light phase according to exponential growth with a specific growth rate (μ_i) set at the initiation of a model run; when cell mass reaches M_{ini} a cell may be eligible to initiate chromosome replication. The circadian gate (C_g) can be viewed as a daily light-dependent restriction point or gate; i.e. a cell must experience x-hours of continuous light on a given day to be eligible to replicate its DNA. Actual initiation of replication is controlled by a probability function (see below) and this circadian gate. Progression through S and G2 phases occurs at the same rate for all cells in which replication has been initiated. New rounds of DNA replication cannot be initiated in such cells until they complete the current round of replication and divide. In this respect (as well as in the inclusion of a circadian gate) this model differs from the classic continuum model, but is

consistent with the present state of knowledge of *Prochlorococcus* and general cyanobacterial cell cycle dynamics (Mori *et al.*, 1996, Shalapyonok et al., 1998).

Cells entering S-phase are chosen randomly at each time-step from the pool of cells that are eligible to begin chromosome replication. The fraction of eligible cells actually entering the S-phase is given by the following function (see Fig. 4.2):

$$f_{divide} = \left(\frac{(\exp(t_{now} - t_{zero}) - 1)}{\exp(t_{now})} + 0.5\right) \qquad \text{(Eq.4.1)}$$

Where t_{now} is the current time and t_{zero} is set to match the timing of the "opening" of the circadian gate. At teach time step, this fraction (f_{divide}) of cells is randomly selected from the group of eligible cells, and DNA replication proceeds in the selected cells.

In order to limit the size of the population, grazing mortality (g) eliminates a constant predetermined fraction of randomly selected cells at each time step. This mortality was turned off for a number of days at the end of each simulation (see below).

Observed population and cell cycle dynamics emerge from the sum of the individual cells behaviors. The model is initialized with a population of cells each having a mass chosen from a normal distribution with a mean ± s.d. of 50 ± 10 fg C cell^{-1}. These values can be modified to initialize a population of varying cell number, with a large or small degree of variability in individual cell sizes. Stochasticity is introduced into the model through this size variability and the selection of cells entering the S-phase.

Observations

Population level statistics (e.g. average cell size) are calculated at each time-step, yielding a 28.8 min. resolution for changes in the model population parameters. The model set-up allows for the observation of individual cells as well as population level dynamics.

Model Results

Sensitivity Analysis and Preliminary Validation

As described above, this model assumes that cell division is controlled by a combination of factors, including a circadian gate for chromosome replication (C_g), rate of biomass accumulation (μ_i), a biomass threshold for chromosome replication (M_{ini}), and the duration of the "G2" phase after chromosome replication (D). A preliminary sensitivity analysis was performed in which I varied these parameters systematically and observed the effect on the shapes and magnitudes of the generated diel phase fraction (%S and G2) curves. One parameter was varied for a number of model runs while the others were held constant, allowing for the effect of the parameter of interest on the bulk population dynamics to be observed.

Changing μ_i had the effect of altering the maximum values of the S and G2 phase fraction curves (as would be expected), and the shape of these curves. Altering the timing of C_g resulted in a corresponding change in the timing of the S-phase. The timing of C_g could also alter the slope of the initial S-phase increase (by forcing an accumulation of cells eligible to replicate their DNA, but unable to do so until the gate is open). Variation in M_{ini} altered the mean size of cells in the population (higher M_{ini} leads to higher average size), and could also induce patterns of varied peak cell sizes from day to day, although this was somewhat dependent upon the growth rate being tested (see Fig.3, and discussion below). Increasing or decreasing D (the duration of G2) had the primary effect of altering the shape, duration and peak of the G2 curve. Larger values for this parameter yielded higher peak values for the G2 curve, as well as a more bell-shaped curve. For a "standard" case, we set M_{ini} = 50 fg C cell^{-1}, D-phase = 2.5h, and C_g = 6h of light.

The Influence of Growth Rate on Diel Population Dynamics

To explore the effect of variation in population growth rate on diel patterns of cell mass and cell cycle progression, I ran the model at a range of μ_i (0.15 – 0.9 d^{-1} in increments of 0.1d^{-1}), holding the other parameters to their "standard" values (see Table 4.1). Results from this analysis showed three basic classes of responses at the growth rates tested.

First, at low growth rates, the phase fraction data showed one peak per day, but the magnitude of these peaks varied from day to day. The amplitude of the diel pattern in average cell size was low, and reached a maximum value that was less than M_{ini}. In the example presented (Fig. 4.3a), the average cell size was ~40 fg C $cell^{-1}$, with a minimum and maximum of ~35 and ~45 fg C $cell^{-1}$ respectively.

At moderate growth rates the variability in the magnitude of the peaks was considerably less than the variability observed at lower growth rates (Fig. 4.3b). The peak values were, as would be expected, significantly higher than those produced by the model at lower growth rates. The amplitude of variation in the diel pattern of average cell size was greater than that observed at lower growth rates. As an example, when $\mu_i = 0.6$ day^{-1}, average cell size varied between ~35 and 55 fg C $cell^{-1}$ (Fig. 4.3b). This behavior is also to be expected: as a higher fraction of the population is involved in cell division each day, the mean cell size will be more strongly influenced by the division cycle.

Finally, at the highest growth rates tested (> 1 doubling d^{-1} or $\mu > 0.69$ d^{-1}) two peaks in S and G2 cells became evident, reflecting successive waves of DNA replication and cell division. At roughly 1.5 doublings per day ($\mu = 0.9$ day^{-1}, Fig. 4.3c), two S- (and corresponding G2-) phase peaks were present on some, but not all days. Essentially, at this growth rate not all cells gain enough biomass to replicate twice each day, so a subset of the population must wait until the

next day to divide. By the time the circadian gate opens on the next day and they are allowed to divide, they have gained more biomass in the light and are able to begin another round of DNA replication immediately after division and to divide a second time in one 24 h period.

Relationship of μ to μ_i

Growth rates for the model are specified as specific cell biomass growth rates, normalized to 24 h (to take into account the lack of growth in the dark). For all model runs, mortality was turned off after day 25. This allowed the actual specific growth rate of the model population to be calculated using observed changes in cell number (henceforth referred to as μ_b). This population growth rate is defined as:

$$\mu_b = \frac{(\log 10(N_f) - \log 10(N_i)) \times 2.303}{t_f - t_i} \qquad \text{(Eq. 4.2)}$$

where N_f and N_i are the cell densities at the end (t_f) and start (t_i) of the experimental time-period of interest. In addition to the actual population growth rate, an estimate of growth rate based on the Carpenter & Chang approach (μ_{CC}) could also be derived for each run (see Chapt. 2 for details).

An interesting observation from this analysis is that on a day to day basis, the population growth rate (μ_b), as determined by the model output, is not constant. Our results show that daily μ_b can vary as much as 4-fold from day to day for a given μ_i (Table 4.2). However, when μ_b is averaged over multiple days (days 28-30 in this case), the mean value for μ_b is very close to the selected value of μ_i (Table 4.2, Fig 4.4). The implications of this daily variability in μ_b (and μ_{CC}) will be discussed below.

I used these model runs to evaluate the accuracy of the Carpenter & Chang (1990) approach for estimating growth rate from cell cycle phase fraction dynamics. For simulated sampling intervals of 0.5 h and 1.5 h, and at growth rates less than or equal to one doubling per

day ($\mu_b \leq 0.69$ day^{-1}), μ_{CC} and μ_b were well correlated, and approximately equal (Fig. 4.5). However once μ_b exceeds 0.69 day^{-1}, this linear relationship no longer appears to hold, as values of μ_{CC} over-estimate the true daily growth rates (μ_b). When the sampling interval was increased to 3 h, values for μ_{CC} tended to underestimate true growth rate for $\mu_b \leq 0.69$ d^{-1}, but by the same token gave much improved estimates for the higher growth rates (Fig. 4.5). This latter result was unexpected, and is not completely understood at this point. It may just be a coincidental result for the few growth rates tested, and needs to be explored more fully.

The μ_{CC} values discussed above were calculated using the curve-fit version of the Carpenter & Chang approach (see Chapt. 2). To test whether the curve-fitting itself was responsible for differences between μ_{CC} and μ_b, particular at higher growth rates, we estimated growth rates using the more traditional manual approach (Fig. 4.5, solid symbols). The manual method of calculating μ did not improve the accuracy of the estimates at high growth rates, and in fact appeared to result in much reduced precision, relative to the curve fit approach.

Model Fit to Experimental Data

As a further evaluation of the model, I compared the model results to selected field data from the previous chapter. Three sets of replicate bottle incubation data were chosen, encompassing low (Fall-3, $\mu = 0.33$ day^{-1}), moderate (Fall-2, $\mu = 0.48$ day^{-1}), and high (Spring-3, $\mu = 0.70$ day^{-1}) growth rates, as estimated by the Carpenter-Chang approach. I set μ_i to match the estimated growth rate values and observed the phase fraction curves on days 28-30 of each model run. Time values for the data were normalized to reflect hours since dawn, as it is represented in our model. Again, mortality was turned off after day 25 to allow for calculation of μ_b. Standard parameter values were modified as necessary, as described below. This exercise was intended to provide a qualitative indication of the ability of the model to replicate salient

features of the observed diel cycle in real *Prochlorococcus* populations. It is obviously not a formal parameter-fitting analysis, although it may provide an appropriate starting point for such analysis in the future.

For the low μ case (μ_{CC} = 0.2 day^{-1}), I increased the duration of the G2-phase to ~4h to better match the peak value of the G2-phase (Fig. 4.6). This is consistent with the results of Burbage and Binder (2007), who found that the duration of G2 increased at low growth rates. The circadian gate (C_g) was set at 7 h from dawn (rather than 6) to more closely match the timing of the rise in S-phase. With this parameter set, the model replicated the peak values well for both S and G2, however it did not match the rate of S or G2-phase decay.

For the moderate growth rate case (μ_{CC} = 0.48 d^{-1}), the standard parameter set was used, except that C_g was again set to 7 h after dawn (Fig. 4.7). In order to match the S and G2 peak magnitudes, however, the input growth rate had to be lowered to 0.40 d^{-1}. Under these conditions, the timing and magnitude of the peaks was simulated well, but as was the case for slow growth, the rate of S- and G2-phase fraction decay were not well represented.

For the high growth rate simulation (μ_{CC} = 0.70 d^{-1}) parameters were the same as for the moderate case. With μ_i set to μ_{CC}, the rise in S- and G2-phase were well represented by the model, although the peak values were slightly over- and under-estimated, respectively. Again, the decay of both phases was more rapid in the model than in the data (Fig. 4.8).

Discussion

This modeling effort provides a foundation for future work involving numerical simulation of *Prochlorococcus* diel behavior. Here it has provided some interesting observations and shows clear avenues for future development. Overall, the model can produce results that are

qualitatively similar to field data, and can serve as a useful tool for hypothesis development and testing in the future.

The model incorporates features of the prokaryotic cell cycle that are supported by the literature. In accordance with Cooper's Continuum model (1979, 1982), I assume that *Prochlorococcus* has no specific G1 tasks that precede chromosome replication, and if other prerequisites are met, a cell may begin chromosome replication immediately following division. In contrast to the classical prokaryotic model, however, the model logic assumes that rounds of chromosome replication in *Prochlorococcus* cannot overlap. This is supported by field and lab observations of successive rounds of replication in rapidly growing *Prochlorococcus* populations (Shalapyonok et al., 1998). The concept of a critical mass acting as an initiator for chromosome replication is well supported by measurements in *E. coli* (Donachie, 1968, Boye *et al.*, 1996), and has more recently been applied experimentally to marine *Synechococcus* and *Prochlorococcus* (Binder, 2000, Burbage & Binder, 2007). The values of M_{ini} and D used are well within the ranges of values measured previously for one *Prochlorococcus* strain (Burbage & Binder, 2007). There is strong evidence for the existence of a circadian rhythm that regulates cell division in cyanobacteria (Mori *et al.*, 1996). Although the specific timing of that gate is not well-characterized, data from previous chapters (as well as many other studies of *Prochlorococcus* dynamics) clearly show the timing of the initial increase in S-phase cells to occur within the time frame used in our model (~6-7 h from sunrise). In terms of direct, experimental evidence, the only unconstrained aspect of the model is the probability function that governs the initiation of chromosome replication in eligible cells (eq. 1), which for the present was arbitrarily chosen.

This model allows us to directly explore issues regarding *in situ* growth rate estimates that were addressed somewhat indirectly in previous chapters. Application of the Carpenter-Chang algorithm to model-generated data supports the notion that the curve-fitting approach yields a more accurate estimate of growth rate than the manual approach, at least for low to moderate growth rates (Fig. 4.5). At high growth rates (> 1 doubling per d), however, the algorithm fails. Although such high growth rates may not be common for *Prochlorococcus*, they have been observed in the field as well as in laboratory cultures on occasion (Shalapyonok et al., 1998). The results also indicate that sampling intervals of 0.5 or 1.5 h (in combination with curve fitting) are sufficient for reasonably accurate determination of low to moderate growth rates. In contrast, simulation of a 3 h sampling interval consistently underestimated the true growth rate of the population. This is consistent with Chang and Carpenter (1990), who suggested that sampling intervals above 2 h resulted in reduced accuracy. That a 3 h sampling interval actually yielded better results than shorter intervals for growth rates above 0.69 d^{-1} is particularly surprising. We are presently not able to satisfactorily explain this result, although it may simply be happenstance.

The model yielded some intriguing results regarding day to day variability among *Prochlorococcus* populations. While model populations generally achieved steady state over the time scales employed here, they nevertheless showed remarkable variability in diel cell cycling and growth rate on a day-to-day basis. Thus, in the slow growth example (Fig. 4.3a) peak magnitude of %S and population growth rate varied from day to day by factors of approximately 2 and 4, respectively. In the high growth rate example, day to day variability between phase fraction dynamics was very obvious: 2 large peaks in %S and %G2 occurred on day 28, 1 peak occurred on day 29, and 1 large and 1 small peak occurred on day 30 (Fig. 4.3c).

Note that this variability occurred under unvarying environmental conditions and constant cellular biomass growth rate. In the natural system, such conditions are unlikely to exist; in fact cellular biomass growth rate can be expected to vary significantly over the course of a single day as both surface light intensity and the depth of the cell varies. Therefore, the day to day variability in population growth rate observed here almost certainly represents a lower bound.

This predicted day to day variability could have important implications for observations of growth rate in natural *Prochlorococcus* populations. If these observations are made over relatively short periods (on the order of 24 h), as they almost always are, then the resultant estimates of growth rate may significantly under- or over-estimate the longer-term growth rate of the population. Furthermore, depending on the ability of grazer communities to track this short-term variation (an issue that could itself be addressed in the future using this model), daily changes in population standing stock might be observed even for populations that are in approximate steady state. In the case of my recent observations (see Chapter 3), some time series do show significant changes in cell concentration over a 24 h period for *in situ* populations of *Prochlorococcus* and *Synechococcus*. Such changes would normally be interpreted as reflections of non-steady state conditions, but the results of this modeling effort suggest that other interpretations are possible. The general implication of these results is that a 24 hour sampling time course may only catch one mode of behavior in the natural population, and the calculated growth rate for that day may not necessarily reflect the longer-term average growth rate of the population. This would be interesting to test in the field (e.g. by measuring growth rate of the same population over successive days).

While initial attempts to match the model output to observations were not as successful as might have been hoped, the fact that in many cases the model can reasonably reproduce the magnitude and timing of the cell cycle phase peaks is encouraging. My initial sensitivity analysis was admittedly crude (manually altering one parameter at a time to get a general idea of what controls the model output), however it does indicate that our fundamental understanding of the system and its controls are sound. A logical next step would be to try to match the data objectively, allowing all state-variables to fluctuate to get a best fit using a Levenberg-Marquardt (or similar) non-linear optimization algorithm.

Incorporation of other refinements for which there is experimental data (e.g. variation of G2 duration and initiation mass with growth rate) may help improve the model as well. If the "decay" of the modeled phase fractions remains unrealistic, the probability function that currently governs the progression of eligible cells into the S-phase may need to be changed. Ultimately this model could provide a basis for understanding the diel variation of growth rate, grazing mortality, and standing stock in natural *Prochlorococcus* populations.

References

Antia, A. N., Carpenter, E. J. & Chang, J. 1990. Species-Specific Phytoplankton Growth-Rates via Diel DNA-Synthesis Cycles .3. Accuracy of Growth-rate Measurement in the Dinoflagellate Prorocentrum-minimum. *Mar. Ecol.-Prog. Ser.* **63**:273-79.

Binder, B. 2000. Cell cycle regulation and the timing of chromosome replication in a marine Synechococcus (cyanobacteria) during light- and nitrogen-limited growth. *J. Phycol.* **36**:120-26.

Binder, B. J., Chisholm, S. W., Olson, R. J., Frankel, S. L. & Worden, A. Z. 1996. Dynamics of picophytoplankton, ultraphytoplankton and bacteria in the central equatorial Pacific. *Deep-Sea Res. Part II-Top. Stud. Oceanogr.* **43**:907-31.

Binder, B. J. & DuRand, M. D. 2002. Diel cycles in surface waters of the equatorial Pacific. *Deep-Sea Res. Part II-Top. Stud. Oceanogr.* **49**:2601-17.

Boye, E., Stokke, T., Kleckner, N. & Skarstad, K. 1996. Coordinating DNA replication initiation with cell growth: Differential roles for DnaA and SeqA proteins. *Proc. Natl. Acad. Sci. U. S. A.* **93**:12206-11.

Burbage, C. D. & Binder, B. J. 2007. Relationship between cell cycle and light-limited growth rate in oceanic *Prochlorococcus* (MIT9312) and *Synechococcus*(WH8103) (Cyanobacteria). *J. Phycol.* **43**:266-74.

Caron, D. A., Lim, E. L., Miceli, G., Waterbury, J. B. & Valois, F. W. 1991. Grazing and Utilization of Chroococcoid Cyanobacteria and Heterotrophic Bacteria by Protozoa in Laboratory Cultures and a Coastal Plankton Community. *Mar. Ecol.-Prog. Ser.* **76**:205-17.

Carpenter, E. J. & Chang, J. 1988. Species-Specific Phytoplankton Growth-Rates via Diel DNA-Synthesis Cycles. 1. Concept of the Method. *Mar. Ecol.-Prog. Ser.* **43**:105-11.

Chang, J. & Carpenter, E. J. 1988. Species-Specific Phytoplankton Growth-Rates via Diel DNA-Synthesis Cycles.2. DNA Quantification and Model Verification in the Dinoflagellate Heterocapsa-triquetra. *Mar. Ecol.-Prog. Ser.* **44**:287-96.

Chang, J. & Carpenter, E. J. 1990. Species-Specific Phytoplankton Growth-Rates via Diel DNA-Synthesis Cycles.4. Evaluation of the Magnitude of Error with Computer-Simulated Cell-Populations. *Mar. Ecol.-Prog. Ser.* **65**:293-304.

Christaki, U., Jacquet, S., Dolan, J. R., Vaulot, D. & Rassoulzadegan, F. 1999. Growth and grazing on Prochlorococcus and Synechococcus by two marine ciliates. *Limnol. Oceanogr.* **44**:52-61.

Christaki, U., Vazquez-Dominguez, E., Courties, C. & Lebaron, P. 2005. Grazing impact of different heterotrophic nanoflagellates on eukaryotic (Ostreococcus tauri) and prokaryotic picoautotrophs (Prochlorococcus and Synechococcus). *Environ. Microbiol.* **7**:1200-10.

Clark, D. J. & Maaløe, O. 1967. DNA replication and the division cycle in Escherichia coli. *Journal of Molecular Biology* **23**:99-112.

Cooper, S. & Helmstetter, C. E. 1968. Chromosome replication and the division cycle of Escherichia coli B/r. *Journal of Molecular Biology* **31**:519-40.

Cooper, S. 1979. A unifying model for the G1 period in prokaryotes and eukaryotes. *Nature* **280**:17-19.

Cooper, S. 1982. The Continuum Model - Statistical implications. *Journal of Theoretical Biology* **94**:783-800.

Donachie, W. D. 1968. Relationship between cell size and time of initiation of DNA replication. *Nature* **219**:1077-&.

Gotham, I. J. & Frisch, H. L. 1981. A simple-model for cell-volume and developmental compartments in nutrient limited cyclostat cultures of algae. *Journal of Theoretical Biology* **92**:435-67.

Guillou, L., Jacquet, S., Chretiennot-Dinet, M. J. & Vaulot, D. 2001. Grazing impact of two small heterotrophic flagellates on Prochlorococcus and Synechococcus. *Aquat. Microb. Ecol.* **26**:201-07.

Hellweger, F. L. & Kianirad, E. 2007. Individual-based modeling of phytoplankton: Evaluating approaches for applying the cell quota model. *Journal of Theoretical Biology* **249**:554-65.

Hellweger, F. L. 2008. The role of inter-generation memory in diel phytoplankton division patterns. *Ecological Modelling* **212**:382-96.

Helmstetter, C. E. & Pierucci, O. 1976. DNA synthesis during the division cycle of three substrains of Escherichia coli B/r. *Journal of Molecular Biology* **102**:477-86.

Jacquet, S., Partensky, F., Lennon, J. F. & Vaulot, D. 2001a. Diel patterns of growth and division in marine picoplankton in culture. *J. Phycol.* **37**:357-69.

Jacquet, S., Partensky, F., Marie, D., Casotti, R. & Vaulot, D. 2001b. Cell cycle regulation by light in Prochlorococcus strains. *Appl. Environ. Microbiol.* **67**:782-90.

Liu, H. B., Nolla, H. A. & Campbell, L. 1997. Prochlorococcus growth rate and contribution to primary production in the equatorial and subtropical North Pacific Ocean. *Aquat. Microb. Ecol.* **12**:39-47.

Mori, T., Binder, B. & Johnson, C. H. 1996. Circadian gating of cell division in cyanobacteria growing with average doubling times of less than 24 hours. *Proc. Natl. Acad. Sci. U. S. A.* **93**:10183-88.

Shalapyonok, A., Olson, R. J. & Shalapyonok, L. S. 1998. Ultradian growth in Prochlorococcus spp. *Appl. Environ. Microbiol.* **64**:1066-69.

Smith, J. A. & Martin, L. 1973. Do cells cycle? *Proc. Natl. Acad. Sci. U. S. A.* **70**:1263-67.

Vaulot, D. & Chisholm, S. W. 1987. A simple-model of the growth of phytoplankton populations in light dark cycles. *J. Plankton Res.* **9**:345-66.

Worden, A. Z. & Binder, B. J. 2003. Application of dilution experiments for measuring growth and mortality rates among Prochlorococcus and Synechococcus populations in oligotrophic environments. *Aquat. Microb. Ecol.* **30**:159-74.

Table 4.1. Cell State Variables

Name	Symbol	Units	Values	Standards
Growth Rate	μ	day^{-1}	0.2 - 1.8	variable
Initiation Mass	M_{ini}	fg C $cell^{-1}$	20 - 80	50
G2 phase duration	D	hours	2 - 10	2.5
Circadian Gate	C_g	hours past dawn	4.8 - 9.6	6

Table 4.2. Growth rates calculated using changes in cell density or curve-fit analysis

Input μ	Biomass Calculated μ					Curve-fit Calculated μ					
	Simulation Day			72 Hour		Simulation Day			72 Hour	90min	180min
	28	29	30	AVG	STDEV	28	29	30	AVG	sampling	sampling
0.15	0.07	0.12	0.25	**0.15**	0.09	0.07	0.10	0.22	**0.13**	0.22	0.17
0.20	0.13	0.22	0.30	**0.22**	0.09	0.12	0.19	0.28	**0.20**	0.27	0.21
0.25	0.34	0.28	0.17	**0.26**	0.09	0.29	0.26	0.15	**0.23**	0.15	0.13
0.30	0.32	0.58	0.13	**0.34**	0.23	0.30	0.50	0.12	**0.31**	0.12	0.09
0.35	0.44	0.22	0.41	**0.36**	0.12	0.42	0.21	0.37	**0.33**	0.38	0.32
0.40	0.46	0.29	0.43	**0.39**	0.09	0.41	0.24	0.38	**0.34**	0.38	0.33
0.45	0.38	0.62	0.43	**0.48**	0.13	0.36	0.57	0.42	**0.45**	0.41	0.39
0.50	0.41	0.57	0.56	**0.51**	0.09	0.38	0.53	0.51	**0.48**	0.50	0.43
0.55	0.57	0.52	0.62	**0.57**	0.05	0.50	0.49	0.59	**0.53**	0.59	0.47
0.60	0.66	0.51	0.69	**0.62**	0.10	0.56	0.44	0.62	**0.54**	0.62	0.51
0.75	0.74	0.70	1.11	**0.85**	0.23	0.85	0.72	1.77	**1.11**	1.70	0.99
0.90	1.27	0.81	0.87	**0.98**	0.25		0.71	1.13	**0.92**	1.12	0.77

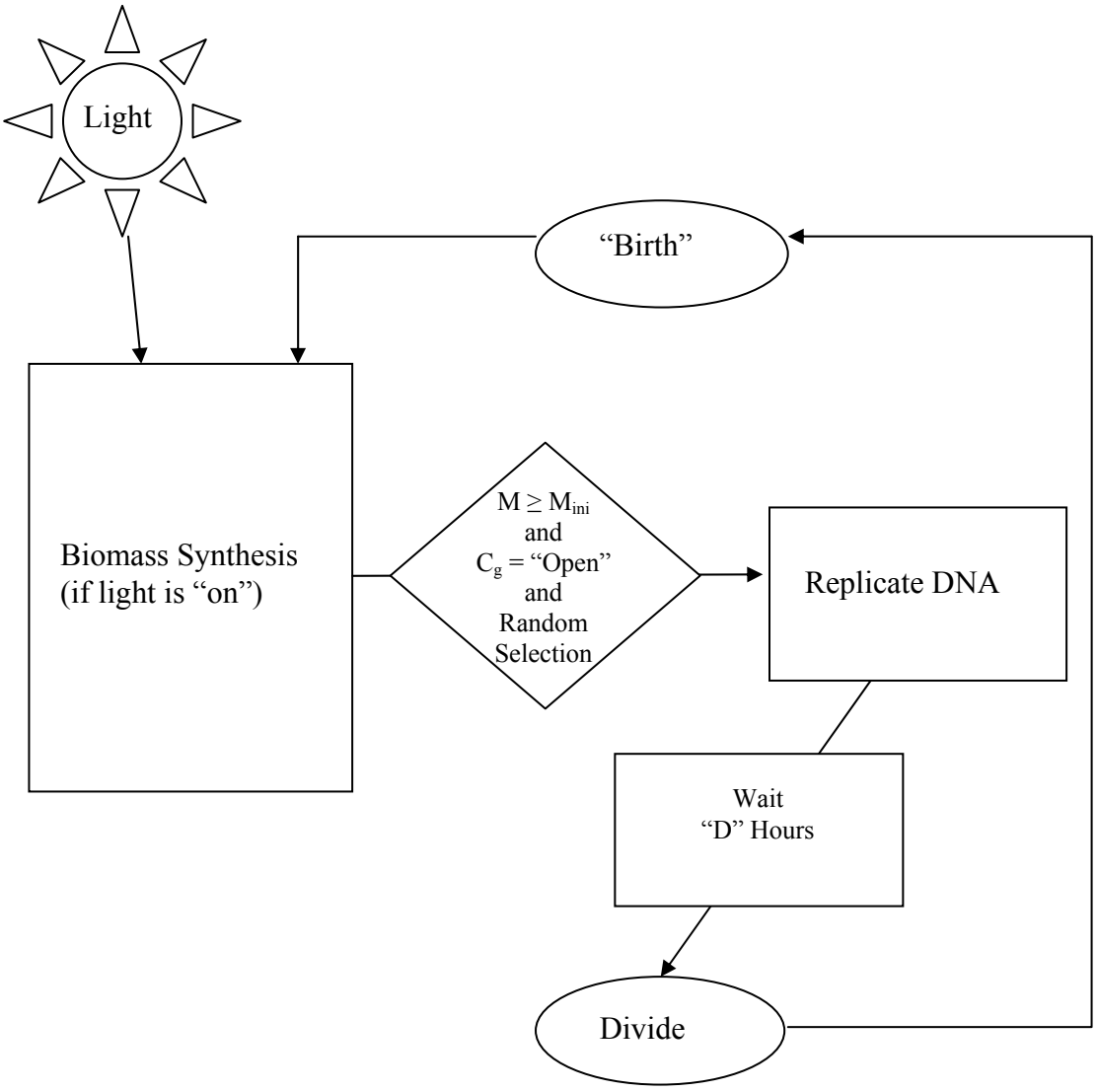

Figure 4.1. A simple conceptualization of the processes experienced by cells in our model

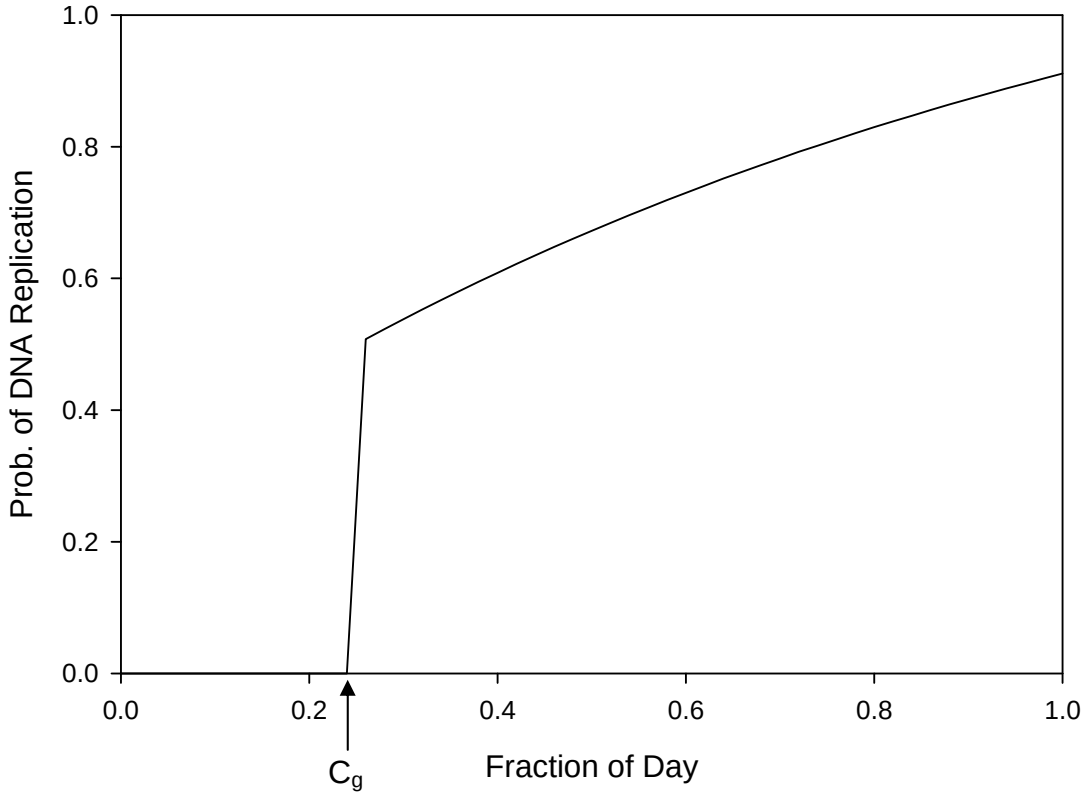

Figure 4.2. Profile of the probability an eligible cell will be selected to begin chromosome replication at a given time-step over the course of a single day. Arrow denotes the timing of the "opening" of the circadian gate.

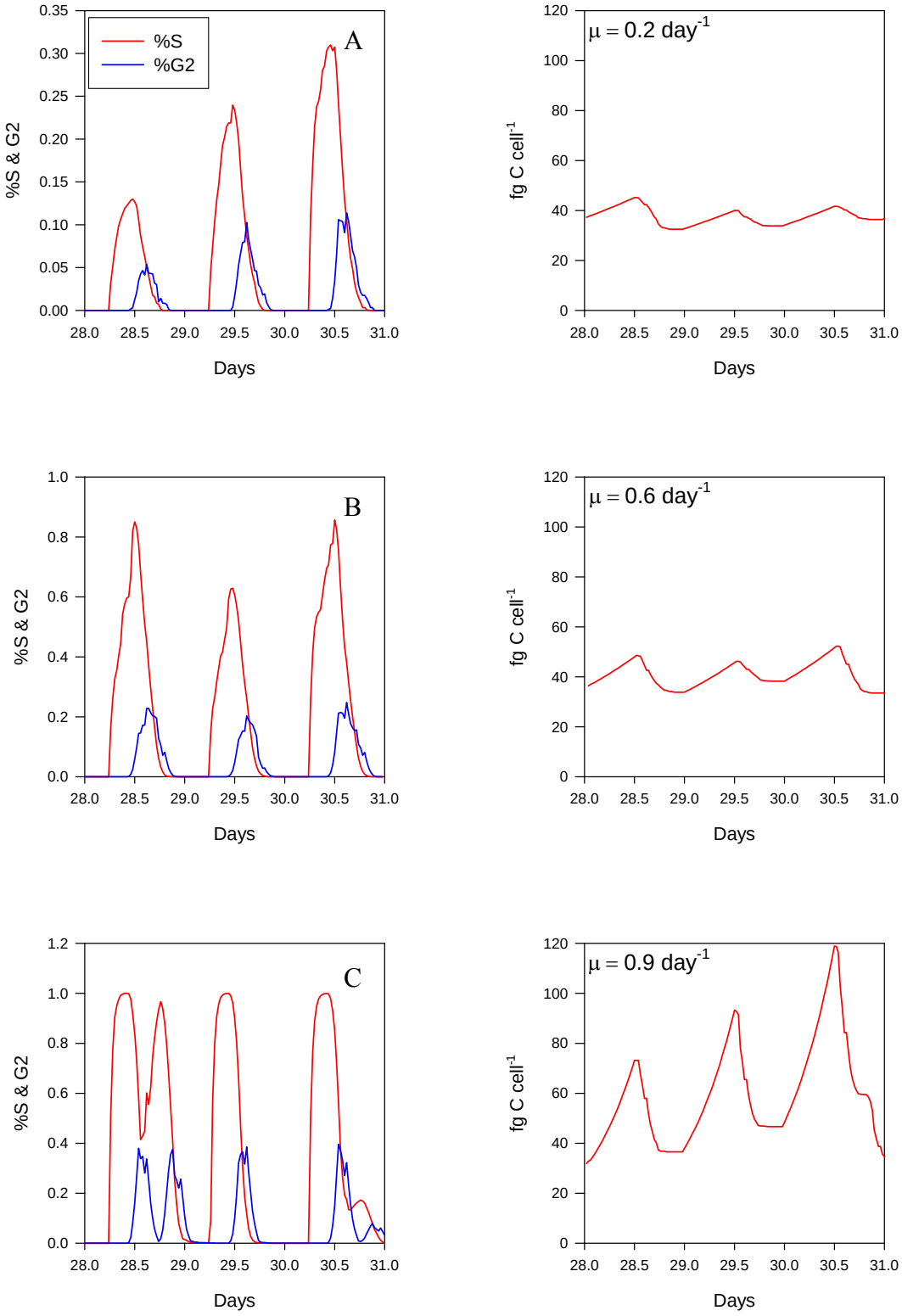

Figure 4.3. Comparison of diel dynamics of phase-fractions (left) and mean cell mass (right) for 3 modeled growth rates.

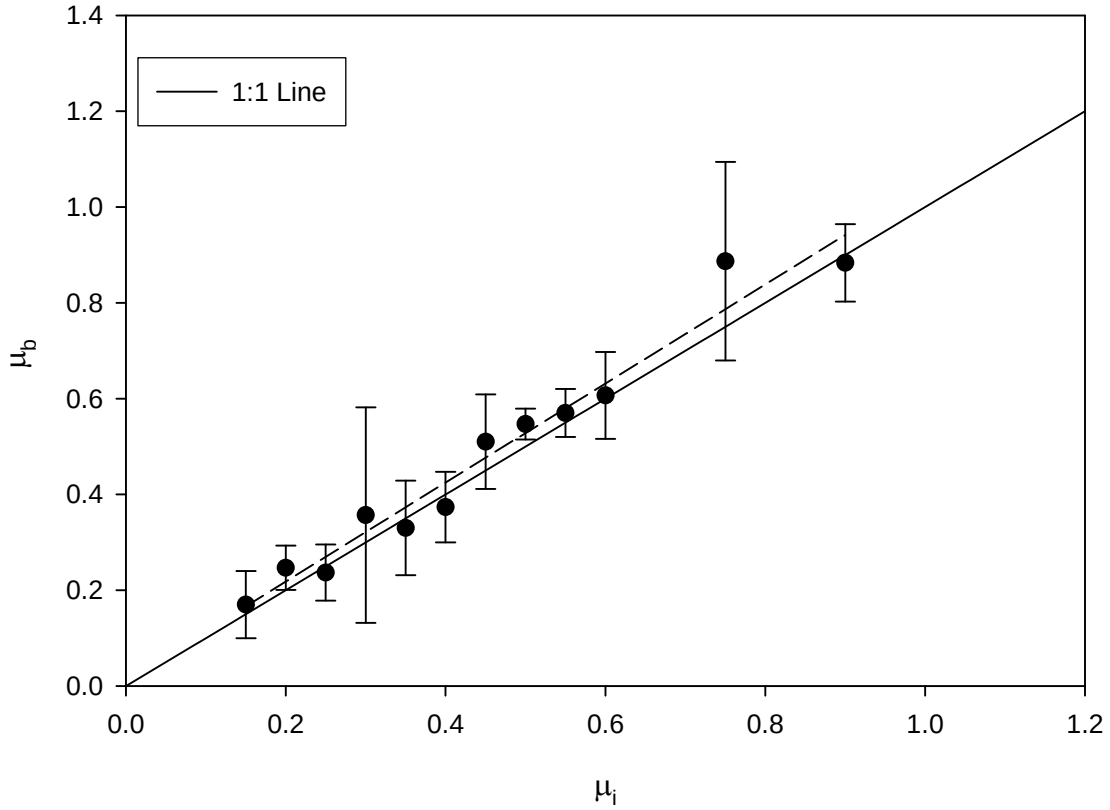

Figure 4.4. Comparison of specified cellular biomass growth rate (μ_i, d^{-1}) vs. the resultant population growth rate (μ_b, d^{-1}). Symbols show mean $\mu_b \pm$ SD (data from Table 2). Broken line is the least-squares fit ($r^2 = 0.99$); solid line indicates 1:1 relationship.

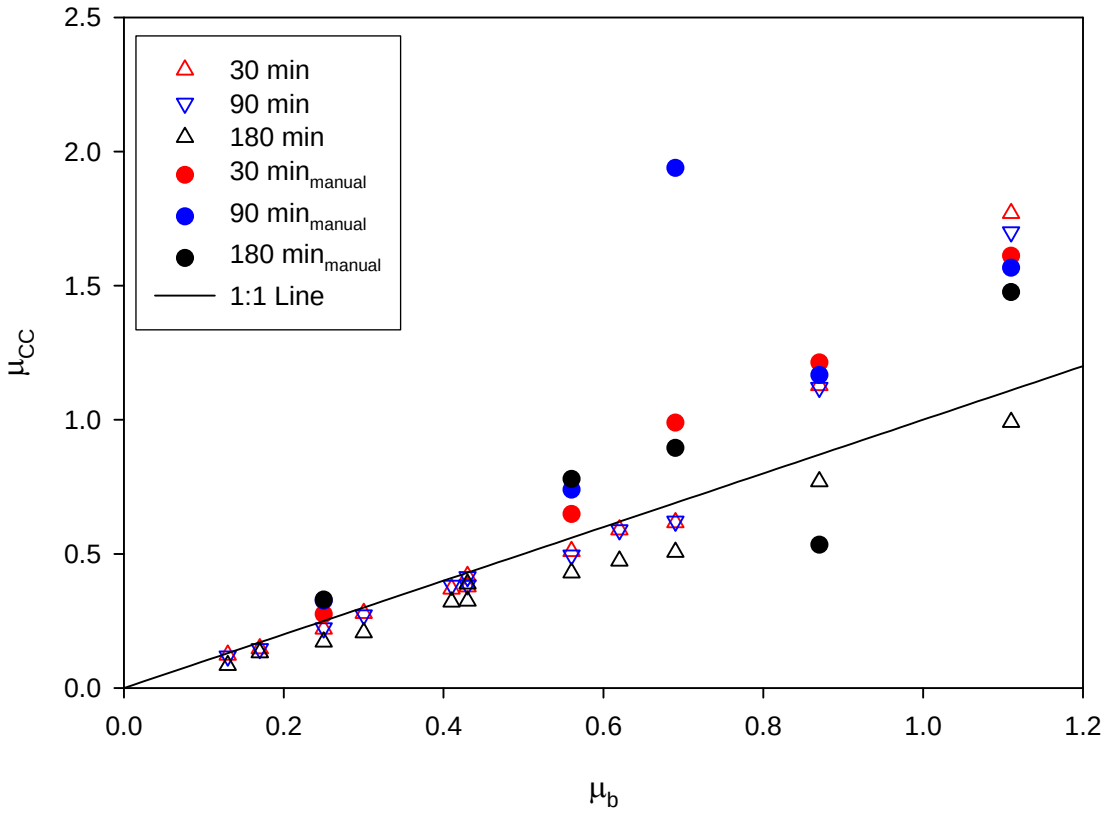

Figure 4.5. Comparison of curve-fit (open symbols) or manually calculated (filled symbols) growth rate estimates (μ_{CC}, d^{-1}) vs. actual growth rate (μ_b, d^{-1}). Line indicates 1:1 relationship. See text for details.

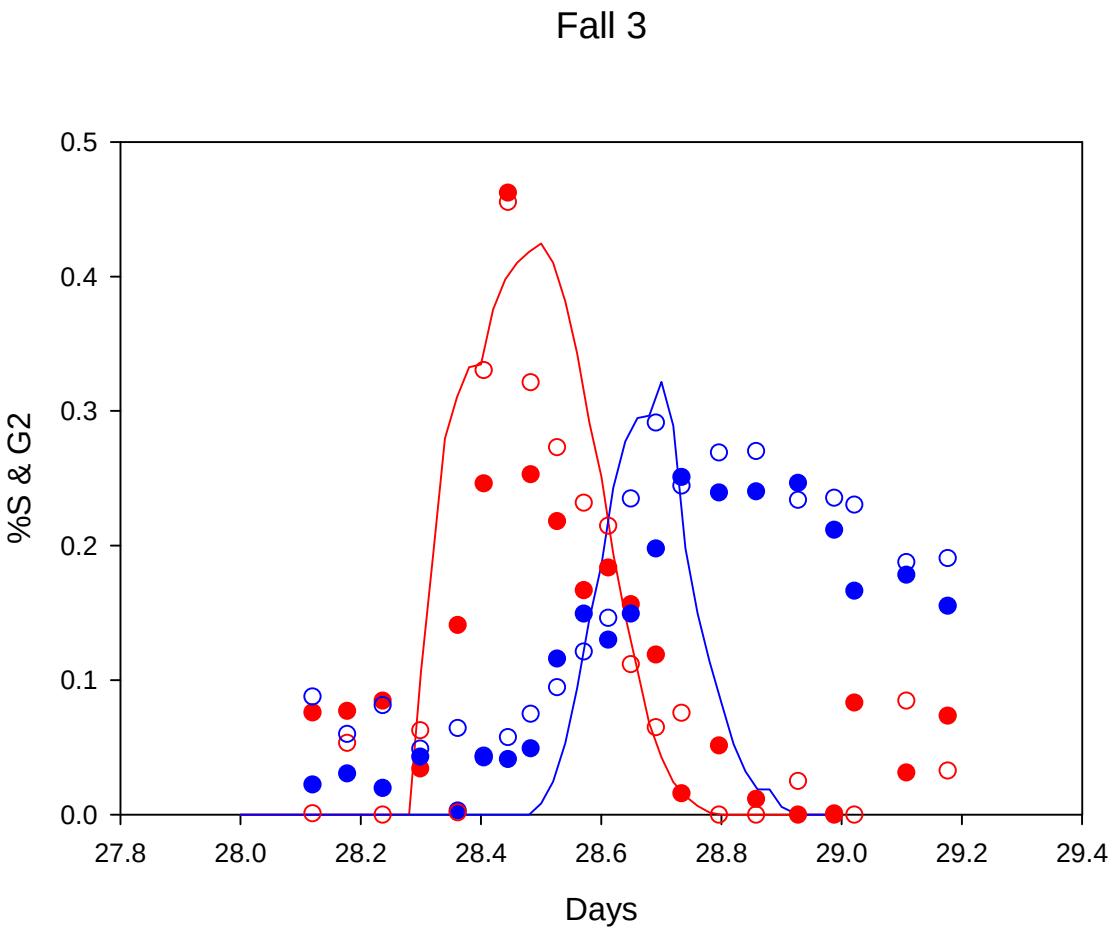

Figure 4.6. Time series of percent population in S (red) and G2 (blue) cell cycle phases measured in bottle incubations (circles) and corresponding model output (lines) for a low growth rate experiment ($\mu = 0.33\ d^{-1}$). Open and closed symbols represent replicate bottles.

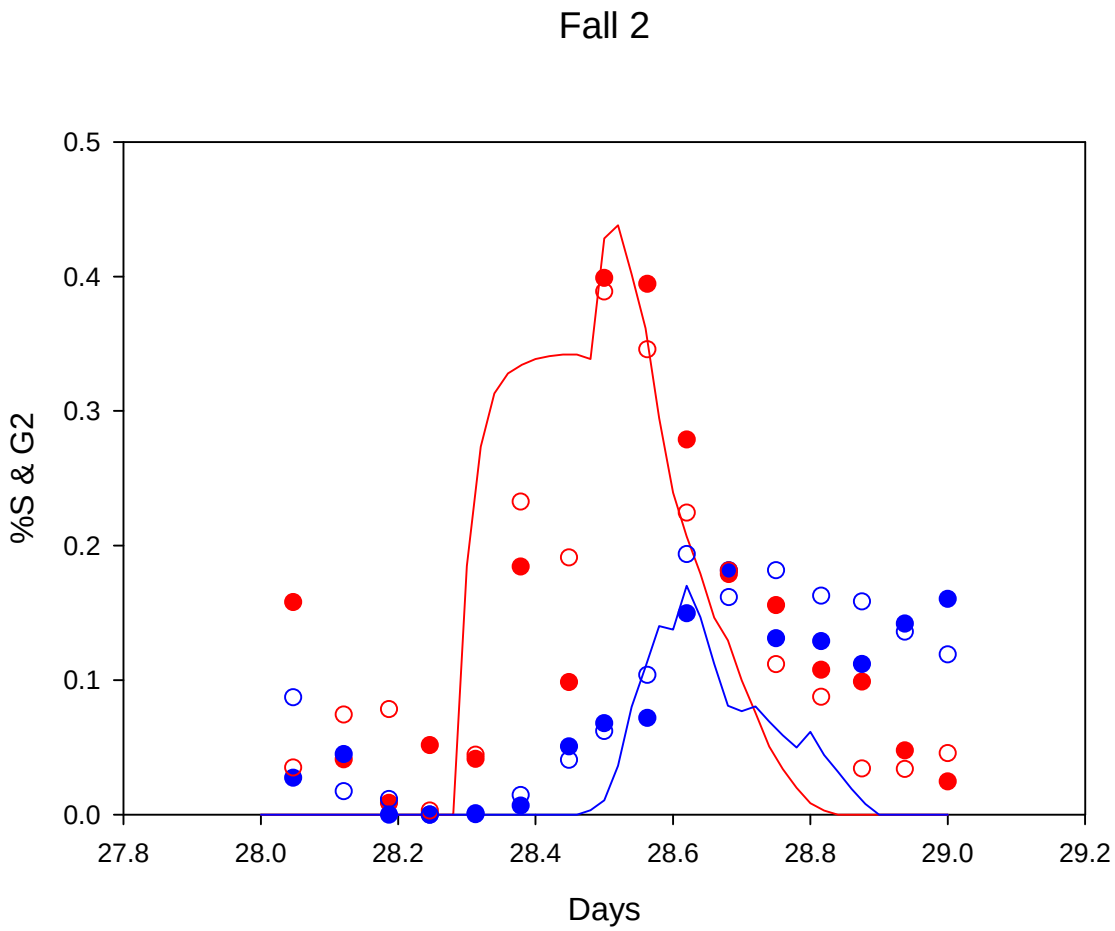

Figure 4.7. Time series of percent population in S and G2 cell cycle phases for the incubation data and model output for a moderate growth rate ($\mu = 0.48\ d^{-1}$). Symbols as in Figure 6.

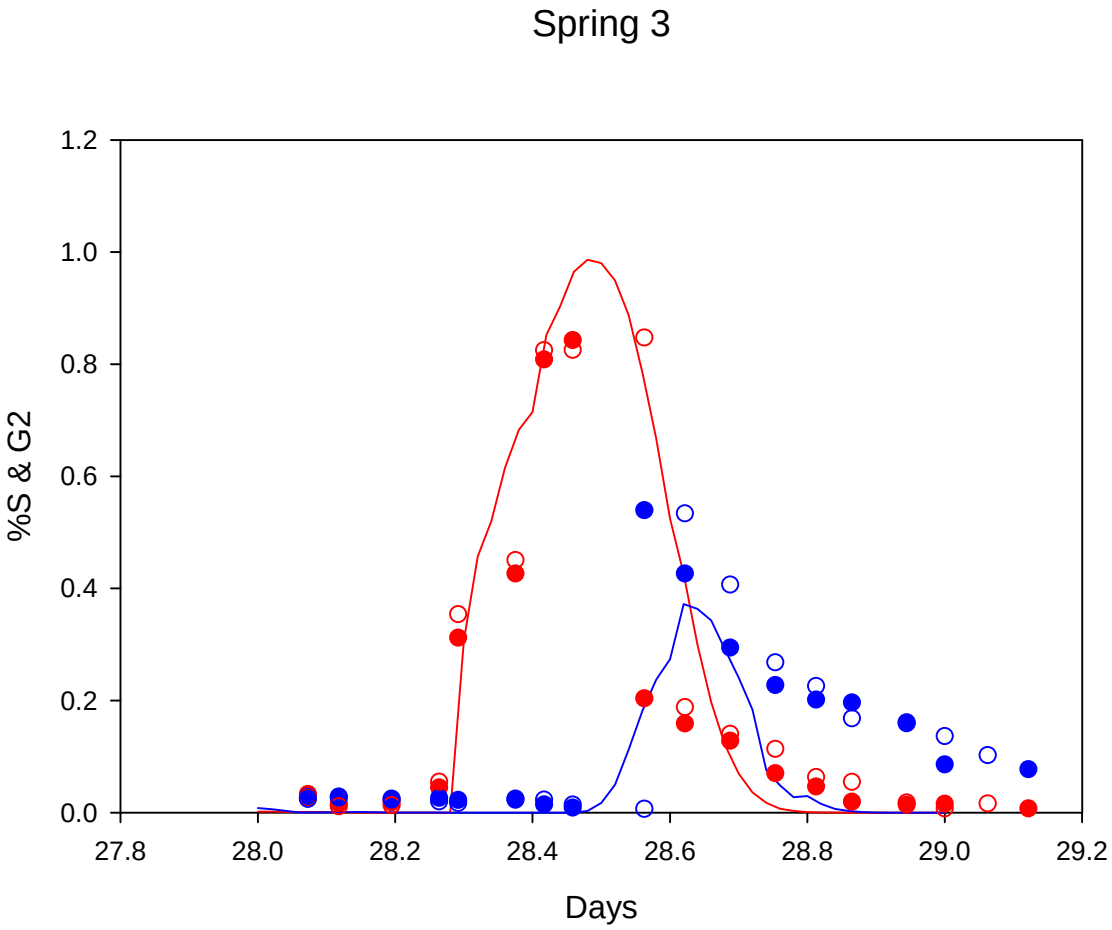

Figure 4.8. Time series of percent population in S and G2 cell cycle phases for the incubation data and model output for a moderate growth rate ($\mu = 0.70\ d^{-1}$). Symbols as in Figure 6.

Appendix

Matlab code for Chapter 4

Driver

```
% driver.m script that steps though and runs model
% Brad J. Blythe
% Date
% UGA
% set the stage
clear all
close all
tic
% A. Call parameter function to initial all simulation settings
[t_span, t_step, pro] = parameters ;
time_step_lag = 4;
%B. Loop thru time and increase cell size
tm(1) = 0.00001;
cnt = 1;
npro = length(pro);
G2_cells = zeros(t_span/t_step+1,1);
G1_cells = zeros(t_span/t_step+1,1);
G0_cells = zeros(t_span/t_step+1,1);
S_cells = zeros(t_span/t_step+1,1);
R_cells = zeros(t_span/t_step+1,1);
av_cell_size = zeros(t_span/t_step+1,1);
av_cell_dna = zeros(t_span/t_step+1,1);
max_size_rep = zeros(t_span/t_step+1,2);
min_size_rep = zeros(t_span/t_step+1,2);
for t = t_step : t_step:t_span
cnt = cnt + 1;
% Now lets start our main loop
% is there light at this time?
lighttime = t - fix(t);
if lighttime <= 0.5;
light = 1;
% disp('day')
else
light = 0;
% disp('night')
end
npro_now = npro;
% This loop just grows the cells
for c = 1 : npro_now
% Calculate Phase fraction data and store it
if pro(c).dna(cnt-1) >=2
G2_cells(cnt-1) = G2_cells(cnt-1) + 1;
elseif pro(c).dna(cnt-1) >1
S_cells(cnt-1) = S_cells(cnt-1) + 1;
elseif pro(c).dna(cnt-1) == 1
G1_cells(cnt-1) = G1_cells(cnt-1) + 1;
else
G0_cells(cnt-1) = G0_cells(cnt-1) + 1;
end
% this step updates size for each cell
```

```
pro(c).size(cnt) = pro(c).size(cnt - 1) + ((pro(c).mu * t_step) * light);
end
% Now check to see which cells can replicate DNA - but don't do it yet.
cell_can_rep = [];
for c = 1 : npro_now
if ((pro(c).size(cnt) > 30) && lighttime >= 0.25 && (pro(c).dna(cnt-1) <= 2)) | ((pro(c).dna(cnt-1)-1) > 1e-6)
cell_can_rep = [cell_can_rep c];
end
end
n_cell_can_rep = length(cell_can_rep);
%This is where we use a function to decide if a cell will begin to
%replicate DNA
t_zero = 0.25;
t_now = t - fix(t);
f_divide = ((exp(t_now - t_zero) - 1) / exp(t_now) + 0.5);
f_div_sav(cnt-1) = f_divide;
% Calculate the number of current cells that WILL replicate DNA at this time
% step
n_cell_will_rep = ceil(n_cell_can_rep * f_divide);
% Randomly select those cells that will divide. To do this, get a random
% permutation of the number of cells that CAN divide. So, if 23 cells can
% divide, we will randomly permute the integers from 1:23. Then select the
% first n_cell_will_rep of these. So if only 6 can replicate, then pick the
% first 6 of these 23 randomly permuted integers. These will be the indices
% representing the cells that WILL divide.
indx = randperm(n_cell_can_rep);
ind_will_rep = indx(1 : n_cell_will_rep);
n_will_rep = length(ind_will_rep);
indx_will_rep = cell_can_rep(ind_will_rep);
% Now get indices of all those cells that will NOT replicate DNA even if
% they potentially can
indx_no_rep = setxor([1:npro_now], indx_will_rep);
n_no_rep = length(indx_no_rep);
% Now we know how many and which cells can replicate, we actually let them replicate their DNA
% and check if they ahve immediately gone to 2 copies of DNA
if length(indx_will_rep) > 0
for c = 1 : n_will_rep
pro(indx_will_rep(c)).dna(cnt) = pro(indx_will_rep(c)).dna(cnt - 1) + (0.102);
if (pro(indx_will_rep(c)).dna(cnt) >= 2) && (pro(indx_will_rep(c)).time_2 == 0);
pro(indx_will_rep(c)).time_2 = t;
end
if pro(indx_will_rep(c)).dna(cnt) >= 2
pro(indx_will_rep(c)).dna(cnt) = 2;
end
end
end
for j = 1 : n_no_rep
pro(indx_no_rep(j)).dna(cnt) = pro(indx_no_rep(j)).dna(cnt - 1);
end
% Loop through all the calls. If they have more than two copies of
% their DNA, and they satisfy the lag criterion, then allow the cells
% to divide
max_size = 0;
min_size = 500;
for c = 1 : npro_now
if (pro(c).dna(cnt) >= 2)
```

```
dna_lag = (time_step_lag - 1)*t_step;
if (t - pro(c).time_2 > dna_lag)
if pro(c).size(end) > max_size
max_size = pro(c).size(end);
end
if pro(c).size(end) < min_size
min_size = pro(c).size(end);
end
pro = makepro(pro, npro+1, cnt, pro(c).size(cnt));
pro(c).size(cnt) = pro(c).size(cnt) - pro(npro+1).size(cnt);
npro = npro+1;
pro(c).dna(cnt) = 1;
pro(c).time_2 = 0;
R_cells(cnt) = R_cells(cnt) + 1;
end
end
end
max_size_rep(cnt,:) = [cnt max_size];
min_size_rep(cnt,:) = [cnt min_size];
% Now we set up the grazing function
grazing_rate = .5;
[pro, npro] = killpro(t, pro, npro, t_step, grazing_rate);
% this updates time array for plotting
lt(cnt) = light;
tm(cnt)=t;
cells(cnt) = npro;
G2 = G2_cells/npro;
G1 = G1_cells/npro;
G0 = G0_cells/npro;
S = S_cells/npro;
cell_size = zeros(npro,1);
cell_dna = zeros(npro,1);
for c = 1 : length(pro)
cell_size(c) = pro(c).size(end);
cell_dna(c) = pro(c).dna(end);
end
non_zero_size = nnz(cell_size);
non_zero_dna = nnz(cell_dna);
av_cell_size(cnt-1) = sum(cell_size)/non_zero_size;
av_cell_dna(cnt-1) = sum(cell_dna)/non_zero_dna;
end
% record some data for later analysis
% calc average cell size & DNA content at each tpt
for t = 1:length(tm)
cnt=1;
procount = 0;
for c = 1:length(pro)
if (pro(c).size(t) ~=0 && pro(c).dna(t) ~= 0)
cellsize(t) = mean(pro(c).size(t));
dna_cell(t) = mean(pro(c).dna(t));
end
end
cnt = cnt+1;
end
cell_size = zeros(length(pro),length(tm));
cell_dna = zeros(length(pro),length(tm));
```

```
for c = 1 : length(pro)
cell_size(c,:) = pro(c).size;
cell_dna(c,:) = pro(c).dna;
end
non_zeros1 = zeros(1,length(tm));
non_zeros2 = zeros(1,length(tm));
for tind = 1 : length(tm)
non_zeros1(tind) = nnz(cell_size);
non_zeros2(tind) = nnz(cell_dna);
end
av_cell_size = sum(cell_size)./non_zeros1;
av_cell_dna = sum(cell_dna)./non_zeros2;
for t = 1 : length(tm)
for c = 1 : length(pro)
end
end
%C. Plot Figure
toc
'drawing'
figure;
for c = 1:length(pro)
%ind = find (pro(c).dna ~= 0);
%index = (tm >=8 & tm <=9);
subplot(3,1,1)
plot(tm, av_cell_size)
ylabel('Avg. Size')
hold on
subplot(3,1,2)
plot(tm, av_cell_dna)
ylabel('dna / cell')
hold on
subplot(3,1,3)
plot(tm, cells)
ylabel('[Pro.]')
xlabel('Days')
end
figure;
for c = 1:length(pro)
ind = find (pro(c).dna ~= 0);
index = (tm >=29 & tm <=30);
subplot(3,1,1)
plot(tm(index), av_cell_size(index))
ylabel('Avg. Size')
hold on
subplot(3,1,2)
plot(tm(index), av_cell_dna(index))
ylabel('dna / cell')
hold on
subplot(3,1,3)
plot(tm(index), cells(index))
ylabel('[Pro.]')
end
figure;
for c = 1:length(pro)
index = (tm >=8 & tm <=10);
subplot (3,1,1)
```

```
plot(tm, S,'b')
ylabel('%S')
subplot (3,1,2)
plot(tm, G2,'r')
ylabel('%G2')
subplot (3,1,3)
plot(tm, G2+S,'g')
ylabel('%S + G2')
xlabel('days')
end
figure;
for c = 1:length(pro)
index = (tm >=29 & tm <=30);
subplot (4,1,1)
plot(tm(index), S(index),'b')
ylabel('%S')
subplot (4,1,2)
plot(tm(index), G2(index),'r')
ylabel('%G2')
subplot (4,1,3)
plot(tm(index), G2(index), 'r', tm(index), S(index),'b')
ylabel('%S + G2')
subplot (4,1,4)
plot(tm(index), G2(index)+S(index),'g')
ylabel('%S + G2')
xlabel('days')
end
ind_exp = find (tm >= 29 & tm <=30);
[tm(ind_exp)' S(ind_exp) G2(ind_exp) cells(ind_exp)' av_cell_dna(ind_exp) av_cell_size(ind_exp)]
```

Makepro

```
% This will be the Script where we make Pro divide
function [pro, growthrate] = makepro (pro, i, current_time, largesize)
%this takes cells that are passed in and divides them into two cells,
%adding a new cell to the array, and then passes them back to the main
%script
growthrate = 0.6; %+ sqrt(0.001) * randn(1); % um d-1
pro(i).mu = growthrate;
pro(i).basesize = 50 + sqrt(100) * randn(1);
if nargin == 4
pro(i).size(current_time) = largesize * 0.5;
else
pro(i).size(current_time) = pro(i).basesize ; % um
end
if current_time > 1
pro(i).dna = zeros(1,current_time-1);
pro(i).dna(current_time) = 1;
pro(i).time_2 = 0;
else
pro(i).dna = 1;
pro(i).time_2 = 0;
end
```

Killpro

```
function [pro_out, npro_out] = killpro(t, pro, npro, t_step, g)
%
% KILLPRO takes a structure of prochloro. and grazes them
%
% t is t he current time
% pro is a structure containing information on the cells
% npro is the number of cells
% t_step is the time step size
% g is the grazing rate
%
% pro_out is the structure of cells after grazing
%
% Is the time right for grazing?
if t < 0
pro_out = pro;
npro_out = npro;
return
end
% Select cells for grazing - we need to figure out which cells will
% actually be grazed
indx = randperm(npro);
grazing_rate = g*t_step;
num_cells_grazed = floor(npro*grazing_rate);
[npro num_cells_grazed];
if num_cells_grazed > 0
% disp('I have done some grazing')
indx_cells_grazed = indx(1 : num_cells_grazed);
% Find the cells that are NOT grazed, discard those cells that have been
% grazed and make a new pro structure
indx_no_graze = setxor([1:npro], indx_cells_grazed);
pro_out = pro(indx_no_graze);
npro_out = length(pro_out);
else
% disp('No cells to graze')
pro_out = pro;
npro_out = npro;
end
```

Parameters

```
function [t_span, t_step, pro] = parameters()
% parameters.m user defined initial conditions and model parameters
% A. Time variables
t_span = 31; % time span (d)
t_step = 0.02; % time step size (d)
% B. Define Prochlorococcus size and growth parameters
npro = 500; % number of cells
pro = [];
for i = 1:npro
[pro] = makepro(pro, i, 1);
end
```

CHAPTER 5

DISSERTATION CONCLUSIONS

This dissertation focuses on understanding the diel population dynamics of *Prochlorococcus* and *Synechococcus*, and the cellular processes driving these dynamics. Natural populations of *Prochlorococcus* and *Synechococcus* display dramatic diel variation in cellular properties (e.g. cell mass and DNA content) as well as in abundance. Although this variation likely influences numerous ecological processes (e.g. bacterial production, microzooplankton growth and grazing), to date it has received relatively little attention. From a practical point of view, diel cell division cycles can be used to estimate growth rates of *in situ* populations, without the need for incubations, and independent of grazing mortality (McDuff & Chisholm, 1982, Carpenter & Chang, 1988). A large part of this thesis is devoted to critically examining the accuracy of this approach for estimating the growth rate in *Prochlorococcus*.

As described in Chapter 2, the basic algorithm for calculating growth rate from cell cycle patterns was developed by Carpenter and Chang (1988), and has since been applied by numerous workers to *Prochlorococcus* populations (Vaulot *et al.*, 1995, Liu *et al.*, 1997, Shalapyonok *et al.*, 1998, Mann & Chisholm, 2000, Worden & Binder, 2003). In a subsequent study, these authors suggested that data-smoothing may increases the accuracy and reliability of the approach (Chang & Carpenter, 1990). In Chapter 2 we analyze this curve-fitting variation of the approach, as applied to natural *Prochlorococcus* populations. Briefly, we expected the curve-fitting

approach would provide more accurate and reproducible estimates of growth rate than the standard, manual approach. However, our results show that the growth rates calculated by these two approaches were not systematically different (Figs. 2.4c, 2.8). Based on the results of this chapter alone, we are unable to show that one method is clearly better than the other for these data, although the resultant growth rate estimates can differ considerably when these two methods are compared.

It is interesting to note that while seasonal patterns of cell abundance observed here were as reported in previous studies, our estimates for μ, Σ and t_d do not cluster together as "Fall" or "Spring" groups when seasons are compared. Thus, *Prochlorococcus* growth rates were not systematically different between seasons, suggesting that top-down factors may be important in controlling the observed seasonal patterns of cell abundance.

In Chapter 3 we undertook a direct comparison of *Prochlorococcus* and *Synechococcus* dynamics in on-deck bottle incubations versus in the water column. Our data strongly suggest that *in situ Prochlorococcus* and *Synechococcus* physiology (as reflected in growth rate) are reasonably unperturbed in bottle incubations of the sort used in our study. Cell cycle patterns (in the case of *Prochlorococcus*) in bottle and natural populations were generally very similar, and growth rate estimates based on these patterns were therefore not significantly different (Fig. 3.9).

Cellular characteristics for incubated populations were quite similar to those of the corresponding natural populations. Patterns in FALS (related to cell mass) were well-replicated between replicate bottles, and generally matched the *in situ* patterns. Patterns of diel variation in chlorophyll fluorescence were likewise similar, although there was some evidence for photo-acclimation in the bottle experiments, presumably reflecting altered light regimes in the

incubator. These apparent physiological changes were clearly small enough to leave overall cellular growth rates unchanged.

Given the apparently unaltered growth rates of *Prochlorococcus* (and by inference, *Synechococcus*) populations in our incubation bottles, the dramatically different diel patterns in cell abundance between the bottles and water-column (Figs. 3.1, 3.2) suggests that grazing mortality was very different (lower) in many of the bottle treatments.

An unintended benefit of the apparently lowered mortality of *Prochlorococcus* and *Synechococcus* in our bottles is that it allows for an interesting comparison of diel mortality patterns between seasons. In some cases (e.g. Fall-3 & 4), the data are consistent with fairly even grazing pressure over the entire diel cycle (Fig. 3.1), and in others an increase in grazing pressure is observed during the evening hours when *Prochlorococcus* is actively dividing (Fig. 3.2). This pattern of increased grazing mortality during the portion of the day when cells are actively dividing has been hypothesized previously for *Prochlorococcus* based on similar sorts of observations (Liu *et al.*, 1997, Worden & Binder, 2003). Further, our data suggest that there may be seasonal difference in the diel pattern of grazing pressure faced by *Prochlorococcus* and *Synechococcus* in the western Sargasso, whether driven by differences in community composition, abundance, or activity. Clearly, more work is required to establish the existence of diel patterns in grazing mortality, and the factors that underlie any such patterns.

Taking all the data together, our comparison of bottle and *in situ* observations suggests that the implicit assumption of relatively unaltered system behavior in bottle incubations does not always hold true. While it is encouraging to find the physiology of *Prochlorococcus* and *Synechococcus* to be relatively unperturbed, grazing mortality among these populations was obviously strongly altered in the bottles. It is clear that care must be taken when interpreting the

results of incubation studies. Without a direct comparison to the *in situ* dynamics of the planktonic community as a whole, observations based on bottle incubations may miss or incorrectly characterize important ecological phenomena.

In the final chapter of the thesis, we developed a population model that will allow us to begin to examine some of the issues brought to light in previous chapters. This individual-based model incorporates known features of the prokaryotic (and *Prochlorococcus*) cell cycle, and uses parameter values that fall within their experimentally determined range. The only aspect of the model that is wholly unconstrained by experimental data is the probability function that governs the initiation of chromosome replication in eligible cells (Eq. 4.1), which for this study was arbitrarily chosen.

Our model allows us to more directly explore some of the issues regarding *in situ* growth rate estimates that were addressed in previous chapters. Application of the Carpenter-Chang algorithm to model-generated data supports the notion that the curve-fitting approach yields a more accurate estimate of growth rate than the manual approach, at least for low to moderate growth rates (Fig. 4.5). At high growth rates (> 1 doubling per d), however, the algorithm fails. Our results also indicate that sampling intervals of 0.5 or 1.5 h (in combination with curve fitting) are sufficient for reasonably accurate determination of low to moderate growth rates.

Perhaps the most intriguing result of the model, in regards to future field studies, was the observation that while model populations generally achieved steady state over the time scales employed; they nevertheless showed remarkable variability in diel cell cycling and growth rate on a day-to-day basis. This predicted day to day variability could have importantly implications for observations of growth rate in natural *Prochlorococcus* populations. If these observations are made over relatively short periods (on the order of 24 h), as they almost always are, then the

resultant estimates of growth rate may significantly under- or over-estimate the longer-term growth rate of the population. The general implication of these results is that a 24 hour sampling time course may only catch one mode of behavior in the natural population, and the calculated growth rate for that day may not necessarily reflect the longer-term average growth rate of the population.

Taken in its entirety, this dissertation has furthered our understanding of the factors driving *Prochlorococcus* and *Synechococcus* dynamics in the western Sargasso Sea. Additionally, it provides validation for a commonly used approach to estimating *in situ* growth rates among these organisms, and points to ways in which this approach may be improved. Finally, the cell cycle-based population model developed here should be a valuable tool for hypothesis development and testing to complement field- and laboratory-based studies concerned with the ecology of picocyanobacteria.

References

Carpenter, E. J. & Chang, J. 1988. Species-Specific Phytoplankton Growth-Rates via Diel DNA-Synthesis Cycles. 1. Concept of the Method. *Mar. Ecol.-Prog. Ser.* **43**:105-11.

Chang, J. & Carpenter, E. J. 1990. Species-Specific Phytoplankton Growth-Rates via Diel DNA-Synthesis Cycles.4. Evaluation of the Magnitude of Error with Computer-Simulated Cell-Populations. *Mar. Ecol.-Prog. Ser.* **65**:293-304.

Liu, H. B., Nolla, H. A. & Campbell, L. 1997. Prochlorococcus growth rate and contribution to primary production in the equatorial and subtropical North Pacific Ocean. *Aquat. Microb. Ecol.* **12**:39-47.

Mann, E. L. & Chisholm, S. W. 2000. Iron limits the cell division rate of Prochlorococcus in the eastern equatorial Pacific. *Limnol. Oceanogr.* **45**:1067-76.

McDuff, R. E. & Chisholm, S. W. 1982. The Calculation of Insitu Growth-Rates of Phytoplankton Populations from Fractions of Cells Undergoing Mitosis - a Clarification. *Limnol. Oceanogr.* **27**:783-88.

Shalapyonok, A., Olson, R. J. & Shalapyonok, L. S. 1998. Ultradian growth in Prochlorococcus spp. *Appl. Environ. Microbiol.* **64**:1066-69.

Vaulot, D., Marie, D., Olson, R. J. & Chisholm, S. W. 1995. Growth of Prochlorococcus, A Photosynthetic Prokaryote, In the Equatorial Pacific Ocean. *Science* **268**:1480-82.

Worden, A. Z. & Binder, B. J. 2003. Application of dilution experiments for measuring growth and mortality rates among Prochlorococcus and Synechococcus populations in oligotrophic environments. *Aquat. Microb. Ecol.* **30**:159-74.